NASA CR-72850

WAED 70.08E

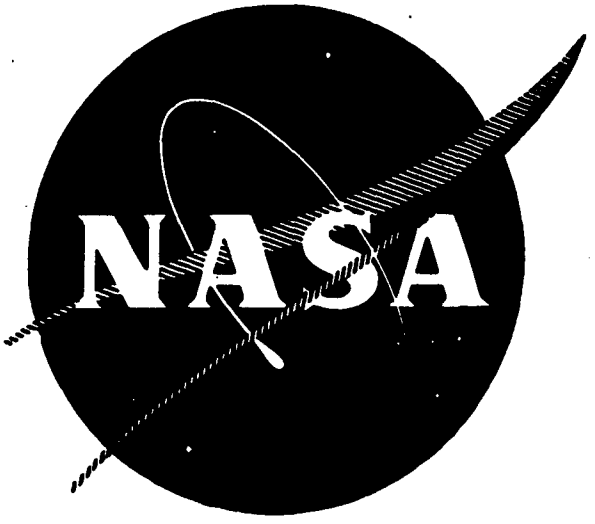

EVALUATION OF HIGH TEMPERATURE ELECTRICAL MATERIALS AND COMPONENTS

by

A. J. Krause, W. S. Neff and J. W. Toth

prepared for

NATIONAL AERONAUTICS AND SPACE ADMINISTRATION

LEWIS RESEARCH CENTER

CONTRACT NAS3-10941

Westinghouse Electric Corporation

Aerospace Electrical Division

Lima, Ohio

1. Report No. NASA CR-72850	2. Government Accession No.	3. Recipient's Catalog No.
4. Title and Subtitle Evaluation of High Temperature Electrical Materials and Components.		5. Report Date April 1970 6. Performing Organization Code
7. Author(s) A. J. Krause, W. S. Neff and J. W. Toth		8. Performing Organization Report No. WAED 70.08E 10. Work Unit No.
9. Performing Organization Name and Address Westinghouse Electric Corporation Aerospace Electrical Division Lima, Ohio 45802		11. Contract or Grant No. NAS3-10941 13. Type of Report and Period Covered Contractor Report
12. Sponsoring Agency Name and Address National Aeronautics and Space Administration Washington, D. C. 20546		14. Sponsoring Agency Code

15. Supplementary Notes
Project Manager, R. A. Lindberg,
NASA Lewis Research Center, Cleveland, Ohio 44135

16. Abstract

This report presents the evaluations from tests, analyses, and examinations of electrical devices that were exposed to ultrahigh-vacuum (10^{-9} torr range) with 1300° F hot-spot temperatures for either 5000 hours or 10,000 hours. Electrical devices included a wound three-phase stator with a beryllia and columbium-1% zirconium bore seal capsule containing potassium (10,000-hour exposure) and two dc solenoids and a single-phase transformer (5000-hour exposure). Evaluations are presented on the functional performance of the various devices, on the device materials relative to device performance, and on overall materials performance relative to aging. The stator, bore seal, and solenoids performed satisfactorily for the durations of their exposures. The transformer primary conductor experienced a failure early in its exposure. No significant material property degradation relative to device performance during aging was found in any material. Satisfactory performance was also recorded for the two thermal-vacuum exposure test chambers with total accumulated times of 19,700 hours each. Conclusions and recommendations from this program are given at the end of the technical sections.

17. Key Words (Suggested by Author(s))	18. Distribution Statement
High-Temperature Vacuum Insulation Aging	Unclassified - Unlimited

19. Security Classif. (of this report)	20. Security Classif. (of this page)	21. No. of Pages	22. Price*
Unclassified	Unclassified		

* For sale by the National Technical Information Service, Springfield, Virginia 22151

NASA-C-168 (Rev. 6-71)

FOREWORD

The work described herein was sponsored by the Space Power Systems Division of the NASA Lewis Research Center. Mr. R. A. Lindberg of NASA was the Project Manager for this program. Mr. T. A. Moss of NASA is also acknowledged for his interest and support in monitoring this work.

The Westinghouse Electric Corporation, Aerospace Electrical Division (WAED) was responsible for the overall technical direction of the program. Mr. J. W. Toth was Program Manager and Mr. W. L. Grant was Principle Investigator. Mr. A. J. Krause was responsible for planning the post-endurance test analyses and evaluation. Mr. W. S. Neff was responsible for conducting and evaluating the post-endurance test analyses of conductor and insulation materials.

Other contributors and consultants who actively participated on this program are listed below:

Westinghouse Aerospace Electrical Division

M. W. Hagadorn
Dr. D. M. Pavlovic
G. R. Keller
R. P. Shumate

Westinghouse Research & Development Center

F. P. Byrne
J. S. Rudolph
C. L. Page
R. D. Nadalin
R. C. Kuznicki

Westinghouse Advanced Reactors Division

J. D. Johnson

Westinghouse Lamp Division

P. J. Walitsky

EIMAC Division of Varian Associates

M. F. Parkman
N. C. Anderson

TABLE OF CONTENTS

TABLE OF CONTENTS (Continued)

TABLE OF CONTENTS (Concluded)

LIST OF ILLUSTRATIONS

LIST OF ILLUSTRATIONS (Continued)

LIST OF ILLUSTRATIONS (Continued)

LIST OF ILLUSTRATIONS (Continued)

LIST OF ILLUSTRATIONS (Concluded)

LIST OF TABLES

LIST OF TABLES (Continued)

LIST OF TABLES (Continued)

LIST OF TABLES (Concluded)

SUMMARY

This topical report presents the evaluations from tests, analyses, and examinations of electrical devices that were exposed to ultrahigh-vacuum (10^{-9} torr range) with 1300° F hot-spot temperatures for either 5000 hours or 10,000 hours. Electrical devices included a wound three-phase stator with a beryllia and columbium-1% zirconium bore seal capsule containing potassium (10,000-hour exposure), and two dc solenoids and a single-phase transformer (5,000-hour exposure). Evaluations are presented on the functional performance of the various devices, on the device materials relative to device performance, and on overall materials performance relative to aging.

The stator, bore seal, and solenoids performed satisfactorily for the durations of their exposures. The transformer primary conductor experienced a failure early in its exposure. This failure has been attributed to motion permitted by winding looseness which in turn was produced by shrinkage of the conductor insulation during firing (ref. 4). No significant material property degradation relative to device performance during aging was found in any other materials. Some magnetic material and electrical insulations actually improved during aging. Several materials experienced changes due to aging alone or interaction with other materials. Grain growth was found in metals and discolorations and deposits were found in both metals and electrical insulations. These changes did not degrade the functional performance of the materials. Satisfactory performance was also recorded for the two thermal-vacuum exposure test chambers with total accumulated times of 19,700 hours each.

Evaluations are summarized on pages 70-75, 123-129, and 131-138 inclusive.

Conclusions and recommendations from this program are given at the end of the technical sections in this report, pages 145-147 inclusive. Flow sheets and outlines of tests, analyses, and examinations planned for the various evaluations are given in the appendix.

SECTION I

INTRODUCTION

Advanced space electric power systems will require magnetic materials, electrical conductors, and electrical insulations capable of long term stable operation at high temperatures in a vacuum or an alkali metal vapor environment. Bore seals, which isolate alternator stators from alkali metal in rotor cavities, are included in designs for these future systems. A series of programs has been directed toward determining the stability of materials and developing the materials and technology required to implement future space electric power systems.

An early program (refs. 1, 2, and 3) defined the physical and electrical properties of materials which might be suitable for space electric power systems. In a later program (ref. 4), selected materials were combined into devices for elevated temperature tests under a simulated space environment. Two sets of devices were constructed with each set consisting of a generator or motor type stator, a transformer, and two solenoids. The first set of devices were installed in thermal ultrahigh vacuum chambers and were subjected to a 5000-hour endurance test under vacuum conditions with a component winding hot-spot temperature of 1100° F. The hot-spot temperature was maintained in part by supplying current to each model (Joule heating) and in part by a heating element in each test chamber. The stator was tested in one vacuum chamber and the transformer and two solenoids were tested in a second vacuum chamber.

While the 1100° F tests were being conducted, the second set of devices was constructed for tests at a 1300° F hot-spot temperature. The basic designs of the devices were the same for each set, but some material changes were introduced, raising the component temperature capability from 1100° to 1300° F. A bore seal capsule, loaded with high-purity alkali metal (potassium), was installed on a pedestal in the stator winding cavity for the 1300° F test.

Following the 1100° F exposure tests, the 1300° F electrical devices and bore seal capsule were thermal-vacuum exposure tested for 5000 hours. The electrical characteristics and the atmospheres of the chambers were monitored periodically. After completion of 5000 hours of testing, the devices remained in the chambers and the chamber sputter-ion

vacuum pumps continued to function. Details of design, model construction, test procedures, and test results are described in reference 4.

The program reported here began with an additional 5000 hours of thermal-vacuum endurance testing of the stator and bore seal capsule. Stator electrical performance and test chamber atmosphere were periodically monitored. Vacuum storage of the transformer and solenoids was continued through the additional stator and bore seal capsule endurance testing. Following completion of the thermal-vacuum endurance tests, all electrical devices were removed from the test chambers and were subjected to tests, analyses, and examinations. Electrical device materials were evaluated on the basis of aging, and any aging effects were defined. Device electrical performance was evaluated in light of possible correlations between measured electrical characteristics and changes in material properties.

Appendix A presents event flow sheets for the planned procedures, processes, tests, analyses, and examinations used in obtaining information on which the evaluations were based. Appendix B gives nominal compositions of metallic materials of construction used in components, fixtures, and thermal-vacuum chambers.

SECTION II

STATOR AND BORE SEAL CAPSULE

A three-phase, ac stator complete with a bore seal capsule containing potassium was exposure tested for a total of 10,000 hours with a hot-spot temperature of 1300° F in a 10^{-9} torr range environment. The electrical conductors were energized during the exposure test thereby applying electrical stresses to the insulation system. Periodically, electrical measurements were taken so that device performance could be determined. Following completion of endurance testing, the final electrical characteristics of the stator were determined. Stator and bore seal materials were then subjected to tests, analyses, and examinations. Electrical performance of the stator and functional performance of the bore seal were evaluated. Bore seal capsule and stator construction materials were evaluated as materials, and the materials evaluations were related to the performance of each device. Descriptions of device construction, exposure testing, details of test procedures, test results, examinations and analyses, and evaluations of devices and materials performances are presented in this section.

STATOR AND BORE SEAL CAPSULE CONSTRUCTION

Figure 1 is a cutaway view of the stator assembly showing primary design features. The main frame was made from a 27 percent cobalt-iron[1] alloy forging, and the laminations were held in the frame by a retaining ring which was also made from a 27 percent cobalt-iron alloy forging. The magnetic stack consisted of 27 percent cobalt-iron alloy laminations, 0.008-inch thick, with an interlaminar insulation coating of plasma-arc sprayed alumina (99.995% Al_2O_3)[2]. The lamination stack was held together by electron beam welds. Electrical conductors were rectangular (0.091 in. x 0.144 in.) Inconel-clad silver (28% Inconel cross-sectional area) wrapped with a 0.006-inch-thick layer of fiberglass served insulation.[3] Slot insulation was provided by ceramic (99% Al_2O_3) U-shaped channels

[1]Hiperco 27 alloy manufactured by Westinghouse Electric Corporation, Blairsville, Pennsylvania.

[2]Linde "A" supplied by Linde Division of Union Carbide Corporation, East Chicago, Indiana.

[3]Anadur "S" applied and supplied by Anaconda Wire & Cable Company, Muskegon, Michigan.

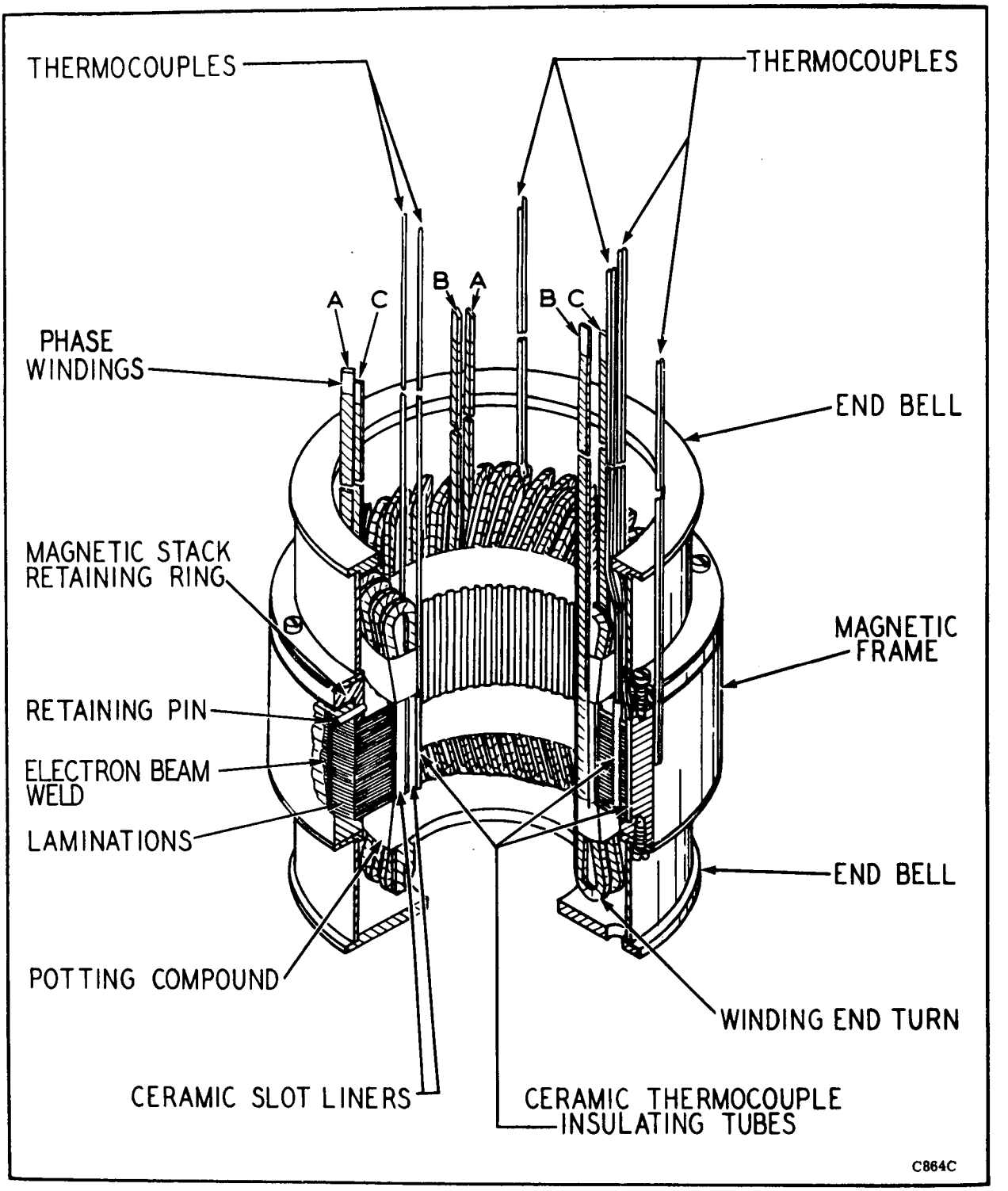

Figure 1. - Cutaway Drawing of Stator Used in the 10,000-Hour, 1300° F Ultrahigh Vacuum Endurance Test

(slot liners), spacers, and wedges. Alumina (99% Al_2O_3) tubes were used as thermocouple insulators in the slot and stack areas. Pairs of thermocouples were installed in the stack, between the outside diameter of the stack and the frame, on the outside diameter of the frame, and on winding end turns. End bells were made from a nickel-base super-alloy[4] which is a nonmagnetic material having a thermal expansion coefficient closely matching that of the 27 percent cobalt-iron alloy. Table 1 summarizes the materials used in the 1300° F stator. Additional information on materials of construction and component fabrication may be found in references 1, 2, 3, and 5.

The lamination stack was representative of one of the two stator stacks of a 15-KVA, 12,000-rpm inductor alternator and of the stator for a 12-horsepower, 12,000-rpm induction motor. The laminations had 36 slots and 36 teeth which were proportioned approximately the same as those of an operating alternator or motor. The ac stator winding was similar to that in a three-phase alternator or motor. The winding was divided into three sections of twelve turns each, and the overlapping of the sections was similar to that which occurs between the phases of an alternator or motor winding. Thus, it was possible to test the stator with a potential between windings and from winding to ground, the same as in an operating alternator.

Figure 2 is a pretest photograph of the bore seal capsule mounted on the pedestal that supported it inside the stator cavity. The bore seal capsule consisted of: (1) a 4-inch outside diameter by 4-inch-long high-purity beryllia[5] (99.8% BeO) tube with a 0.1-inch-thick wall, (2) two 4-inch outside diameter by 3.6-inch inside diameter by 0.2-inch-long high-purity beryllia back-up rings, (3) two columbium-1% zirconium alloy end bells, and (4) a columbium-1% zirconium alloy fill tube. Figure 3 shows the capsule design details. The wall of the large beryllia tube was 0.2-inch thick at the ends to provide a greater brazing area at the seal. The end bells were made hemispherical to equalize stresses when a differential pressure was imposed on the capsule. The active metal brazing alloy used to make the ceramic-to-metal seals consisted of 60Zr-25V-15Cb. (Background on bore seal technology is given in references 3 and 6.) After assembly and leak testing, the capsule was clean-fired at 1470° F and at a pressure of less than 5×10^{-6} torr. Potassium loading and electron beam welding of a closure plug were accomplished in a chamber with a pressure in the 10^{-6} torr range (ref. 6).

---

[4]Hastelloy Alloy "B" manufactured by the Stellite Division of Union Carbide Corporation, Kokomo, Indiana.

[5]Thermalox 998 supplied by the Brush Beryllium Company, Elmore, Ohio.

Table 1. - Summary of Materials Used in 10,000-Hour, 1300° F Ultrahigh Vacuum Endurance Tested Stator

Part	Material	Reference For Additional Detail
Frame	Iron-27% Cobalt Forging[a]	Reference 1
Frame Ring	Iron-27% Cobalt Forging[a]	
Laminations	Iron-27% Cobalt Sheet - 0.008-inch thick[a]	
Interlaminar Insulation	Plasma-arc sprayed Al_2O_3[b] (99.995%)	Reference 2
Slot Liners	Al_2O_3 (99%)	Reference 2
Spacers	Al_2O_3 (99.5%)	Reference 2
Wedges	Al_2O_3 (99%)	Reference 2
Thermocouple Insulators	Al_2O_3 (99%)	Reference 2
Conductor Insulation	Glass fiber (double serving) overcoated with a proprietary oxide-loaded silicone wire enamel[c]	
Potting Compound	Boron nitride chopped fiber cement	
Conductors (rectangular) (0.091 x 0.144 inch)	Inconel-clad silver	Reference 2
End Bells, Hardware	Nickel-base Super Alloy[d]	
Lamination Plates	Nickel-base Super Alloy[d]	
Spring Pin	AMS 5506	
Thermocouples	Inconel Sheath - Platinel II Wire System[e]	

(a) Hiperco 27 Alloy supplied by Westinghouse Electric Corp., Blairsville, Pa.
(b) Linde A supplied by Linde Division of Union Carbide Corp., East Chicago, Ind.
(c) Anadur "S" supplied by Anaconda Wire and Cable Co., Muskegon, Mich.
(d) Hastelloy B manufactured by the Stellite Division of Union Carbide Corp., Kokomo, Ind.
(e) Platinel II manufactured by Engelhard Industries, Inc., Newark, N.J.

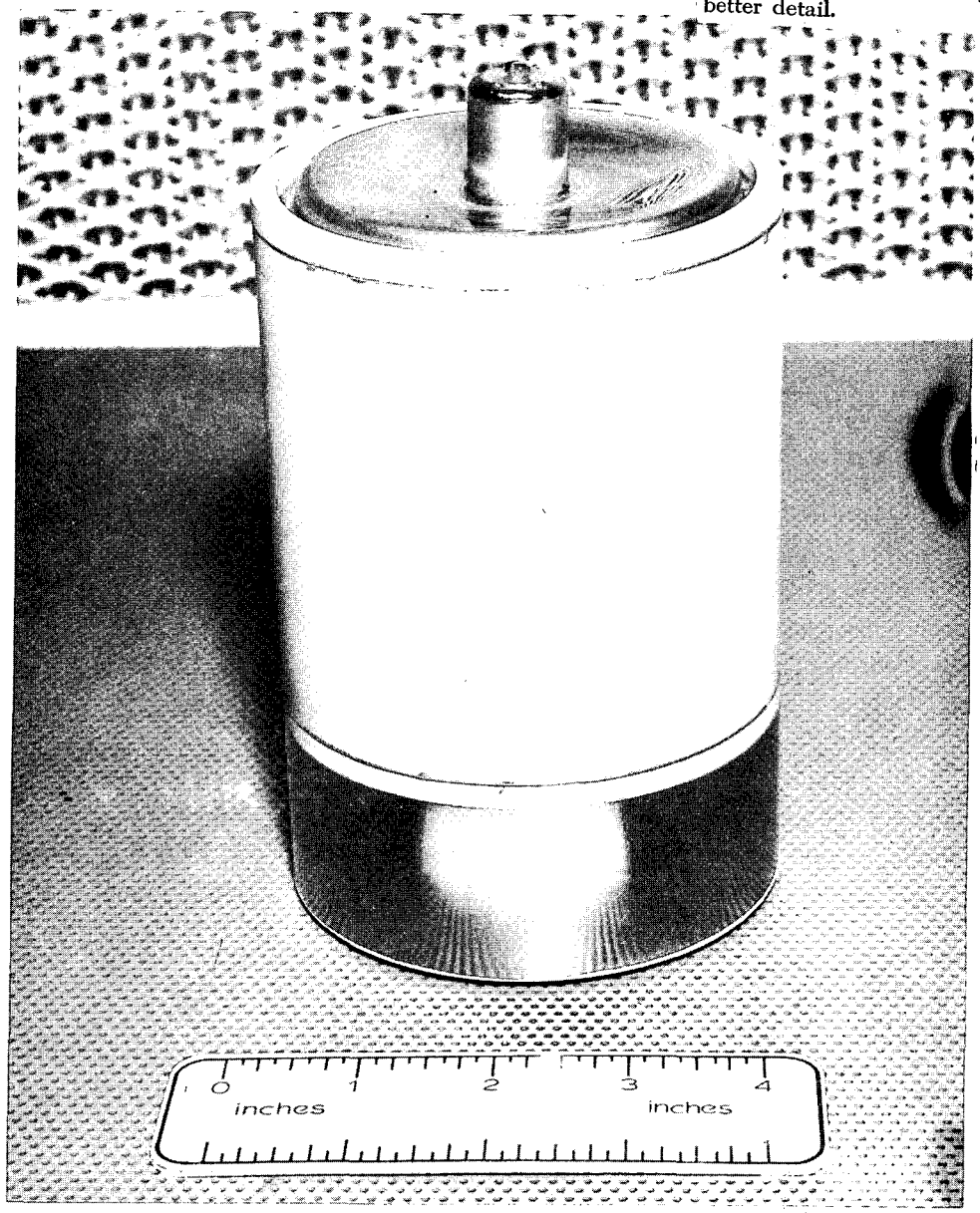

Figure 2. - Photograph of 99.8% Beryllia (Cb-1%Zr) Bore Seal Capsule Brazed with 60Zr-25V-15Cb Alloy. Bore Seal, Containing Potassium was used in the Stator Endurance Test

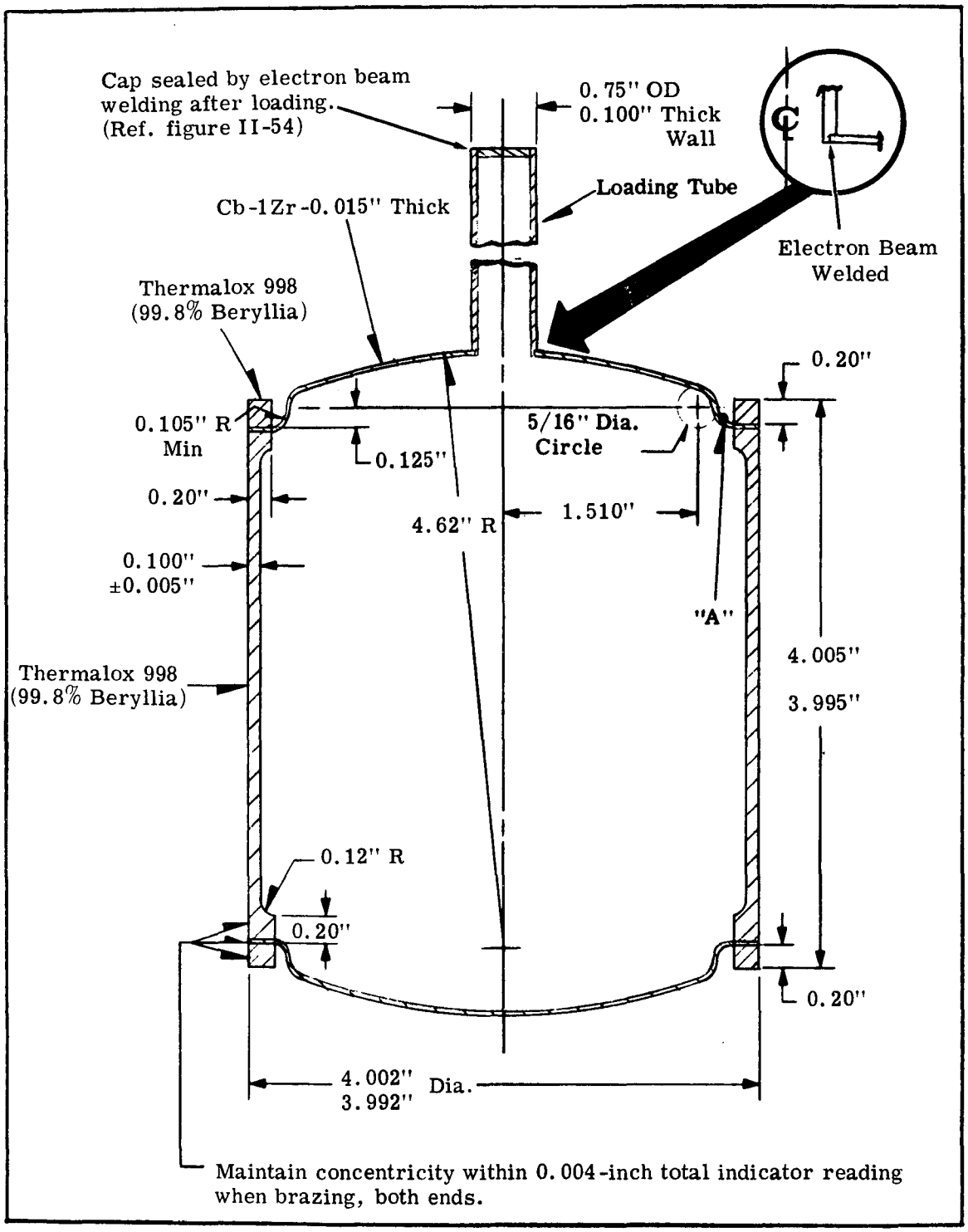

Figure 3. - Design of the Bore Seal Capsule Used in the 10,000-Hour, 1300° F Endurance Test

Figure 4 is a photograph of the two thermal-ultrahigh vacuum chambers used for endurance testing. Each chamber was of double-wall construction with baffles between the walls to channel cooling water flow. The chamber top cover was also double walled to provide a path for cooling water. Each chamber was pumped by a 500 liter/second ion pump (visible at the rear of the left chamber) with titanium sublimation pumping elements for additional pumping capacity. When clean, dry, and empty, each chamber was capable of continuous operation with the test zone temperature at 2200° F and at a pressure below 5.0×10^{-9} torr. The stator and bore seal capsule were endurance tested in the chamber appearing at the left side of the photo, and the

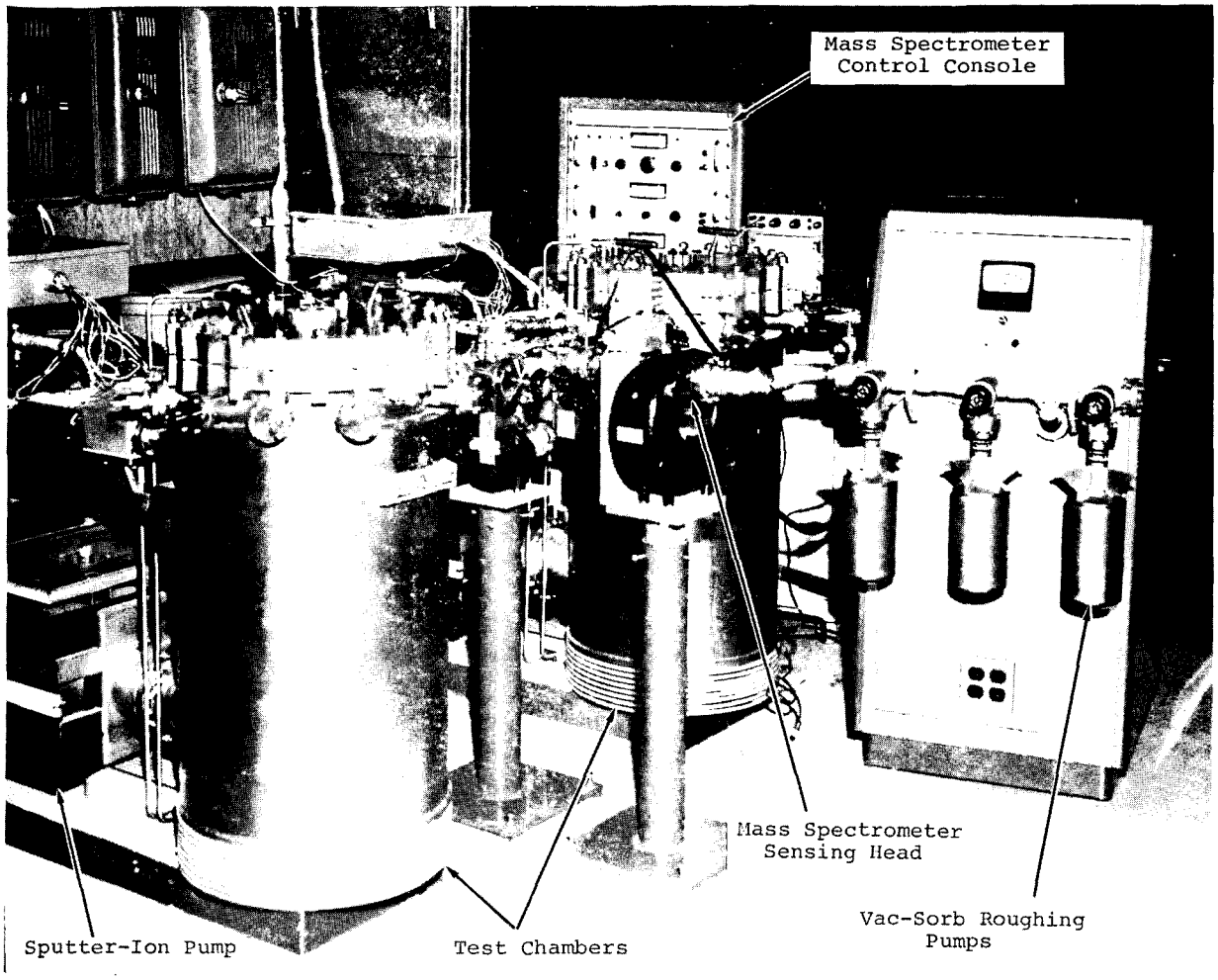

Figure 4. - Vacuum Furnaces Showing Mass Spectrometer Magnets For Residual Analyzer and Sorption Roughing Pumps

This page is reproduced at the back of the report by a different reproduction method to provide better detail.

other chamber contained the transformer and two solenoids. The photo also shows the sensing head and magnet for a residual gas analysis mass spectrometer, and an adsorption roughing pump cart. The residual gas analyzer control console is in the background.

Figure 5 is a cutaway drawing of one of the thermal ultra-high vacuum chambers with the stator, less bore seal capsule, installed in the furnace hot zone. For the endurance test, the bore seal capsule was supported on a pedestal which centered it vertically in the stator stack. Prior to installing the stator in the endurance test chamber, thermocouples were installed in the stator at a laminar flow bench work station. During installation of the stator in the chamber, stator winding leads were inserted in short lengths of alumina tubing to provide electrical insulation as they passed through the top heat shields. The winding leads were brazed to oxygen-free high conductivity copper feedthrough bus bars inside the chamber. Sheathed thermocouples were passed through hollow low expansion iron-nickel-cobalt alloy[6] feedthrough tubes and were brazed to the tubes externally to form vacuum-tight joints.

STATOR AND BORE SEAL CAPSULE ENDURANCE TEST PROGRAM AND ELECTRICAL DATA

Heat to maintain the stator hot-spot temperature was obtained from two sources. During the endurance test, the stator was supplied with three-phase, 400-Hz power with a potential of approximately 485 volts between phases. Current in each phase was maintained at 50 amperes to induce Joule (I^2R) heating in the conductors. The calculated phase I^2R loss at test temperature was 115 watts per phase, or 345 watts total for the stator. The remainder of the heat required was supplied by a heating element which was an integral part of the test chamber.

Electrical data were taken each week during the endurance test to monitor stator conductor resistance stability and insulation system performance. A residual gas analysis trace of the test chamber environment was also recorded each week.

Figure 6 shows a normalized plot of conductor resistance as a function of time at 1300° F for the 10,000-hour test period.

---

[6]Kovar supplied by Westinghouse Electric Corporation, Blairsville, Pennsylvania.

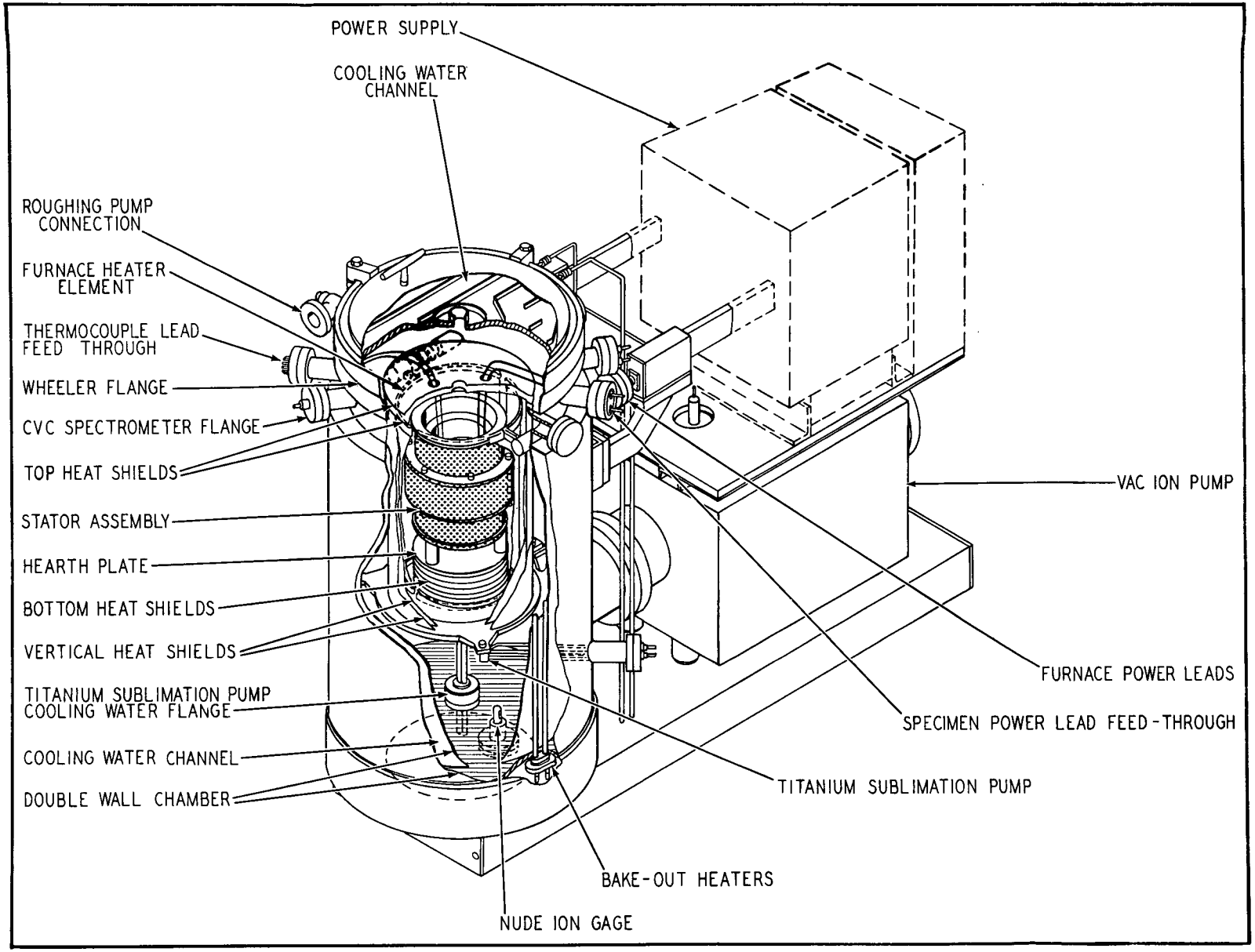

Figure 5. - Cutaway View of Vacuum Furnace Showing the Test Stator Installed

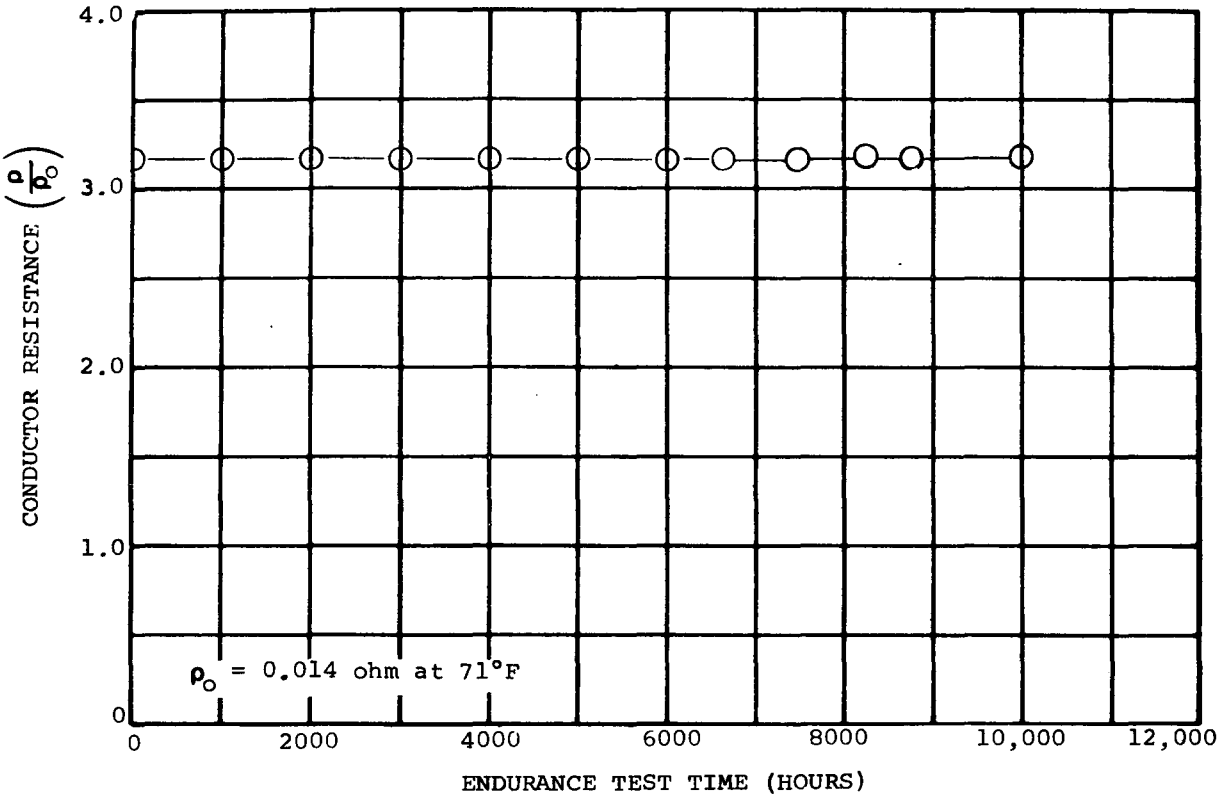

Figure 6. - Stator Conductor Resistance as a Function of Endurance Test Time at 1300° F Hot-Spot (Slot) Temperature in Ultrahigh Vacuum

No change in resistance was observed in any of the three conductors during the course of the test. Figure 7 is a plot of actual dc insulation resistance values, phase-to-phase and phase-to-ground, as a function of time for the 10,000-hour test period. There was a gradual improvement in insulation performance during the total test period, as indicated by estimated trend lines. Figures 8 and 9 are trend plots showing ac leakage current as a function of endurance test time. Phase-to-phase leakage current decreased by a ratio of approximately 3:1, and phase-to-ground leakage by a ratio of approximately 9:1.

Figure 10 is a plot showing the major gas component partial pressures in the stator test chamber as a function of time for the 10,000-hour test period. Ion gage pressure is lower than the partial pressure summation because of relative sensing

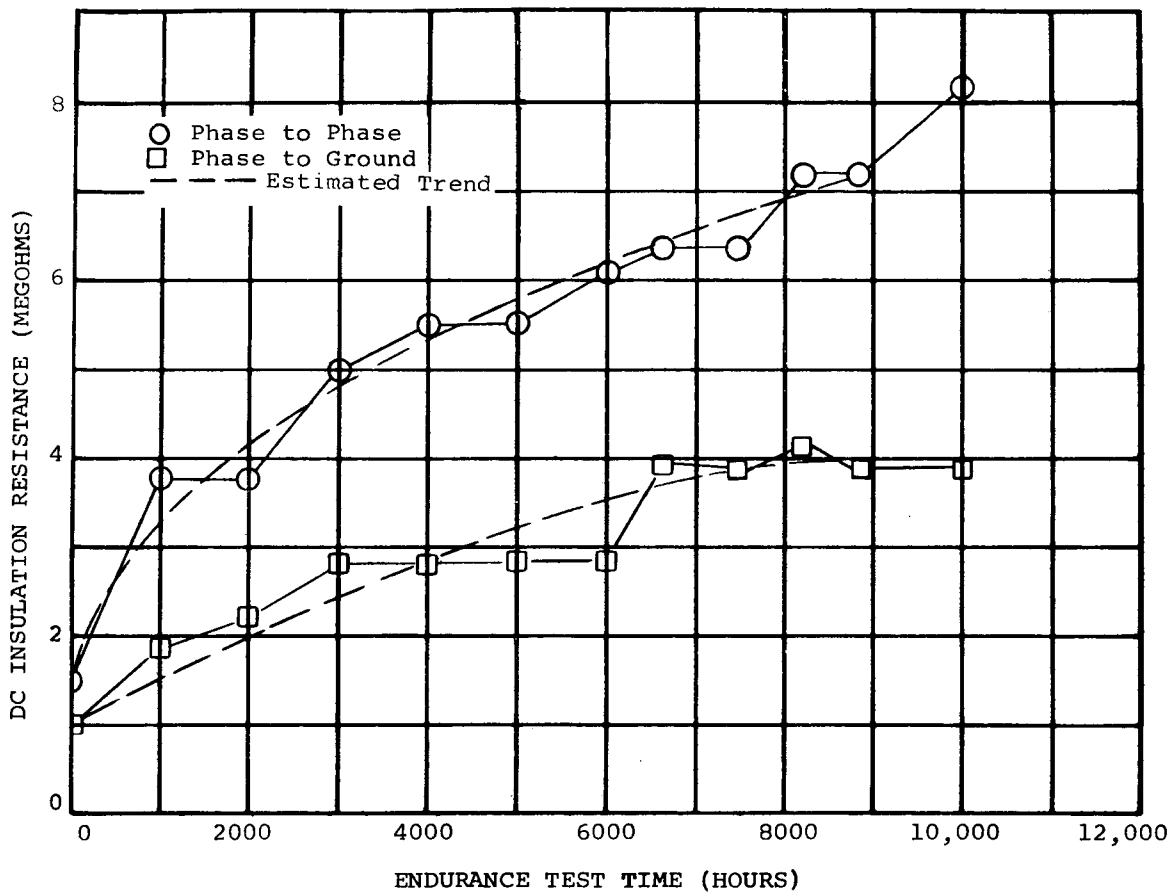

Figure 7. - Stator DC Insulation Performance as a Function of Endurance Test Time in Ultrahigh Vacuum with 1300° F Hot-Spot (Slot) Temperature. Five Hundred Volts DC was Applied Between Phases and Between Each Phase to Ground.

locations. The ion gage was located near the bottom of the chamber in line with the ion pump throat, with a short conductance path to the pump. The residual gas analyzer sensing head was attached to a feedthrough near the top of the test chamber, with a relatively long conductance path to the ion pump, resulting in a higher total pressure at the sensing head. Water vapor was the predominant gas detected in the test chamber throughout the test, followed by nitrogen plus carbon monoxide. Figure 11 is a plot of the various partial pressures normalized to initial gas partial pressures.

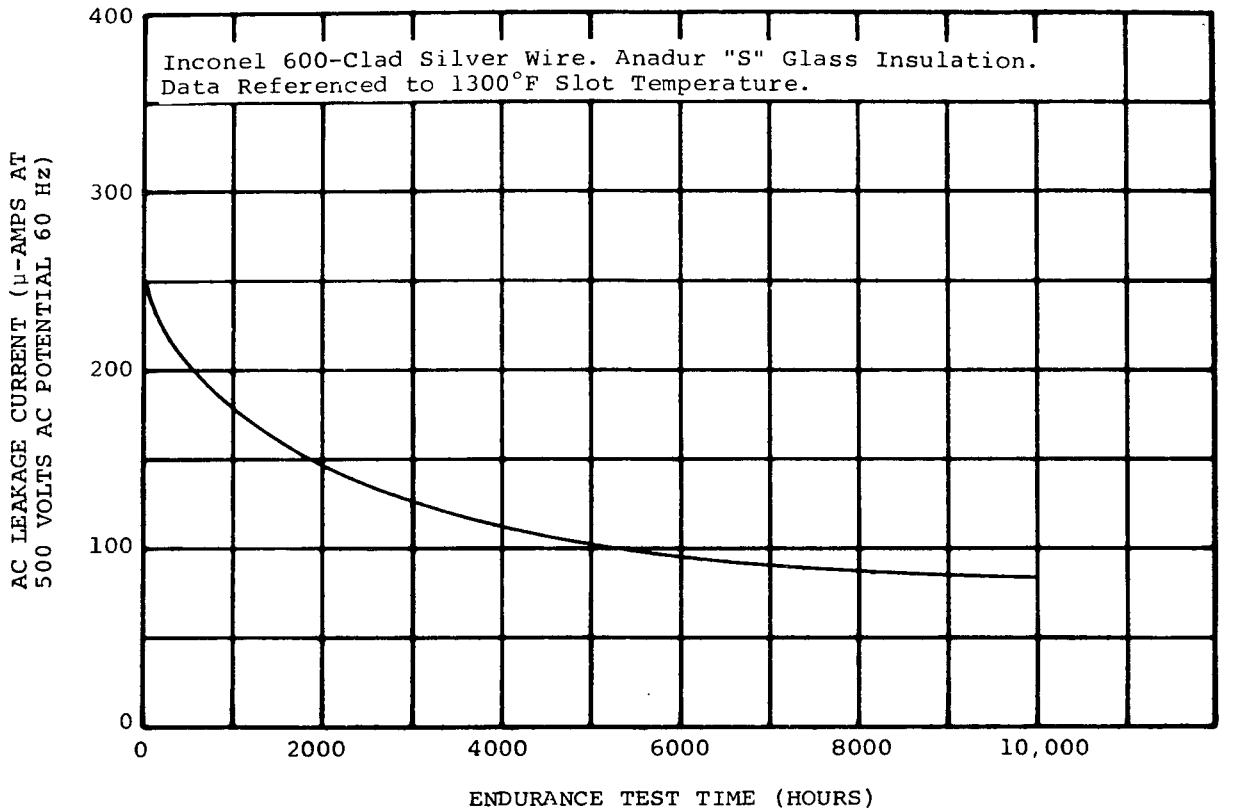

Figure 8. - Stator Insulation System Performance. Phase-to-Phase Current Leakage as a Function of 1300° F Hot-Spot Ultra-high Vacuum Endurance Test Time.

After the 10,000-hour test electrical data and residual gas analysis traces were obtained, power was removed from the stator windings and the chamber heating element power was increased to stabilize the stator assembly at 1300° F. Voltage breakdown values between phases and from phase-to-ground were determined using a self-protecting ac voltage corona tester. Incipient breakdown voltages are shown in table 2. These tests were non-destructive for the stator insulation system. It is believed that a probable cause for the different and descending breakdown voltage values is that a small increase in outgassing rate of the insulation was produced by the application of the test voltage stress. The phase-to-phase and phase-to-ground test sequence was always performed in the reported order over a short time period. Thus, outgassed material of a preceding test combination caused a higher but unknown pressure in the slot area which in turn produced a lower incipient breakdown voltage value.

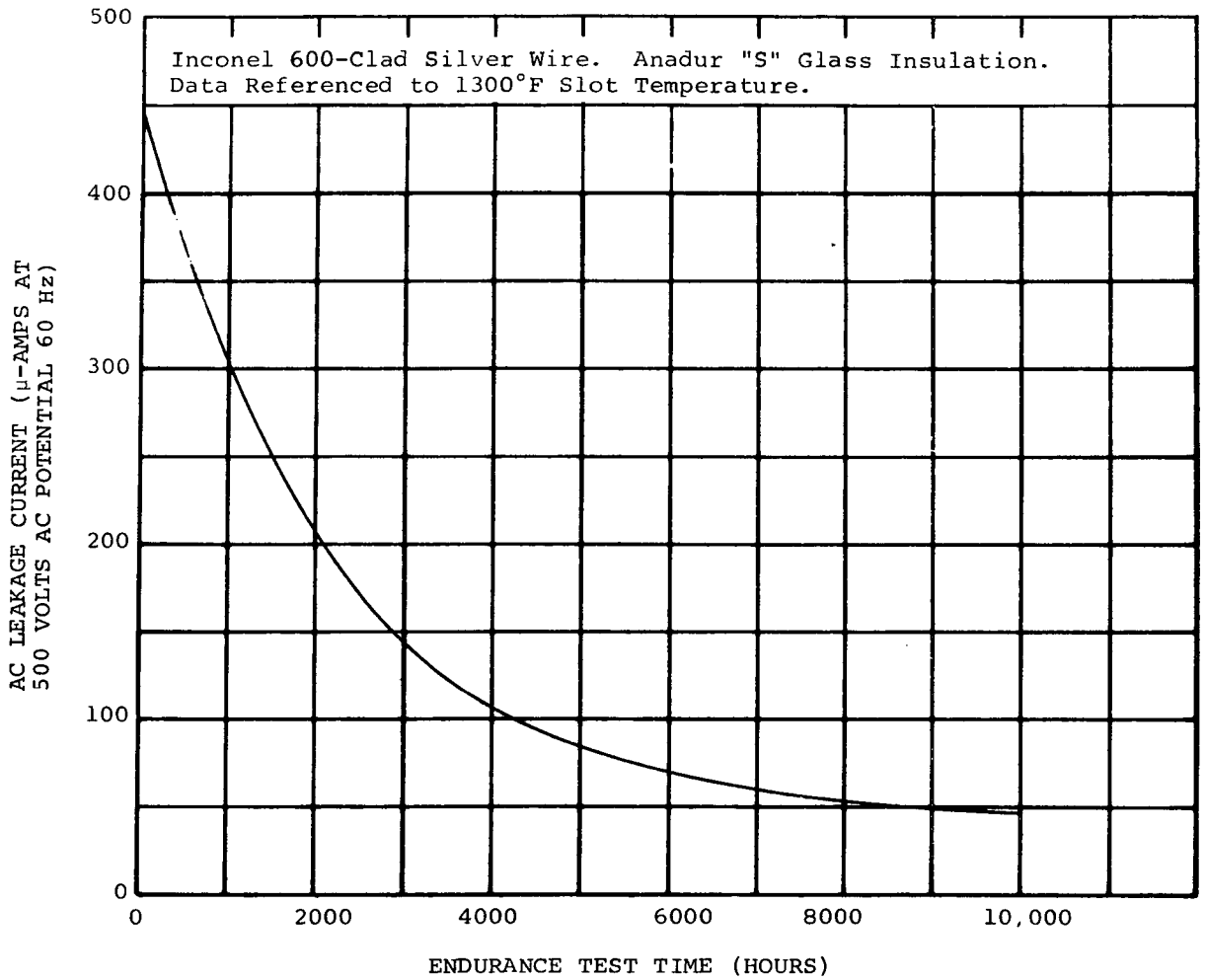

Figure 9. - Stator Insulation System Performance. Phase-to-Ground Current Leakage as a Function of 1300° F Hot-Spot Ultra-high Vacuum Endurance Test Time.

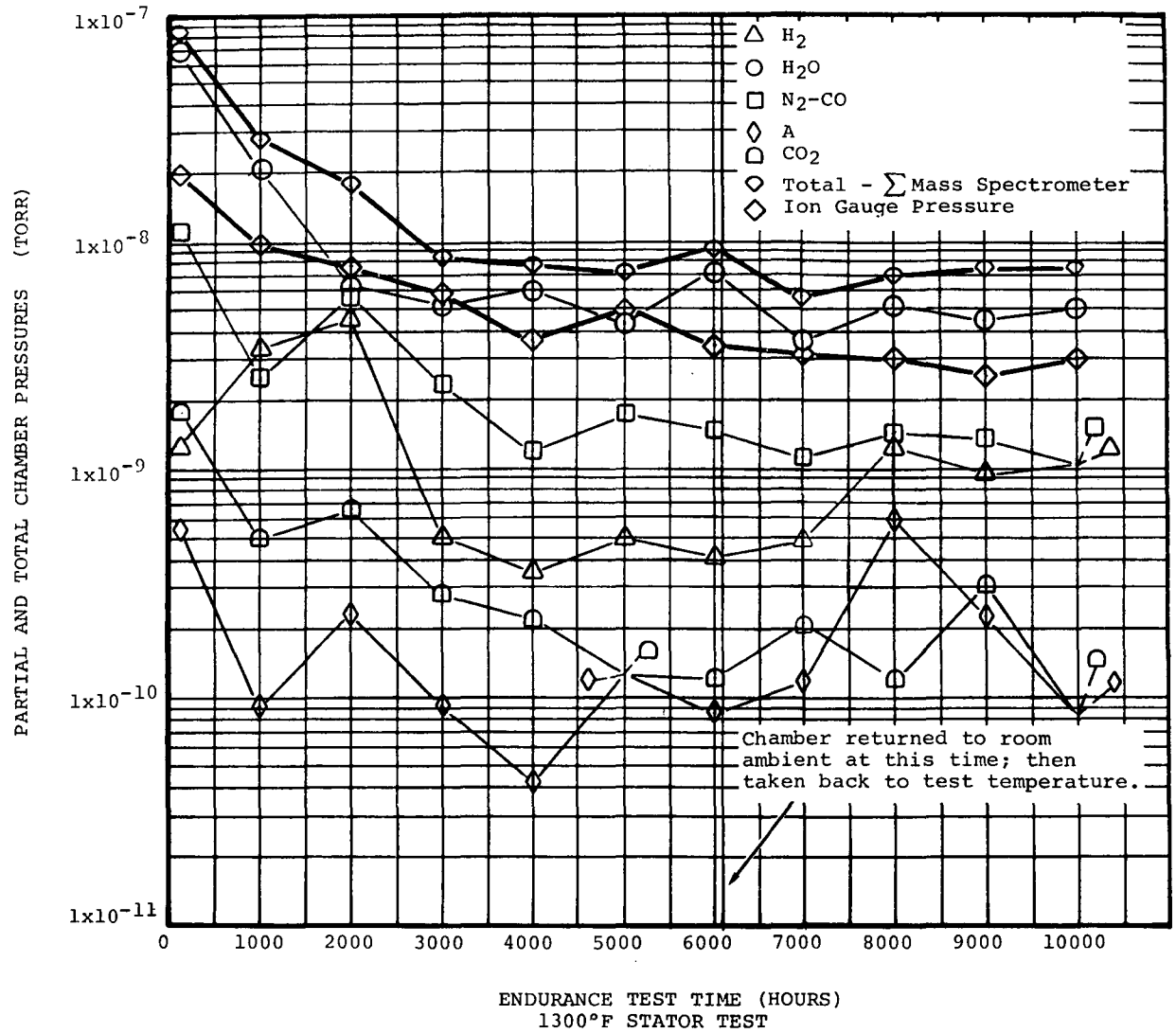

Figure 10. - Partial Pressures of Gases in the Stator Test Chamber as a Function of Test Time for the 10,000-Hour Test Period at 1300° F in Ultrahigh Vacuum.

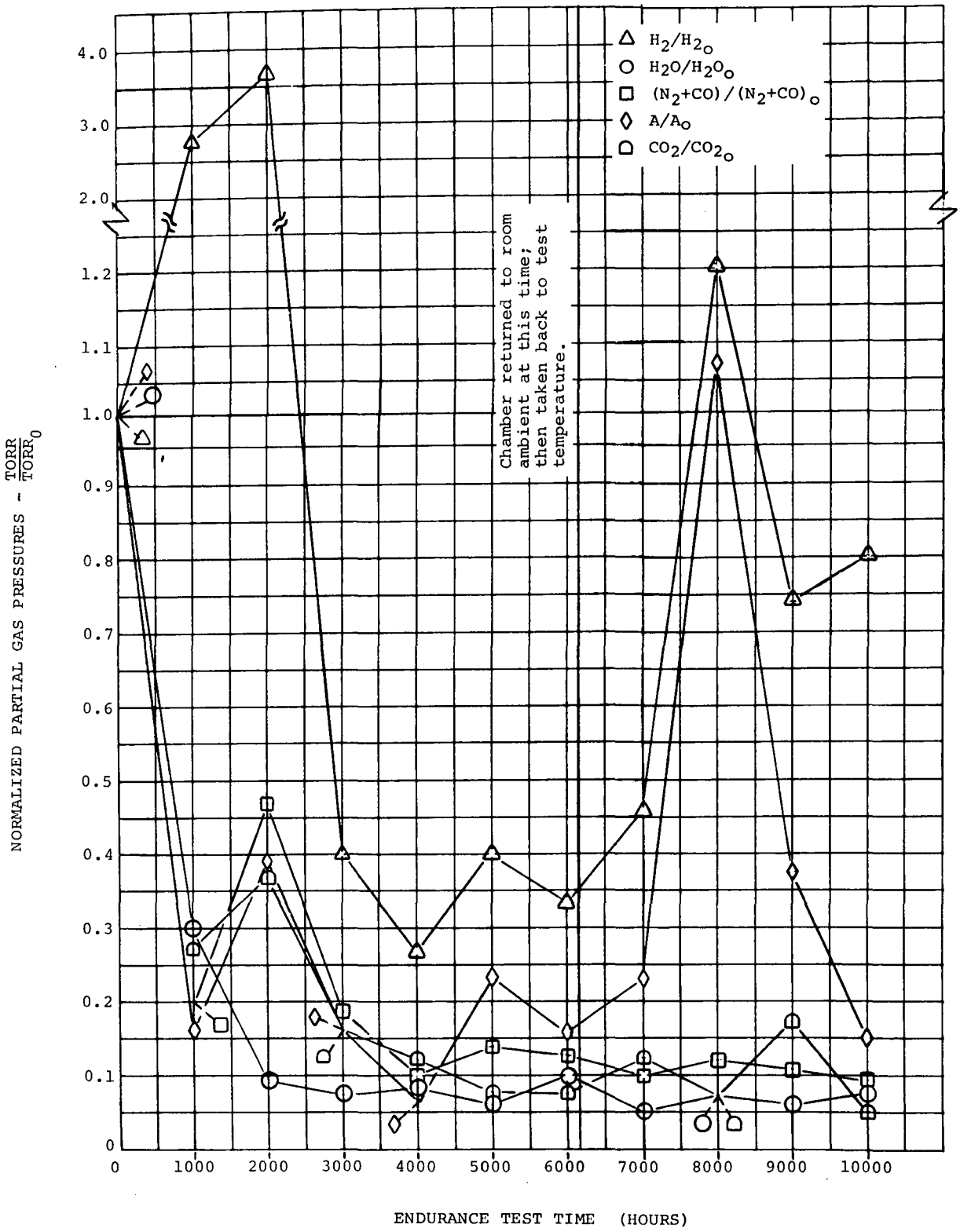

Figure 11. - Normalized Plot of Stator Test Chamber Partial Pressures of Gases as a Function of Time Analyzed Periodically During the 10,000-Hour, 1300° F Hot-Spot Ultrahigh Vacuum Endurance Test. Base Line - Zero Test Hours.

Table 2. - Stator Incipient Phase-to-Phase and Phase-to-Ground AC Breakdown Voltages at 1300° F After 10,000-Hour Endurance Test.

Phase-to-Phase	Volts AC	Phase-to-Ground	Volts AC
A-B	2000	A-Gd	2000
A-C	1750	B-Gd	1450
B-C	1300	C-Gd	1200

The test chamber temperature was reduced to room temperature in steps using heater element power to stabilize the temperature at each step. Electrical performance data were taken at each stabilized temperature. Insulation performance over the temperature range was essentially the same as that observed when temperature was increased in steps for the second 5000-hour of exposure test. Conductor resistance followed point-for-point along the curve that had been defined for increasing temperature.

After all room temperature data in vacuum had been obtained, the chamber pressure was raised to room ambient pressure using dry nitrogen as the cover gas. Figure 12 is a photograph of the top of the test chamber after removal of the chamber cover. Two groups of eight thermocouples can be identified in the picture. The three-phase winding leads are identified as A, B, and C. The stator ground wire is also indicated. Winding leads were brought through the top heat shields in rectangular alumina sleeves.

Figure 13 is a view of the chamber interior with top heat shields removed showing the stator and the bore seal capsule. Figure 14 shows the chamber with the stator and bore seal capsule removed. The general cleanliness of the test volume can be noted by the stator support post reflections on the chamber heating element. Figure 15 shows the stator and bore seal capsule on a laminar flow clean bench after removal from the chamber. Figure 16 is a photograph of the bore seal capsule and support pedestal. No evidence of potassium leakage was noted as the stator and bore seal capsule were removed from the test chamber. A stator lamination, slot wedge, and winding end turn stain pattern was evident around the capsule outside diameter. (See figure 2 for pretest appearance of the capsule.) The source of these stains was determined as part of the post-test evaluation. Figure 17 is a view into the stator stack and winding cavity. Anadur "S" conductor insulation on the winding end turns had split when the windings were initially formed. After completion of the Anadur cure cycle, the insulation was

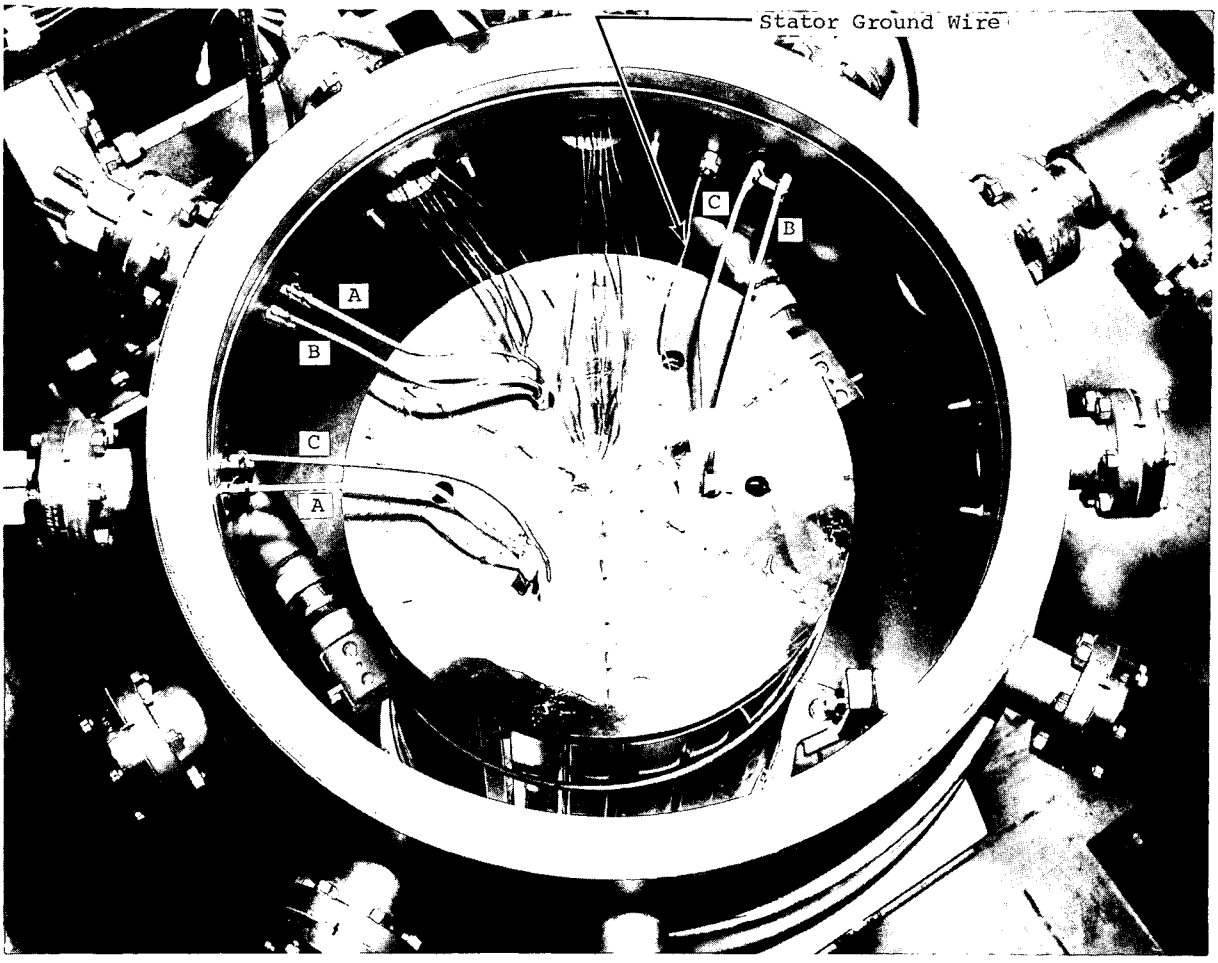

Figure 12. - Photograph of the Stator Test Chamber After 10,000-Hour, 1300° F Ultrahigh Vacuum Endurance Test With the Top Cover Removed. Phase Winding Leads are Identified.

This page is reproduced at the back of the report by a different reproduction method to provide better detail.

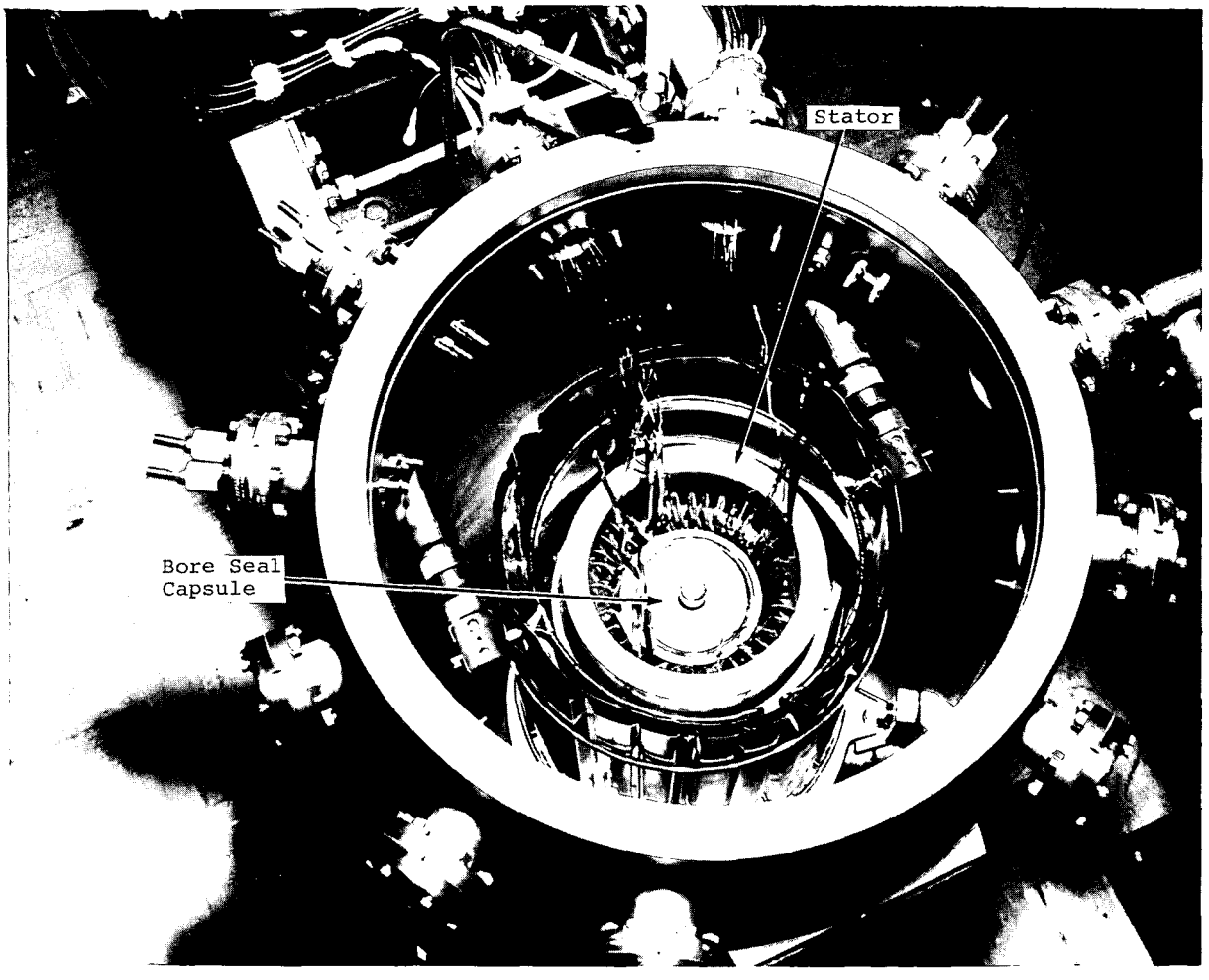

Figure 13. - Photograph of the Stator and Bore Seal Capsule in the Test Chamber After Removal of the Top Heat Shield and After the 10,000-Hour, 1300° F Ultrahigh Vacuum Endurance Test.

This page is reproduced at the back of the report by a different reproduction method to provide better detail.

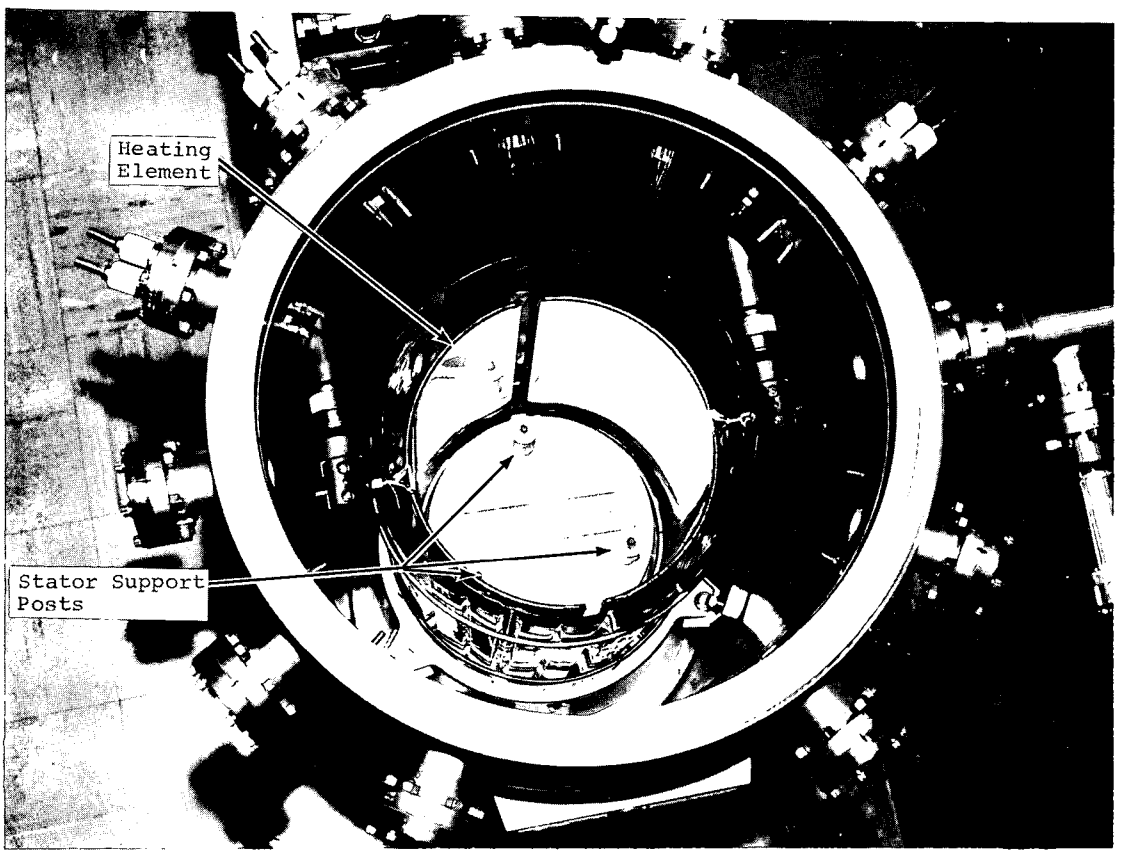

Figure 14. - Photograph of the Interior of the Test Chamber After Removal of the Stator and Bore Seal Capsule After the 10,000-Hour, 1300° F Ultrahigh Vacuum Endurance Test.

This page is reproduced at the back of the report by a different reproduction method to provide better detail.

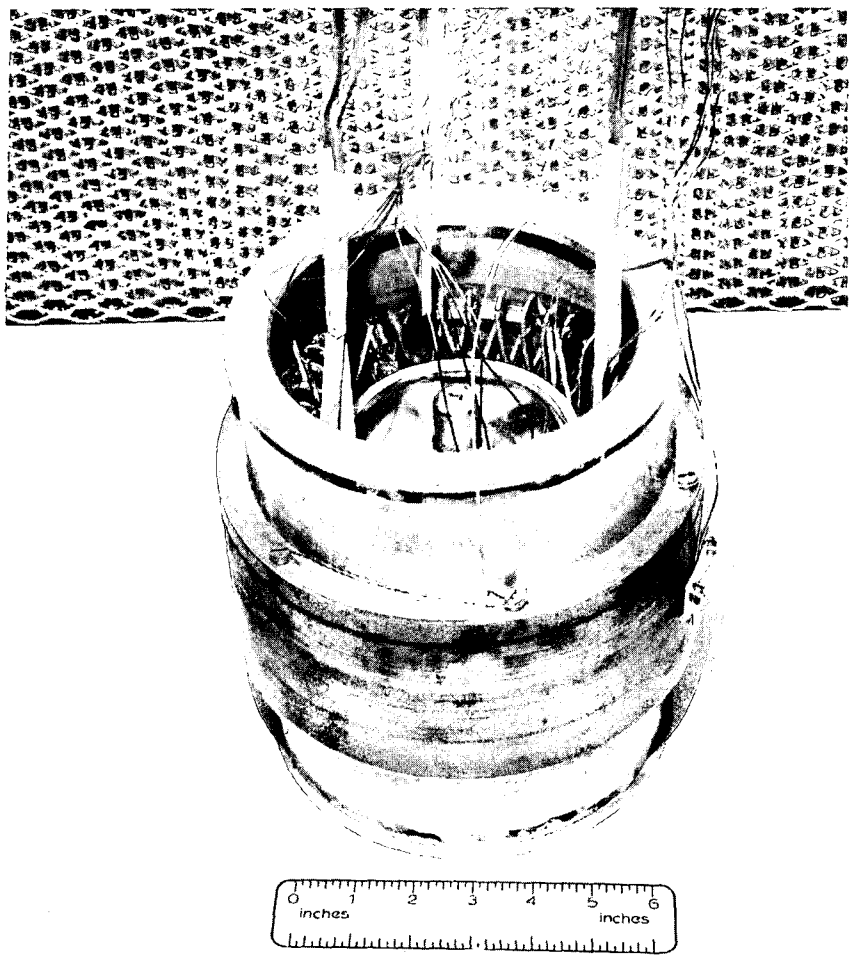

Figure 15. - Photograph of the Stator and Bore Seal Capsule After the 10,000-Hour, 1300° F Ultrahigh Vacuum Endurance Test. Refer to figure 1 and table 1 for location and identification of stator materials.

This page is reproduced at the back of the report by a different reproduction method to provide better detail.

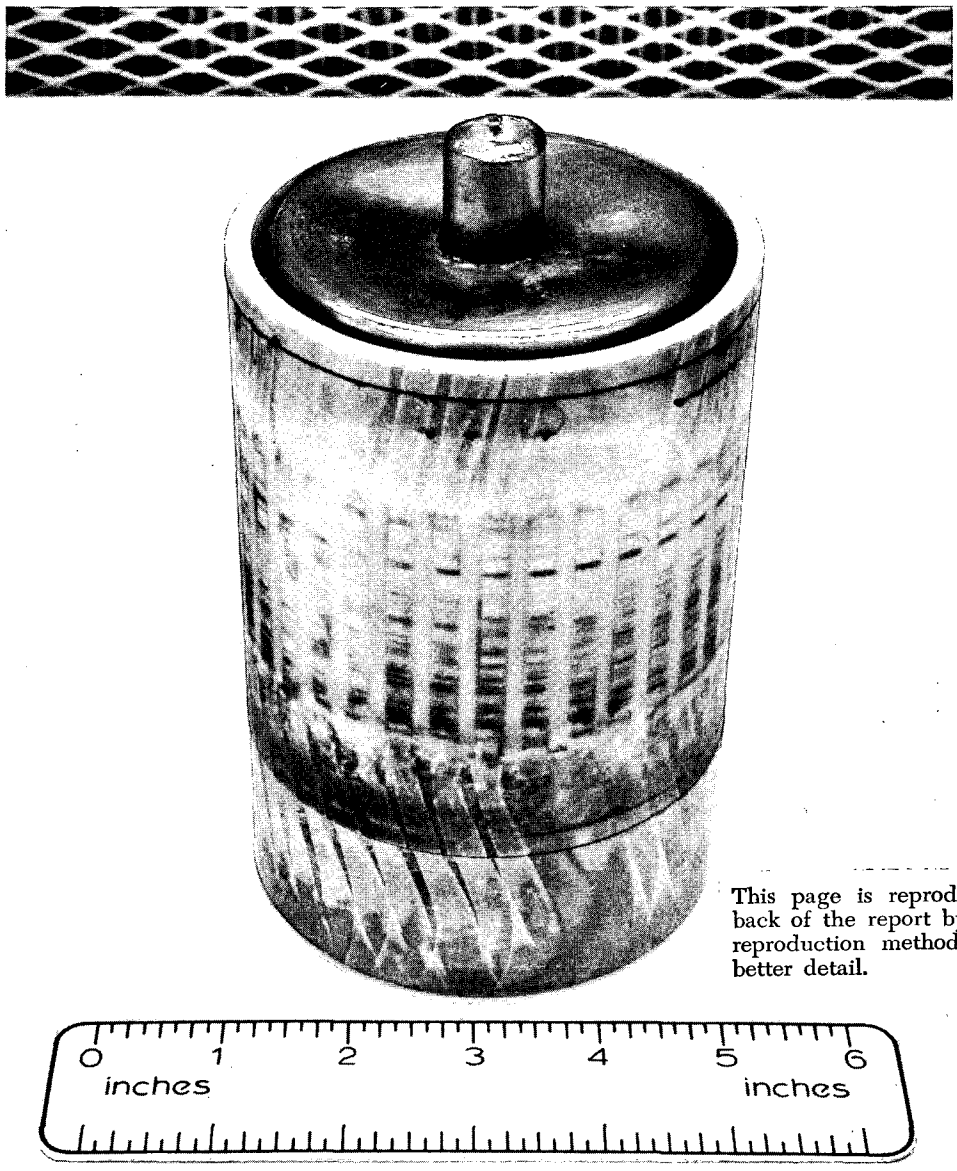

This page is reproduced at the back of the report by a different reproduction method to provide better detail.

Figure 16. - Photograph of the Bore Seal Capsule and Support Pedestal After the 10,000-Hour Potassium Exposure Test at 1300° F in Vacuum.

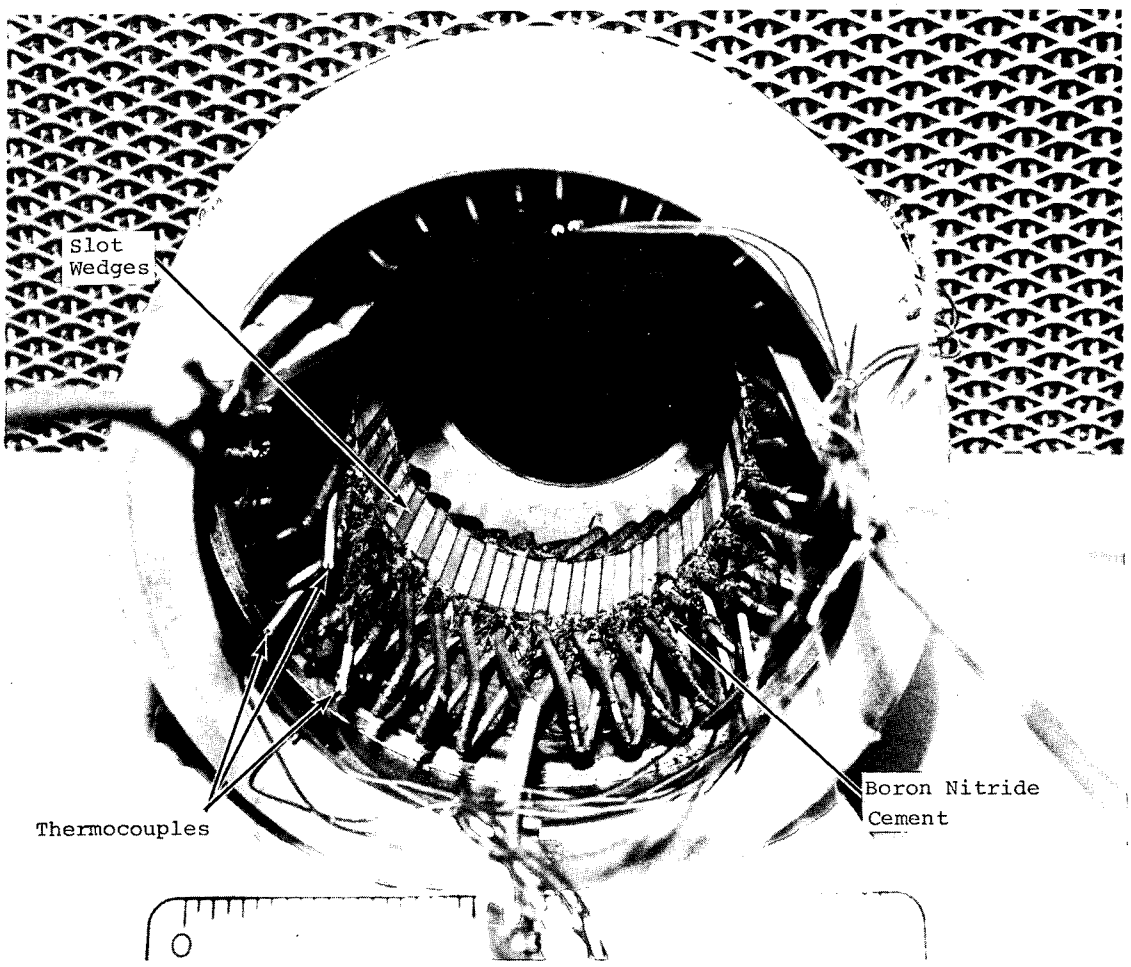

Figure 17. - Photograph of the Stator Interior After Completion of a 10,000-Hour Test at 1300° F in Vacuum.

This page is reproduced at the back of the report by a different reproduction method to provide better detail.

more brittle and some pieces had flaked off. Other pieces were dislodged during installation and removal of the bore seal capsule. The initial appearance of the cured Anadur "S" was an off-white color. The chopped boron nitride fiber cement which was used at the slot ends and the alumina wedges used in the slots were also initially an off-white color. The exposed surfaces of the insulation components were all somewhat darker, presenting a gray appearance.

After removal from the test chamber, the stator was placed on a laminar air flow clean bench and electrical performance was measured at room ambient pressure and temperature. These data are compared with pre-endurance test data in table 3. Room temperature conductor resistance in the three-phase windings did not change as a result of 10,000-hour test in vacuum (10^{-9}

Table 3. - Comparison of Stator Room Temperature Bench Test Electrical Data Taken Before and After a 10,000-Hour Endurance Test in Ultrahigh Vacuum with a 1300° F Hot-Spot Temperature.

MEASUREMENT	PHASE WINDING (a)	BEFORE ENDURANCE TEST		AFTER ENDURANCE TEST	
		OHMS	TEMPERATURE (°F)	OHMS	TEMPERATURE (°F)
Conductor Resistance	A-A	0.0140	71	0.0140	78
	B-B	0.0138	71	0.0140	78
	C-C	0.0139	71	0.0140	78
		MEGOHMS @ 500 Vdc	TEMPERATURE (°F)	MEGOHMS @ 500 Vdc	TEMPERATURE (°F)
DC Insulation Resistance	A-B	140	71	3.0×10^3	78
	A-C	155	71	3.0×10^3	78
	B-C	175	71	2.6×10^3	78
	A to Ground	6.5	71	1.1×10^3	78
	B to Ground	6.5	71	1.0×10^3	78
	C to Ground	9.0	71	1.0×10^3	78
		MICROAMPS @ 500 Vac	TEMPERATURE (°F)	MICROAMPS @ 500 Vac	TEMPERATURE (°F)
AC Leakage Current	A-B	46	71	12	78
	A-C	43	71	31	78
	B-C	56	71	27	78
	A to Ground	96	71	28	78
	B to Ground	89	71	26	78
	C to Ground	72	71	28	78

(a) Phase windings are designated A-A, B-B, C-C, A to Ground, B to Ground, and C to Ground.

torr range) at 1300° F hot-spot temperature. The pretest dc insulation resistance and ac leakage current data were taken immediately after stator assembly had been completed, and thus were not influenced by the effects of outgassing. The improved post-test performance was a result of the component outgassing which occurred at high temperature in high vacuum over a long period of time.

EVALUATION OF STATOR ELECTRICAL AND BORE SEAL CAPSULE FUNCTIONAL PERFORMANCE AFTER 10,000-HOUR, 1300° F SIMULATED SPACE ENDURANCE TESTING

Each endurance tested device was evaluated on the basis of its functional performance. These evaluations were based on comparisons of functional properties and characteristics determined before, during, and after endurance testing. The following gives evaluations of stator electrical performance and bore seal capsule functional performance.

Stator Electrical Performance

Analysis of electrical data from the stator prior to endurance testing, during endurance test, and after the endurance test shows no degradation in electrical performance. Conductor resistance did not change as a result of the endurance test. Figure 6 shows a constant conductor aging-temperature resistance to room-temperature resistance ratio for the 10,000 hours of endurance test. Table 3 shows no significant change in conductor room temperature resistance from pretest values to post-test values. Phase-to-phase and phase-to-ground insulation resistance values increased (improved) throughout the endurance test (as is shown in figure 7) and the post-test values measured in air were considerably higher than pretest values measured under similar conditions (as is shown in table 3). A second indication of insulation performance is the cnange in the ac leakage currents. Both phase-to-phase and phase-to-ground leakage currents improved throughout the endurance test (see figures 8 and 9) and were lower after the endurance test than before. (These latter measurements were made in air and are shown in table 3. The cause for improved insulation performance was component outgassing which occurred during the endurance test.

Bore Seal Capsule Functional Performance

The function of a bore seal is to isolate the environment in a motor or alternator rotor cavity from that in the stator. The functional performance of the bore seal capsule was evaluated on the basis of its ability to contain potassium without leaking during the endurance test. Bore seal capsule performance was satisfactory in that it did not leak potassium during a 10,000-hour, 1300° F endurance test.

POST 10,000-HOUR ENDURANCE TEST PROCEDURES, TESTS, EXAMINATIONS, AND ANALYSES

Following endurance testing each device was visually examined for deposits and/or discolorations; then it was disassembled and re-examined according to a previously specified plan (see appendix A). Specimens of previously specified materials were selected on the basis of their ability to contribute to the evaluation of the materials system, and were further examined, analyzed, and tested. Details of specific procedures, tests, examinations, and analyses and their results on the bore seal capsule and stator follow.

Bore Seal Capsule

Subsequent to the endurance test, the bore seal capsule was examined and processed according to the previously defined plan. Selected areas were intensively examined, tested, and analyzed. The following paragraphs describe the investigation of the bore seal capsule and results obtained.

Exterior Deposits. - After removal from the stator, the bore seal was visually examined. A deposit with the same pattern as the iron-27% cobalt alloy stator laminations was noted on the beryllia bore seal tube as well as a general darkening of the beryllia surface to a light gray color. Figure 16 shows the bore seal after removal from the stator. A band of dark gray deposits was also seen on each end of the beryllia tube.

Samples of deposits from the beryllia tube were removed and analyzed. Sample removal was performed using a diamond tipped scribe. Qualitative emission spectrochemical analyses were performed on bore seal deposit samples. Analyses of samples and their location are given in table 4.

Iron was a major constituent in all three areas with the iron-27% cobalt stator magnetic material the probable source. Nickel was common to deposits sampled at each location on the

Table 4. - Emission Spectrochemical Analysis of Deposits From the Bore Seal Capsule Exterior After 10,000 Hours Exposure in the Stator at 1300° F at a Pressure in the 10^{-9} Torr Range.

Sample	Major Constituents (>10 percent of deposit)	Minor Constituents (<10 percent of deposit)
Black Deposit - Center Periphery	Fe, Mn	Ti, B, Co, Ni, Zr, V, Cu
Light Gray Deposit - Bottom Periphery	Fe, Ni	Zr, Mo
Dark Gray Deposit - Bottom Periphery	Fe, Ni	Zr, Mn, V

bore seal capsule beryllia tube, and was a major constituent in the lower end deposits. Manganese was common to the darker deposits and was a major constituent in the darkest. Both manganese and nickel are present in the stator magnetic material in quantities of less than one percent (see table in appendix B). The transfer of manganese can be understood from vapor pressure-temperature information (ref. 7). Iron, nickel, and cobalt have vapor pressures immediately below the test operating conditions. Their presence in a bore seal capsule deposit is associated with the long term close proximity to the stator magnetic material. Titanium and vanadium, then boron, zirconium and molybdenum, have vapor pressures increasingly below endurance test operating conditions. Titanium was used in the test chamber sublimination pump. Vanadium and zirconium are constituents elements in the active metal braze. The bore seal capsule assembly end bells contain one percent zirconium. One source for molybdenum in the test chamber is in the nickel base super alloy used for the pedestal. Copper, present as a trace in the center deposit, could have come from Inconel 600 (see table in appendix B).

Potassium Unloading and Analyses. - The bore seal capsule was radiographed to determine the location of the potassium and the location of possible internal flaws. Potassium was found on the fillet at the lower end (aging position) of the bore seal capsule at the transition where the bore seal wall changes from 0.100-inch thick to 0.200-inch thick. No flaws in the columbium -1% zirconium metal, the beryllia ceramic, or the 60 percent zirconium-25 percent vanadium-15 percent columbium (60Zr-25V-15Cb) brazing material were found.

Preparation for bore seal capsule unloading began with the transfer of potassium from the lower region (aging position) to the fill tube for ease of removal. The capsule was positioned on its support pedestal (fill tube down) with the pedestal on a water-cooled heat sink (titanium sublimation pump condenser plate) in a vacuum furnace and was instrumented with thermocouples. The furnace was then evacuated, baked out, and the bore seal heated to 500° F. The chamber pressure ranged from 8.8×10^{-8} to 8.4×10^{-8} torr. During two hours at 500° F, and subsequent cooling, potassium was transported as a vapor to the fill tube where it condensed. Subsequent to removing the potassium to the fill tube, the bore seal capsule was radiographed to verify the potassium's location. Radiographs showed that the majority of the potassium had been collected in the fill tube. The bore seal was then transferred to an evacuable glove box for potassium unloading.

High purity reagents were processed in preparation for potassium unloading. A flame spectrophotometer was calibrated with standard solutions having from 10 to 500 parts per million of potassium. High purity reagents (distilled, boiled water and spectrographic grade methanol) were analyzed for potassium content using the calibrated flame spectrophotometer. No potassium was detected in either reagent (sensitivity of two parts per million).

Unloading of potassium from the bore seal capsule was accomplished in a glove box under a cover of high purity argon. The bore seal and accessories for bore seal opening and potassium removal (plastic wash bottles and plastic beakers) were subjected to two evacuation-backfill cycles in the glove box. The gas used for backfilling was high purity argon with a guaranteed minimum purity of 99.996 percent argon and maximum oxygen and moisture contents of 7 and 15 parts per million, respectively.

Bore seal capsule opening was accomplished using a clean tubing cutter. The majority of the potassium was removed either with the cut-off portion of the fill-tube or was scraped from the fill-tube with a clean, stainless steel spatula. Potassium was observed to have a clean specular appearance. The remainder of the potassium was removed from the bore seal capsule interior by reacting it with reagents. Several methanol rinses were performed before the first methanol was analyzed by flame spectrophotometer for potassium. The first analysis indicated a potassium content of 60 parts per million. A second analysis, after more rinsing, indicated 22 parts per million of potassium in the methanol. After further rinsing, no potassium could be detected in the rinse methanol (i.e., the potassium content was substantially less than 5 parts per million). Distilled water was used in a second series of rinses with the final rinse analyzed. No detectable potassium remained in the bore seal capsule.

Potassium from the bore seal capsule was processed in preparation for chemical analysis. Previously analyzed high purity potassium chloride was also processed as a standard so that impurities resulting from processing could be determined. A solution was made using approximately 7.5 grams of the high purity potassium chloride and the same quantities of water and methanol that had been used in unloading the bore seal capsule. The standard solution and that from the bore seal were evaporated from plastic beakers (in a ventilated hood and heated in a water-filled double boiler) until a volume of approximately 100 milliliters remained. Seven drops of phenolphthalein (a pH indicator) were added to each solution. The bore seal solution was then brought to a neutral pH using a 10 percent solution of spectrographic grade hydrochloric acid and distilled water. The bore seal solution was then made acidic by the addition of one-third milliliter of hydrochloric acid. (The effect of the addition of hydrochloric acid to the bore seal solution was to make a potassium chloride solution from the water plus potassium methylate solution.) An amount of hydrochloric acid solution, equal to that added to the bore seal solution, was also added to the standard potassium chloride solution. Both solutions were then evaporated to salts and the salts dried in air at 230° F.

Table 5 gives the results of spectrographic analyses for metallic impurities in the starting potassium and the processed bore seal potassium as well as those for the starting potassium chloride and the processed potassium chloride. The calculated net potassium impurity increase is based on the total impurity content less the starting material content and the impurity pick-up due to processing (as indicated in impurity difference between base potassium chloride and processed potassium chloride).

Table 5. - Metallic Impurities, By Spectrographic Analysis, of 10,000-Hour, 1300° F Exposed Bore Seal Capsule Potassium and Process Control Potassium Chlorides.

Impurity (parts per million by weight = micrograms of element per gram of potassium ±30 percent relative based on potassium)

Element	Potassium as Loaded in Bore Seal[a]	Base Potassium Chloride[b]	Processed Potassium Chloride[b]	Bore Seal Potassium After Exposure and Processing[b]	Calculated Bore Seal Potassium Impurity Increase After 10,000-Hour Exposure
Ag	1	<0.5[e]	<0.5[e]	<0.5[e]	<0.5[e]
Al	3	9	30	150	117
B	<5	<0.5[e]	0.5	2.6	2.1
Ba	<3	(f)	(f)	(f)	(f)
Be[c]	<1	<0.5[e]	<0.5[e]	22	22
Bi	(f)	<5[e]	<5[e]	<5[e]	<5[e]
Ca	4	10	125	190	61[d]
Cb	(f)	<10[e]	<10[e]	21	21
Cd	(f)	<50[e]	<50[e]	<50[e]	<50[e]
Co	<5	<10[e]	<10[e]	<10[e]	<10[e]
Cr	<1	<20	<20	<20	<20
Cu	<1	6	21	58	37
Fe	5	4	81	92	6
Ge	(f)	<20[e]	<20[e]	<20[e]	<20[e]
In	(f)	<20[e]	<20[e]	<20[e]	<20[e]
Mg[d]	<1	<2[e]	20	27	7
Mn	<1	<0.5[e]	3.8	7.2	3.4
Mo	<5	<2[e]	<2[e]	<2[e]	<2[e]
Na	3	(f)	(f)	(f)	(f)
Ni	<1	<5[e]	6	19	13
Pb	<1	<10[e]	17	16	<10
Pt	(f)	<20[e]	<20[e]	440	440
Rh	(f)	<5[e]	<5[e]	950	950
Si	10	<6	19	41	12
Sn	<1	<6[e]	<6	7	7
Sr	<1	<0.5[e]	<0.5[e]	<0.5[e]	<0.5[e]
Ti	<5	<3[e]	4	3	<3
V[c]	<1	<2[e]	<2[e]	<2[e]	<2[e]
Zr[c]	<10	<5[e]	<5[e]	<5[e]	<5[e]

(a) Batch analyses supplied by Mine Safety Applied Research, Evans City, Pa.
(b) Spectrographic analyses by Westinghouse Power Systems, Waltz Mill Site, Madison, Pa.
(c) These are the major elements specified for analysis.
(d) The indicated quantities of these elements are not considered to be significant.
(e) < means less than, and indicates the limit of detection for the element, or a limit due to contamination.
(f) Not determined.

There was no increase in vanadium or zirconium level in the bore seal capsule potassium. Both beryllium and columbium levels in the bore seal potassium had increased approximately 20 parts per million (approximately 80 micrograms of each) as a result of the 10,000-hour 1300° F exposure. Bore seal capsule beryllia was the probable source of beryllium. During the active metal brazing process, beryllia at the braze alloy-beryllia interface was reduced to the metal which has a relatively high vapor pressure. Beryllium may have then been deposited on the inside of the bore seal capsule and subsequently dissolved in the potassium. Columbium was present in both the columbium-1% zirconium end members and in the 60Zr-25V-15Cb braze alloy. The absence of an increase of either vanadium or zirconium in bore seal capsule potassium indicates that the probable source of columbium in the potassium was the columbium-1% zirconium end member material. Platinum and rhodium contaminations in the bore seal potassium were possibly from the platinum - platinum-10% rhodium thermocouples used inside the capsule during active metal brazing at 2462° F at a pressure in the 10^{-6} torr range. Minor metallic impurities in the potassium (copper, manganese aluminum, nickel, iron, and calcium) were present as metal oxides in the beryllia tube (see table C-1, ref. 6). It is likely that these minor impurities either: (1) reacted directly with thermodynamically less stable oxides in the ceramic, or (2) reacted with metals reduced from metal oxides as a result of active metal brazing. Tin (and Cu, Mn, Al, Ni, and Fe) were trace impurities in the columbium-1% zirconium (see table C-2, ref. 6).

Determination of the Flexural Strength of Bore Seal Capsule Beryllia. - After potassium unloading, the bore seal capsule and the cut-off portion of the fill-tube were dried overnight at 230° F in a circulating air furnace and then weighed. The difference in weights between before and after potassium loading was 3.9 grams, with all weights determined on the same calibrated balance.[7] Radiographs were again taken and examined to determine if any flaw, possibly hidden previously by potassium, could be found in the bore seal capsule. No flaws were found.

The bore seal capsule and a vacuum furnace were then prepared for bore seal clean firing. The bore seal was positioned on its support pedestal and instrumented with a sheathed thermocouple attached to the exterior of the bore seal capsule beryllia tube. After evacuating and baking the vacuum chamber, the bore seal capsule was heated. Clean firing was accomplished at

[7]The calibrated balance was a Model P-1200 Mettler balance.

1832° F, twenty minutes at temperature, and at a chamber pressure of 2×10^{-7} torr. The purpose of clean firing was to remove any remaining traces of moisture and/or potassium hydroxide.

Visual and microscopic examinations performed on the clean fired bore seal capsule revealed that both the basic beryllia and its deposits had a lighter color than before clean firing. The bore seal capsule was subsequently secured in a plastic bag to maintain cleanliness.

The bore seal capsule was sectioned in a facility equipped for cutting beryllia[8]. A longitudinal plane was specified and the bore seal capsule was cut into two sections using a diamond cut-off wheel. Two ceramic-to-metal brazed joint specimens were selected, one each from the top and bottom brazements, and were removed from one bore seal capsule section. Each brazed joint specimen was mounted in a metallurgical mount and a specified surface was prepared for microscopic examinations, electron microprobe analyses, and microhardness determinations.

An area in the bore seal capsule was selected for obtaining the beryllia modulus-of-rupture bars. This area was within the 0.100-inch-thick wall region, with the specimen axes parallel to the beryllia tube's axis. Figure 18 shows the location and numbering sequence of these specimens. Specimen removal was accomplished by using a diamond wheel. Rough cut specimens were diamond-ground to give the square section shown in figure 19. The 0.95-inch dimension was selected to remove the radii of curvature from the bore seal capsule inside and outside surfaces. A bevel was ground on the end of each bar to indicate the inside (toward the potassium exposed) surface.

Flexural strengths were determined on each beryllia modulus-of-rupture bar. A four-point-loading fixture having the same dimensions as was used in a previous program (ref. 6) was used here. Modulus-of-rupture bars were divided into three groups for tests. One group had the side toward the potassium (inside of the beryllia bore seal) in compression and consisted of specimens numbered 1, 4, 7, 10, and 13. A second group of modulus-of-rupture specimens had the side toward the potassium in tension and consisted of specimens 2, 5, 8, 11, and 14. The remaining group of specimens had the bore seal capsule cross-section in compression and consisted of specimens 3, 6, 9, 12, and 15. Table 6 gives individual and average flexural strength values, as well as standard deviations and coefficients of variation, for bore seal capsule specimens both aged and unaged.

---

[8]EIMAC Division of Varian Associates, 201 Industrial Way, San Carlos, California.

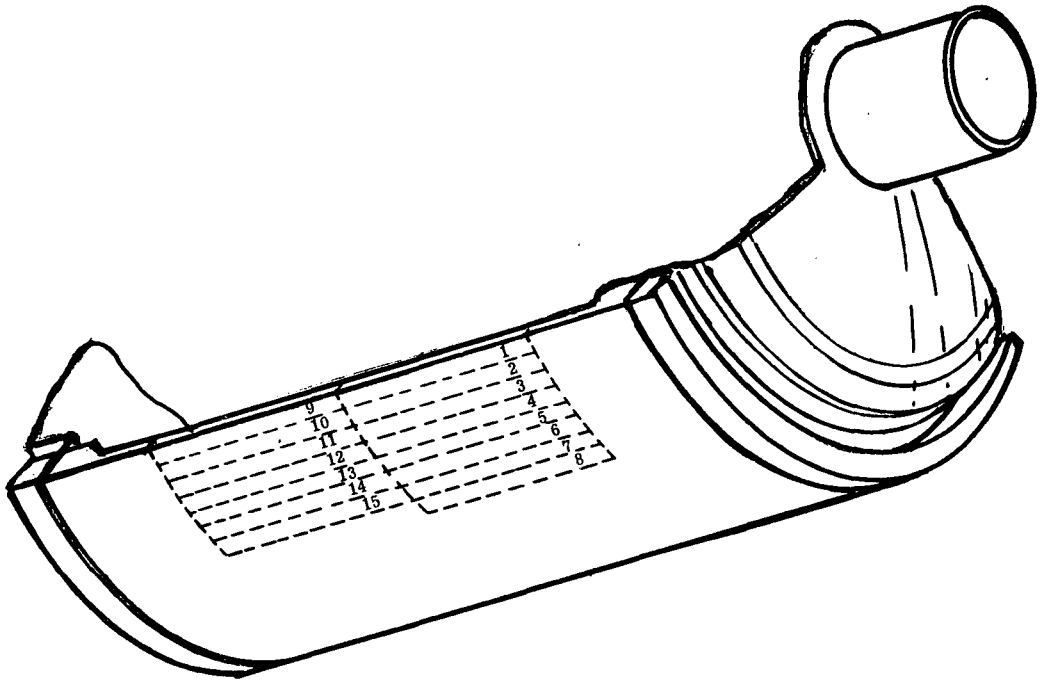

Figure 18. - Sketch of Beryllia Bore Seal Capsule Assembly Section Showing the Location of Modulus-of-Rupture Specimens.

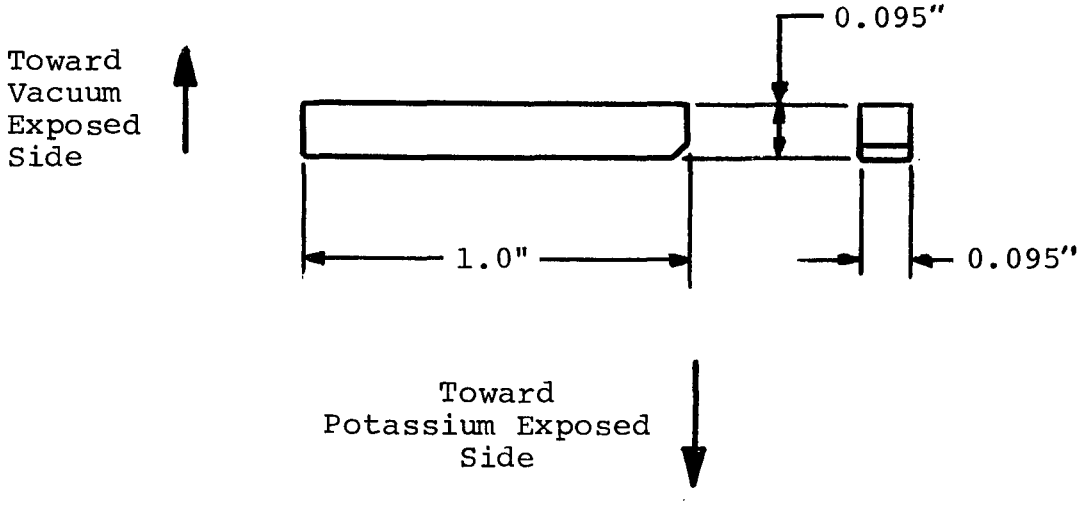

Figure 19. - Beryllia Modulus-of-Rupture Specimen After Cutting and Grinding.

Table 6. - Flexural Strength of 99.8 Percent Beryllia[a] Bore Seal Ceramic Specimens Before and After Aging in Potassium at 1300° F for 10,000 Hours.

Specimen Type	Specimen No.	Flexural Strength (psi)	Standard Deviation (psi)	Coefficient of Variation[c]
Potassium Side in Compression (vacuum side in tension) Aged Bore Seal	1 4 7 10 13 Arithmetic Mean	30,800 22,100 23,500 23,800 23,800 25,000	3,250	13.0
Potassium Side in Tension (vacuum side in compression) Aged Bore Seal	2 5 8 11 14 Arithmetic Mean	20,800 26,300 22,400 26,300 18,300 22,800	3,500	15.4
Cross Section in Compression-Aged Bore Seal	3 6 9 12 15 Arithmetic Mean	26,400 23,400 25,300 25,000 25,000 25,000	1,080	4.3
For Comparison Inside or Outside Surface in Compression-Unaged Bore Seal	Arithmetic Mean of 5 Specimens	24,700[b]	3,400[b]	13.8
Cross Section in Compression-Unaged Bore Seal	Arithmetic Mean of 5 Specimens	24,800[a]	2,700[b]	10.99

(a) Thermalox 998 supplied by the Brush Beryllium Company, Elmore, Ohio
(b) From work on NASA Contract NAS3-6465 (Reference 4)
(c) Coefficient of Variation = $\frac{s}{\bar{x}}$ = $\frac{\text{Standard Deviation}}{\text{Arithmetic Mean}}$

There are no significant differences in average flexural strength values among the aged groups, thereby indicating no penetrating effects due to either vacuum or potassium exposure. There are no significant differences in average flexural strength values between any of the aged specimens and unaged specimens, thus indicating no effect due to aging at 1300° F for 10,000-hours.

Interior Deposits. - After the bore seal capsule was sectioned, deposits were observed on the ceramic interior. The interior of one half of the bore seal capsule is shown in figure 20. A definite line of deposits may be seen around the interior circumference at approximately the same level as the top of the previously discussed condensed potassium fillet. A general cover of light deposits may be seen on other beryllia areas with pattern of heavier deposits in some areas. These deposits all exhibited a metallic appearance. Qualitative spectrographic analyses were performed on both these deposits and the clean beryllia substrate. Platinum was the major element in the deposit. No platinum was found in the clean substrate beryllia. Rhodium was specifically looked for but was not found in the deposit on the bore seal interior. The solubility limit of platinum in potassium may have been reached during cooling and condensation when the bore seal capsule was cooled from the 1300° F exposure temperature, thus causing excess platinum to deposit on the capsule wall. (The heaviest deposit appeared at the top of the condensed potassium fillet.) Rhodium, the predominant impurity element in bore seal capsule potassium (see table 5) apparently was not present to the limit of solubility. The suggested source for platinum and rhodium is from a section of platinum - platinum-10% rhodium thermocouple, possibly remaining in the capsule after brazing or clean firing.

Analyses of Bore Seal Capsule Ceramic-to-Metal Brazed Joints. - Two previously mentioned bore seal capsule brazed joint specimens were scanned by an electron microprobe.[9] Specimens were longitudinal cross sections from opposite ends of the capsule and each contained columbium-1% zirconium from an end bell brazed with a 60Zr-25V-15Cb alloy to 99.8 percent beryllia (molybdenum metallized) from the capsule tube on one side and to 99.8 percent beryllia from a back-up ring on the other side. Scans for vanadium, columbium, and zirconium, were made across the potassium side and the vacuum side seals of

[9]The analysis was performed using the Materials Analysis Company Model 400 microprobe located at the Analytical Techniques Section of the Westinghouse Lamp Division, Bloomfield, N.J.

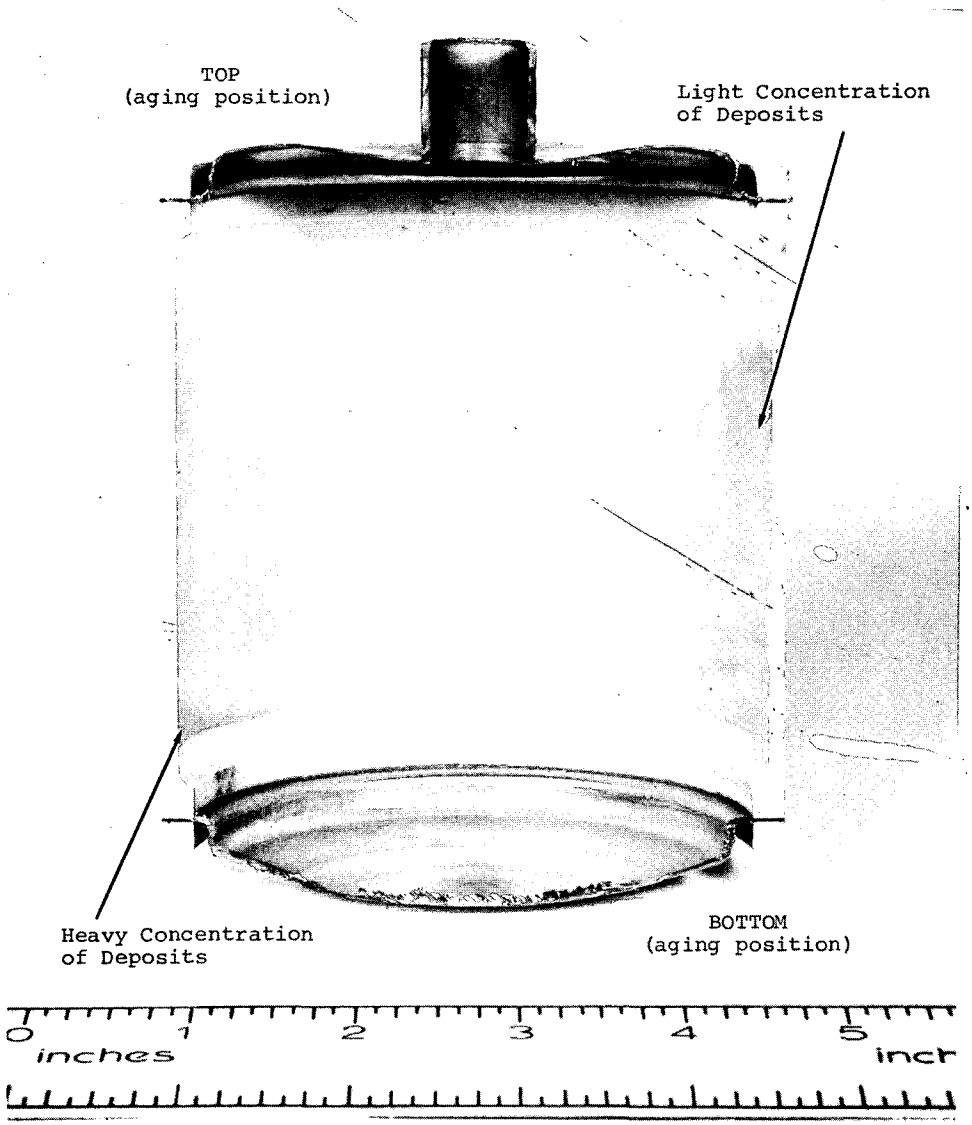

Figure 20. - Beryllia Bore Seal Capsule Interior After 10,000-Hour, 1300° F Potassium Vapor Exposure.

This page is reproduced at the back of the report by a different reproduction method to provide better detail.

both the top and bottom specimens as shown in figures 21 and 22. Scan directions are marked and the various interfaces are identified. Additional scans were made in selected areas for potassium and molybdenum. Electron microprobe scans were obtained by driving the sample at 10 microns/minute under the electron beam (30-kV, 0.025 microamperes specimen current) and recording the x-ray output on a chart recorder.

X-ray counting rates for pure element standards were determined before and after each elemental scan. Counts were accumulated for five 100-second intervals for each element of interest. Each interval was taken on a fresh spot on the standard. Background counts were obtained in a similar manner. For the background, the spectrometer setting was changed a fixed amount above and below the spectral peak and the count rates averaged. Using the recorder charts to obtain count rates allowed shifting of one elemental scan relative to the other in order to compensate for slight changes in starting points. (If counts had been obtained by counting at fixed positions across the braze, proper alignment of starting points would not have been possible.) Therefore, to insure accuracy of alignment, count rates were read directly from the calibrated chart recorder at five micron intervals. Data was accumulated in this manner for zirconium, columbium, and vanadium,

An oxygen Kα x-ray signal, generated by a 7-kV electron beam and 0.5 microampere specimen current, was obtained by using the beryllia as a standard. Counts were taken far from the braze area, i.e., toward the center of the beryllia. These standard counts were compared with the oxygen count rate from the braze areas. For one particular point analyzed in the braze area, the oxygen content was approximately six weight percent. A qualitative scan in that area indicated contents both above and below the six weight percent level.

In a search for potassium, potassium bromide was used to provide a standard potassium Kα x-ray signal. Spot checks were made throughout all four brazes (potassium and vacuum-exposed sides of the top and bottom brazed joints), in the columbium-1% zirconium, and in the beryllia. Detectability limits were calculated by taking the standard assumption that a signal 20 percent above background would be distinguishable. The same criterion was used for all other elements. The potassium detectability limit was approximately 300 part-per-million (0.03%). No potassium above background was detected anywhere in any of the braze alloy, in the columbium-1% zirconium, or in the beryllia.

Molybdenum was detected at about the 0.3 percent to 0.4 percent level at the interfaces between the beryllia and the

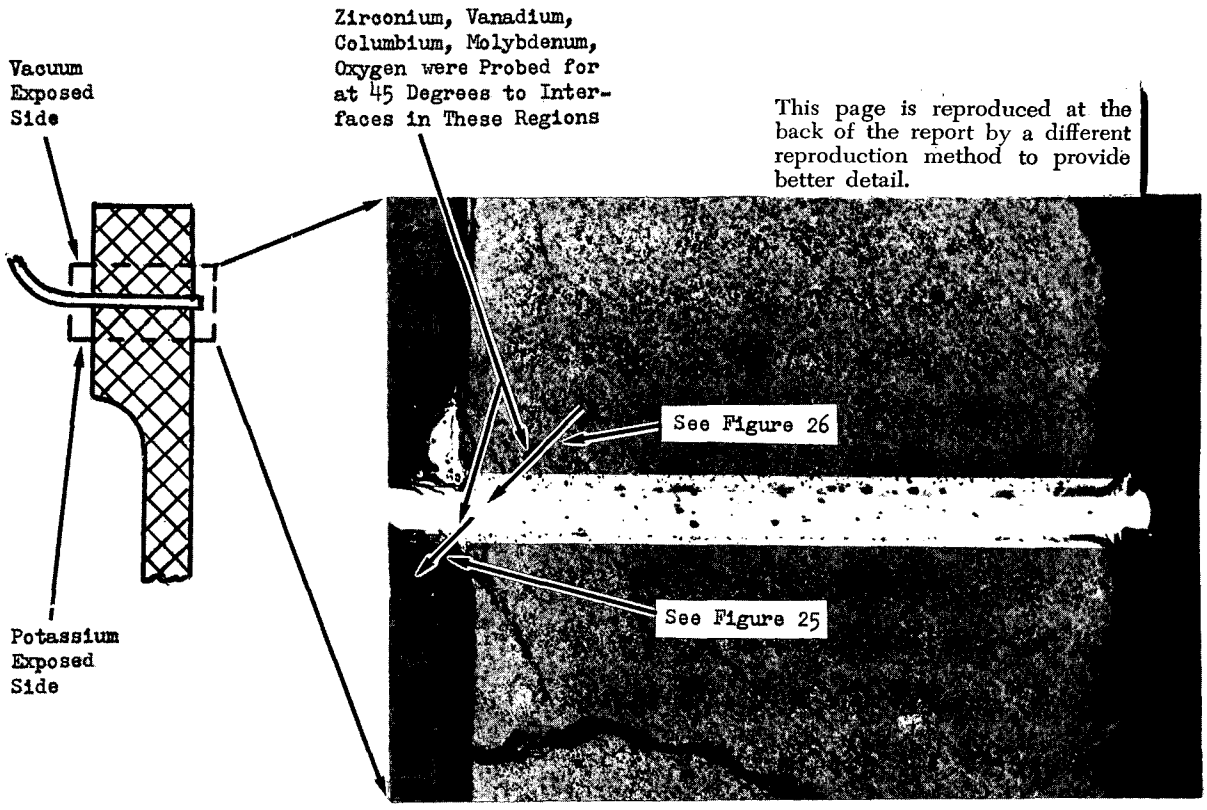

Figure 21. - Photograph Showing Cross Sections of Brazed Joints From Top of 4-Inch Diameter by 4-Inch High Bore Seal Capsule After Exposure to Potassium at 1300° F For 10,000 Hours. (16X)

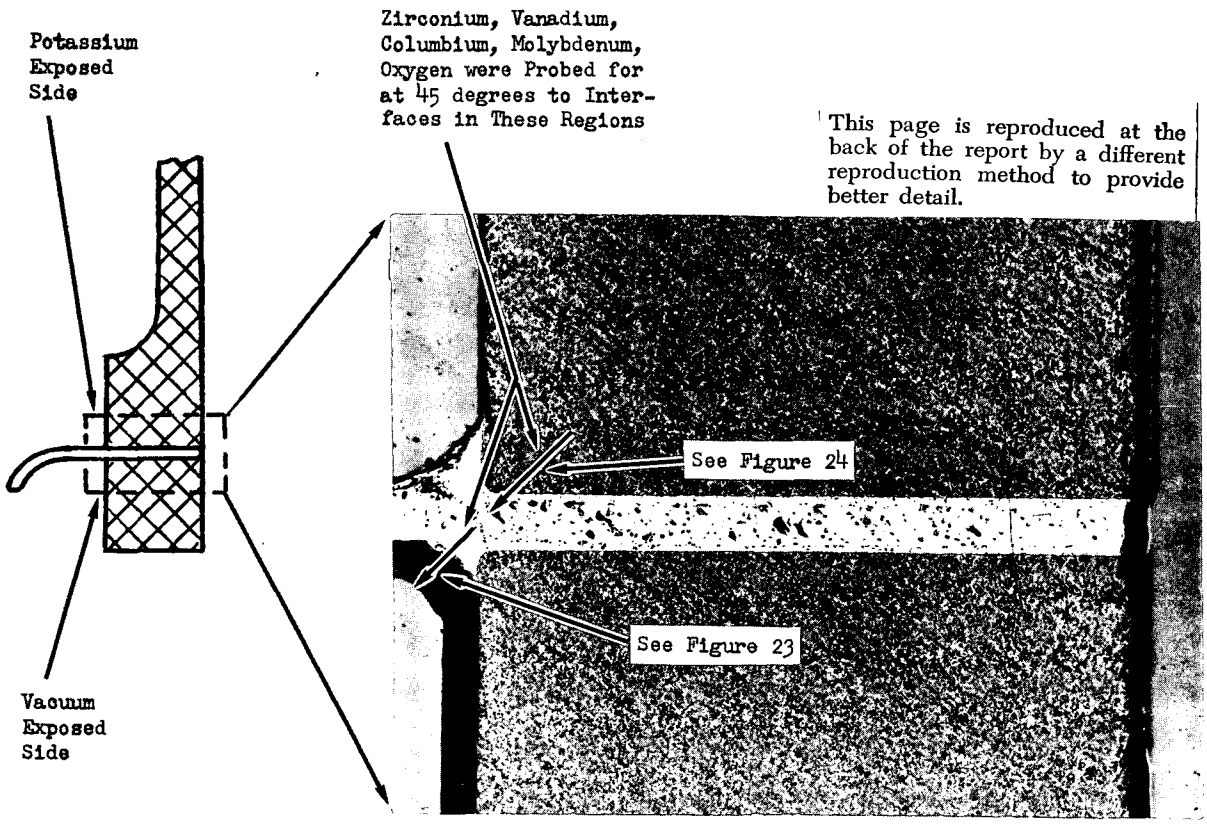

Figure 22. - Photomicrograph Showing Cross Sections of Brazed Joints From Bottom of 4-Inch Diameter by 4-Inch High Bore Seal Capsule After Exposure to Potassium at 1300° F For 10,000 Hours. (16X)

braze alloy. The detectable limit was approximately 0.1 percent. The molybdenum signal reached background as the scan left the vicinity of the beryllia and entered further into the braze alloy. Molybdenum had been vapor deposited on the beryllia (as an aid to wetting) prior to brazing. The minute amount of the molybdenum in the areas near the beryllia was ignored when calculating total braze constituents.

Oxygen was detected in most areas of the braze alloy; although in some areas it was very low. The detectable limit for oxygen using the beryllia standard was approximately 0.75 percent to 1.0 percent. It should be emphasized that there is most likely some beryllium included in the oxygen plot. Past experience with seals of this type indicates that some of the beryllium ions will diffuse into the braze area during brazing. The oxygen (plus beryllium) content was calculated by difference with a maximum set at 10 weight percent. The results of electron microprobe analyses for oxygen along with those for zirconium, columbium, and vanadium are shown in figures 23, 24, 25, and 26.

Examination of figures 23, 24, 25, and 26 reveals that the braze alloy joints are not very homogeneous and that each joint structure is somewhat different. The bottom braze alloy structures appear to be less homogeneous than the top braze alloy structures. Most homogeneous of the probed joints is the potassium side of the top seal (figure 25). (It should be noted that this probe trace began in the columbium-1% zirconium end member, crossed a fillet of braze alloy, and terminated at the edge of the fillet.) The probe trace for the other side of the top seal (figure 26) shows this braze alloy to be less homogeneous. Columbium from the columbium-1% zirconium end member appears to have diffused into the braze alloy during the brazing cycle. (This probe trace began in the beryllia, traversed the braze alloy, and terminated in the columbium-1% zirconium.) Comparing figure 24 with figure 26 one can see that the figure 24 braze alloy is much less homogeneous, has narrower zirconium-rich regions, and has substantially more columbium. The columbium content in figure 24 braze changed from 65 percent to 15 percent in ten microns. It appears that the zirconium precipitated, leaving a matrix rich in columbium and vanadium. The figure 24 braze alloy is approximately half the thickness of the figure 26 braze alloy. Figure 23 shows a braze alloy fillet on the other side of the figure 24 brazement. This fillet is less homogeneous than the fillet in figure 25 but more homogeneous than the braze alloy in figure 24. The columbium content in the figure 23 braze alloy is not as high as that in the figure 24 braze alloy. In the top seal braze alloys (figures 25 and 26), the vanadium and columbium seem to be related in that

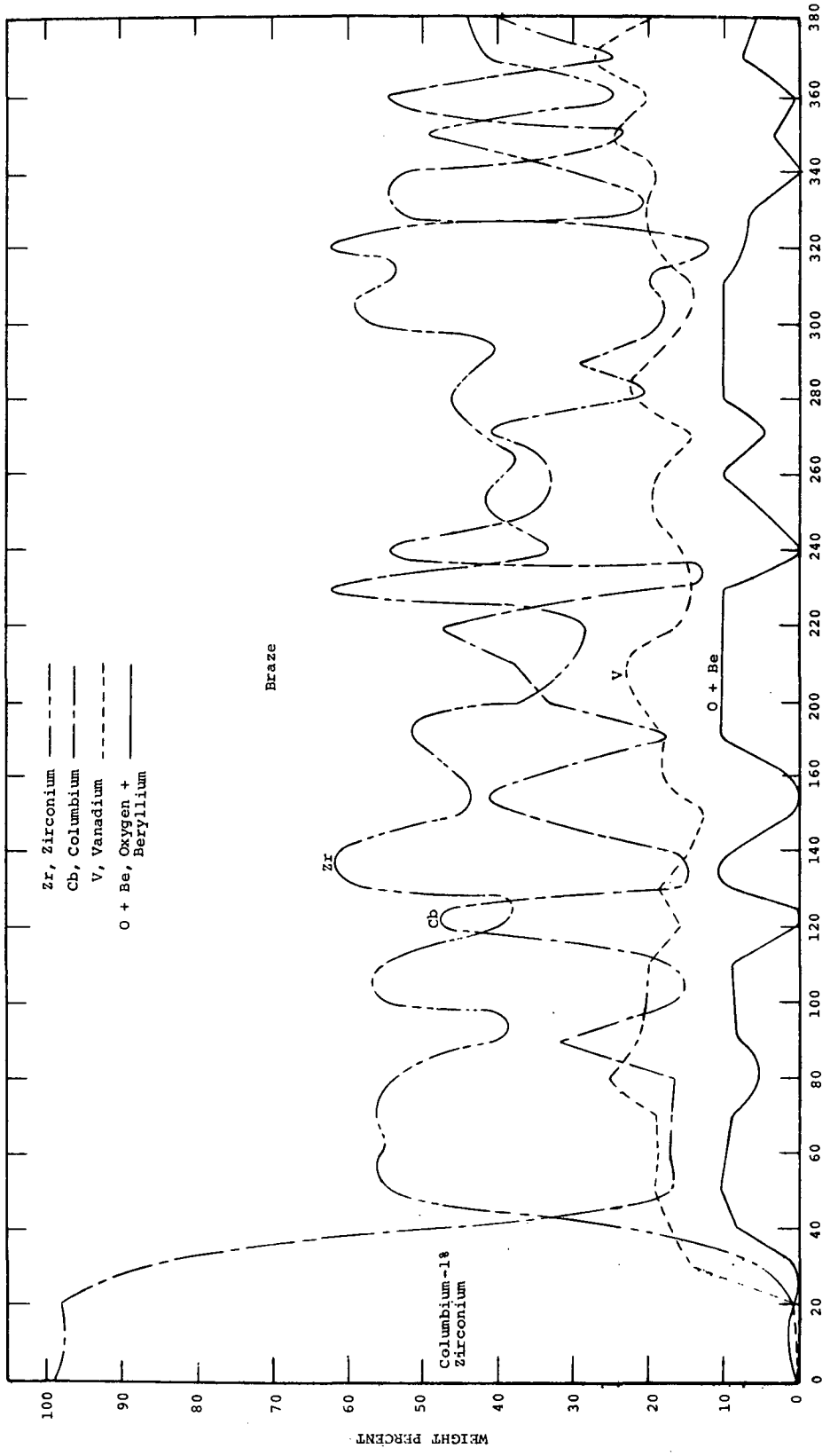

Figure 23. - Electron Microprobe Analyses Across Potassium Exposed Side of Aged (10,000 Hours at 1300° F) Bore Seal Capsule (Columbium-1% Zirconium and 60Zr-25V-15Cb Braze Alloy) Bottom Seal.

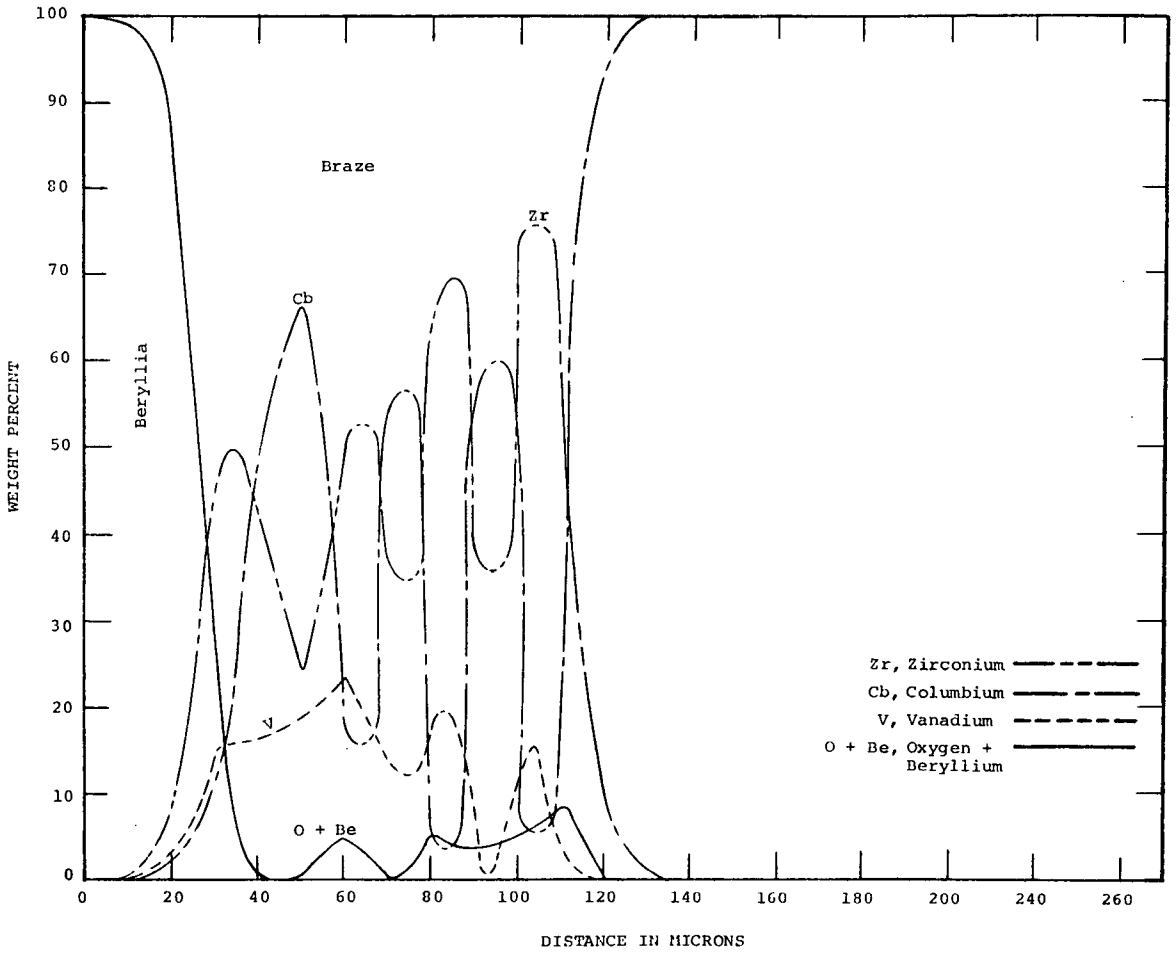

Figure 24. - Electron Microprobe Analyses Across Vacuum Exposed Side of Aged (10,000 Hours at 1300° F) Bore Seal Capsule (Beryllia, 60Zr-25V-12Cb Braze Alloy, and Columbium-1% Zirconium) Bottom Seal.

both constituents increase and decrease in roughly the same places. This trend does not seem to be as evident in the bottom seal braze alloys (figures 23 and 24).

The probably cause for differences in brazed joint structures is differences in brazing time-temperature relationships for each joint. The generally less homogeneous bottom braze alloy structures (with relatively more columbium present) suggest either high temperature, longer time at temperature, or both, when compared with the top brazes. The relatively lower uniform aging temperature (1300° F), when compared with the apparently non-uniform brazing temperature (in the order of 2500° F), suggests that the brazing cycle established the brazed joint structures, not aging.

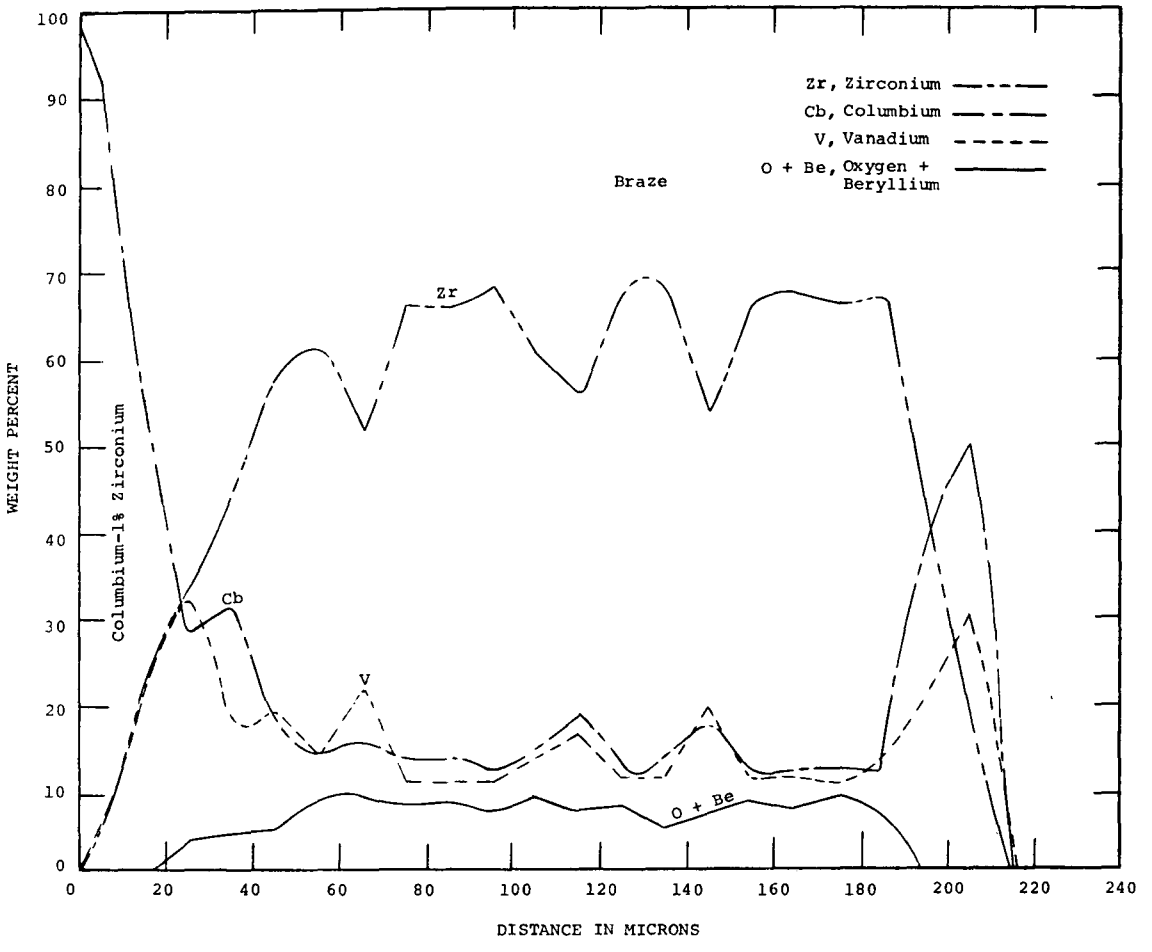

Figure 25. - Electron Microprobe Analyses Across Potassium Exposed Side of Aged (10,000 Hours at 1300° F) Bore Seal Capsule (Columbium-1% Zirconium and 60Zr-25V-15Cb Braze Alloy) Top Seal.

Microscopic Examinations of Brazed Joints. - Microstructures of bore seal capsule brazed joints were compared with each other and with those of unaged (as-brazed) specimens shown in reference 6, figure 40. Identification of phases is difficult since there are probably quaternary and ternary as well as binary structures present. One structure with probable identification, shown in figure 27 with bright field illumination and in figure 28 with dark field illumination, is in the braze alloy adjacent to the beryllia. Dark field and polarized illumination shows the structure to be of an intermetallic type, not an oxide. Electron microprobe analyses show high zirconium content in the braze alloy near the beryllia. The beryllium-zirconium phase diagram (ref. 8) shows an intermetallic, $ZrBe_2$,

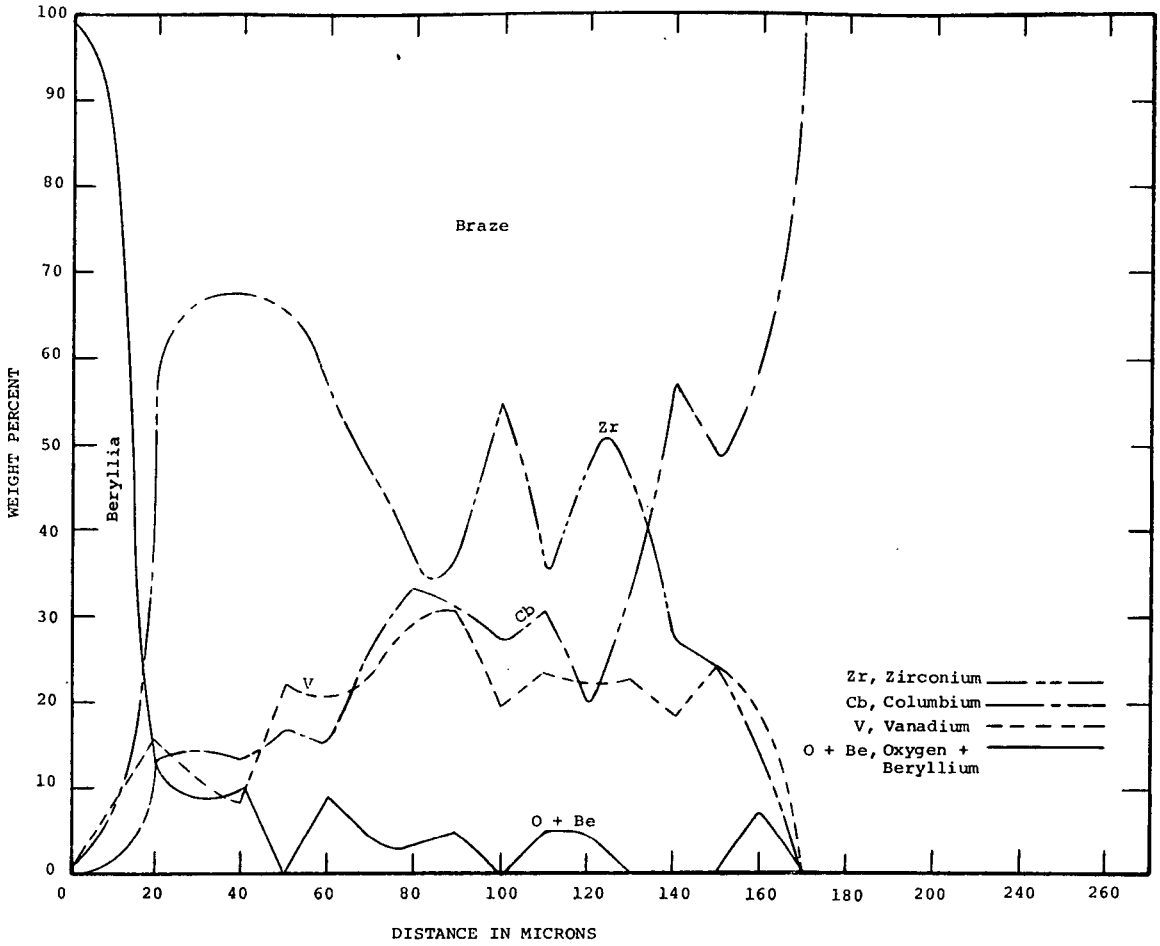

Figure 26. - Electron Microprobe Analyses Across the Vacuum Exposed Side of Aged (10,000 Hours at 1300° F) Bore Seal Capsule (Beryllia, 60Zr-25V-15Cb Braze Alloy and Columbium-1% Zirconium) Top Seal.

with 83 weight percent zirconium. The probable composition of the areas referenced in figures 27 and 28 is $ZrBe_2$. Another structure identified from microprobe analyses is the zirconium peak shown in both figures 24 and 25 at 55 microns into the braze from the edge of the columbium-1% zirconium. These peaks correspond to the 80Zr-20Cb eutectoid.

Good wetting characteristics of the braze alloy with respect to both columbium-1% zirconium and beryllia are evident in figures 27 and 29. Joint integrity was retained.

This page is reproduced at the back of the report by a different reproduction method to provide better detail.

Figure 27. - Photomicrograph of Beryllia/Braze Interface of Bottom Brazed Joint of Bore Seal Capsule After 10,000 Hours at 1300° F Exposure. (750X, Bright Field)

Figure 28. - Photomicrograph of Beryllia/Braze Interface of Bottom Brazed Joint of Bore Seal Capsule After 10,000 Hours at 1300° F Exposure. (750X, Dark Field)

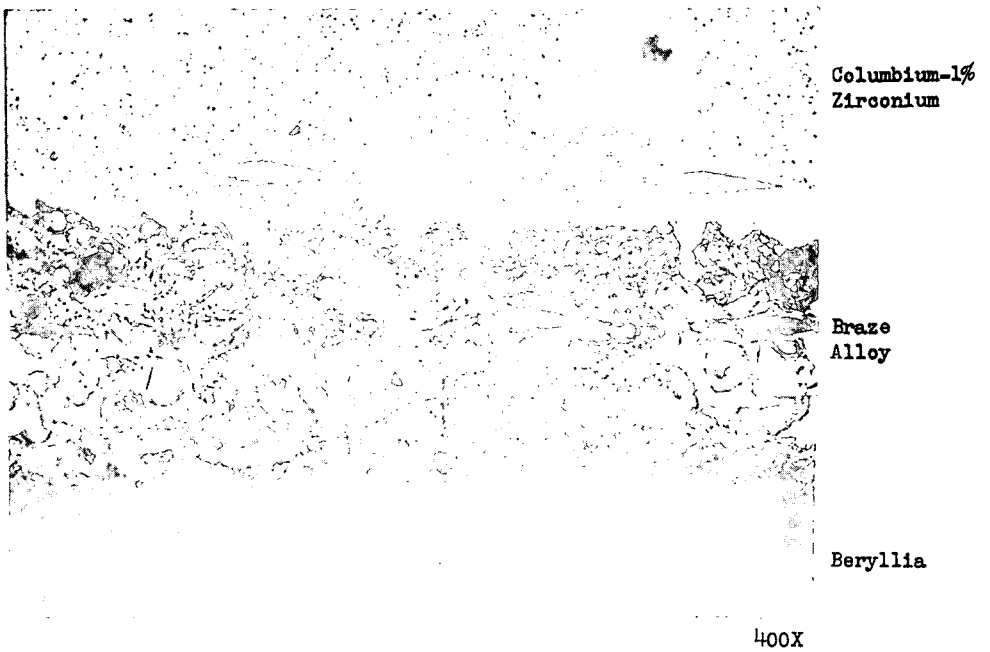

Figure 29. - Photomicrograph of Bottom Bore Seal Capsule Brazed Joint After 10,000 Hours 1300° F Exposure. Joint is Between Columbium-1% Zirconium and Beryllia Using 60Zr-25V-15Cb Braze Alloy. (400X)

Microhardness Surveys of Brazed Joints. - Microhardness surveys were made from the columbium-1% zirconium end members into the braze alloy on both top and bottom bore seal capsule brazed joints. Hardnesses of clearly defined areas are given in table 7. Differences in hardness between the top joint and the bottom joint are not significant.

Post Endurance Tests of 1300° F Stator

Subsequent to the 1300° F endurance test, the stator was examined and processed according to the previously defined plan. Selected areas, based on preliminary findings, were further examined, tested, and analyzed. The following paragraphs describe the processing of the stator and the results obtained.

Table 7. - Microhardness Values at Selected Locations in the 10,000-Hour, 1300° F Ultrahigh Vacuum Exposed Bore Seal Capsule Brazed Joints.

Location	Knoop Hardness Value With the Specified Load	
	25 grams	100 grams
Columbium-1% Zirconium End Member		
Top Brazed Joint	126	
Bottom Brazed Joint	137	
Columbium-1% Zirconium-Braze Alloy (60Zr-25V-15Cb) Diffusion Zone		
Top Brazed Joint	116	
Bottom Brazed Joint	122	
Braze Alloy (60Zr-25V-15Cb)		
Top Brazed Joint		1014
Bottom Brazed Joint		1092

Visual Examination of the Stator After Removal from the Test Chamber - A visual examination of the stator, performed immediately after removal from the test chamber, revealed some gray discoloration of the insulation materials and a general dulling of the exposed metallic surfaces attributed to deposition of evaporated materials during thermal-vacuum aging. The exposed surfaces of the conductor insulation were gray. Many of the conductor insulation "S" glass fibers on the conductor end turns had been fractured during winding, thereby causing some fraying; but this condition had not progressed further during the aging (see figure 17). The glass fibers were mechanically weak with low interfiber bonding. The adhesion of the wire insulation to the Inconel cladding was also weaker than after firing. The Inconel surface under the insulation was bright and not discolored.

During assembly, boron nitride fiber cement had been applied to the insulated conductors and the laminated stator core where the conductors exited the core. Adhesion between the

boron nitride fiber cement and the surface of the conductor insulation was weak at the conclusion of the test. The outer surface of the boron nitride cement had darkened during aging. The contacting interfaces of the cement and fibrous conductor insulation showed little darkening from aging.

After the post endurance test bench testing and visual inspections had been completed, one stator quadrant was disassembled to obtain samples of the various component parts for post-endurance test materials evaluation. Aging characteristics and compatibilities of the materials in this device were studied for effects of the environment and possible interactions of adjacent materials.

Analyses of Stator Conductor Insulation. - Spectrographic analyses were performed on unaged and aged inorganic conductor electrical insulation in several conditions. The objectives of these spectrographic analyses were: (1) to identify extraneous elements present as deposits or discolorations, and (2) to estimate relative amounts of the deposited elements. In normal spectrographic procedures, milligram quantities of the specimens to be analyzed are loaded into an electrode and compared against equivalent weight quantities of known materials of similar basic composition. This technique improves the accuracy of the semiquantitative estimates. However, the deposit specimens in this study were extremely small and it was not feasible to weigh them. This limitation was partially compensated for by comparing the totally arced sample of the unknown against a similarly arced series of standard samples in which the number of micrograms per element for each arcing operation was known. The series of standards for these analyses represented four orders of magnitude respectively: 0.01, 0.1, 1.0, and 10.0 micrograms of each of 49 elements. When arced, with the spectra recorded on film, a one-to-one correspondence of signal (optical density of the pertinent lines) to the microgram level of the observed elements was produced. Visual comparison of these film optical densities of known element lines to similar lines in the unknown material provided an approximation of the quantity in micrograms of the elements found.

Table 8 gives results of spectrographic analyses for two stator conductor electrical insulation specimens and those of unaged conductor electrical insulations equivalent to that used in the stator. Review of the relative compositions of unaged and aged conductor electrical insulation reveals changes in several elements out of the sixteen detected. The values reported for zinc show definite reduction from about 0.25 to 0.1 percent or less. Where the insulation was exposed directly to the chamber vacuum and not covered with boron nitride fiber cement, the zinc value dropped to 0.05 percent. The covering

Table 8. - Analyses of Conductor Electrical Insulation, Unaged and Aged for 10,000 Hours at 1300° F in Ultrahigh Vacuum

CONSTITUENT / SAMPLE	PERCENT															
	Si	Al	Mg	B	Na	Ca	Be	Ti	Cr	Mn	Fe	Co	Ni	Cu	Zn	Ag
Unaged Transformer Standard	27[a]	13[a]	2.4[a]	1	0.5	5	<0.001	0.05	0.01	(b) <0.01	0.5	(b) <0.02	0.05	0.06	0.3	0.01
Unaged Solenoid Standard	>10	>10	>10	1	0.5	5	<0.001	0.05	<0.01	(b) <0.01	0.2	(b) <0.02	0.1	0.04	0.2	0.1
Aged in Stator For 10,000 Hours at 1300° F, 10^{-9} torr Range and 292 V, 400 Hz	>10	>10	>10	1	0.2	10	0.02	0.05	0.05	0.1	0.5	0.02	0.05	0.04	0.05	<0.01
Aged With Boron Nitride Compound in Stator For 10,000 Hours at 1300° F, 10^{-9} torr Range and 292 V, 400 Hz	>10	>10	>10	1	0.5	10	0.005	0.05	0.05	0.2	0.5	0.05	0.1	0.03	0.1	(b) <0.01

(a) - Quantitative wet chemical analysis. All other analyses are semiquantitative spectrographic.
(b) - Not detected. Limits of detection are as shown after < sign.

of boron nitride fiber cement hindered the evaporation of the zinc oxide, thus reducing the loss. Sodium values showed a tendency for reduction, particularly in the absence of the boron nitride fiber cement. The aged samples showed relatively large increases in beryllium values. The exposed insulation value indicated an increase from less than 0.001 percent to 0.002 percent. The beryllium values for the conductor insulation covered by boron nitride fiber cement increased from less than 0.001 percent to 0.005 percent. This increase is attributed to the evaporation of beryllium from the bore seal brazing alloy. Metallic beryllium was formed during the active metal brazing process by reduction of beryllium oxide. If this contaminant would remain in the elemental state, then the electrical properties of the insulation covering could be ultimately degraded as the deposit accumulated throughout the insulation structure. Manganese levels increased with the source believed to be the aluminum oxide ceramic parts. The values for calcium were increased, both with and without adjacent boron nitride fiber cement. A possible mechanism for this increase may be interaction of the glass/refractory oxide matrix with the aluminum oxide slot liners and wedges which contain some calcium.

A ten milligram sample of fired and unaged conductor electrical insulation was quantitatively analyzed for alumina (Al_2O), silica (SiO_2), and magnesia (MgO) by fusing with sodium carbonate. The results were:

Al_2O_3	25.9%
SiO_2	58.4
MgO	4.1
	88.4%

The remainder of the sample consisted of oxides of boron, (B), sodium (Na), calcium (Ca), titanium (Ti), chromium (Cr), iron (Fe), nickel (Ni), copper (Cu), and zinc (Zn) with traces of beryllium (Be) and silver (Ag) noted.

Microscopic Examination of Conductor Insulation. - A transverse section of aged stator Inconel-clad silver conductor with Anadur "S" insulation was prepared for microscopic examination. A photomicrograph of this section is presented in figure 30 accompanied by that of an unaged specimen, figure 31. Examination of the aged specimen showed that the "S" glass fibers remained discrete and were not dissolved to a significant degree by the glass/refractory oxide matrix of the Anadur "S" insulation. The non-uniform appearance of the insulation coating in figure 30 was caused by the mechanical disturbances of sectioning,

This page is reproduced at the back of the report by a different reproduction method to provide better detail.

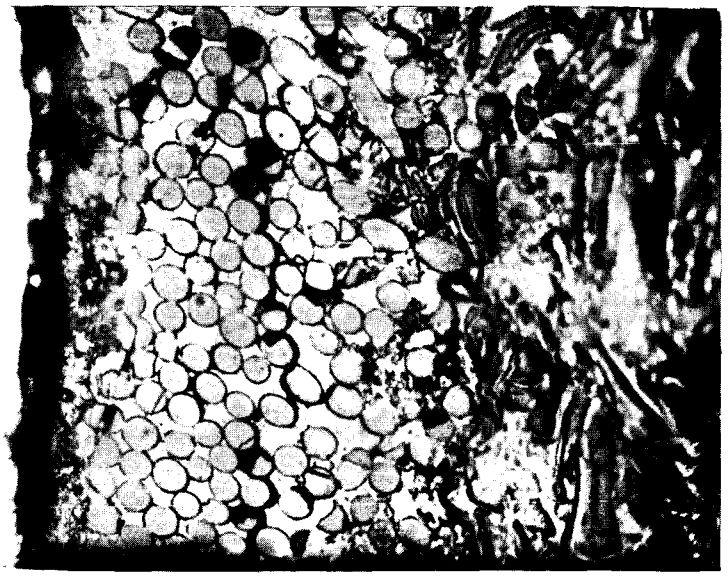

Figure 30. - Photomicrograph of Stator Conductor Electrical Insulation After Aging (10,000 Hours at 1300° F Ultrahigh Vacuum). (400X)

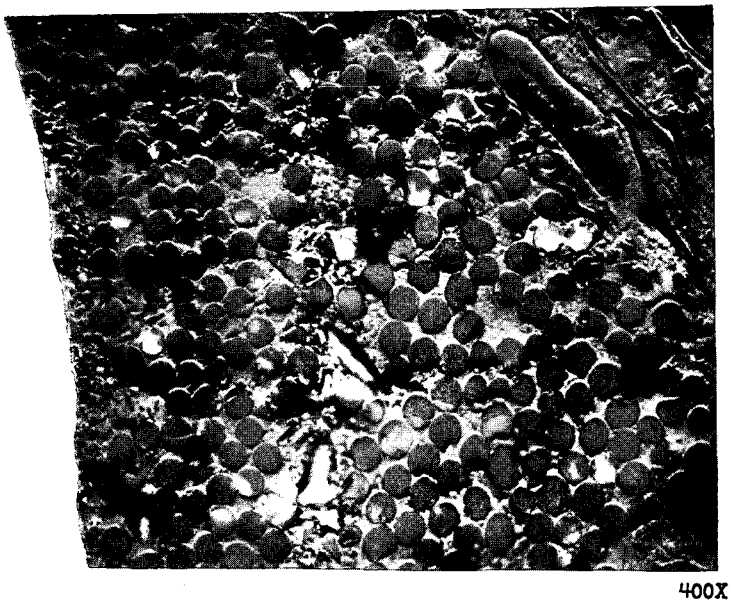

Figure 31. - Photomicrograph of Unaged Transformer Secondary Conductor Electrical Insulation. (400X)

mounting and polishing, acting on the inflexible insulation structure. Adhesion of the Anadur "S" to the conductor was low, thus contributing to the separation shown in the photomicrograph of the aged specimen.

Spectrographic Examination of Rigid Insulation. - Sampling of deposits on the aluminum oxide ceramic components was performed by removing the zones of interest with a tungsten carbide-tipped tool while minimizing disturbance of the substrate. The substrate was also sampled with the same instrument. Both deposit and substrate specimens were loaded into graphite electrodes for spectrographic analysis. The analytical technique has been described in the segment on Post Endurance Tests of 1300° F Stator of this section in the paragraph on Analysis of Stator Conductor Insulation. Estimates of element levels, developed by this technique, are presented in table 9. The accuracy of this data is considered to be one-third to three times the stated values.

Analysis of slot liner dark spots showed reduction of magnesium and manganese levels and increase in cobalt when compared with the substrate. Analyses of feedthrough ceramic dark spots showed, in comparison to the substrate, depletions of silicon, magnesium, manganese, and iron, and increases in nickel and copper.

Electron Microprobe Analysis of Rigid Insulation Discoloration. - Electron microprobe analyses were performed on an aluminum oxide slot liner from the stator. Dark spots had developed during the aging. These spots had been examined by emission spectrographic analysis (reported in table 9) and were found to contain relatively more cobalt than the substrate. Nickel, the major element in Inconel 600, was selected as the second element for analysis. Sections from both light (substrate) and dark spot areas were examined for nickel and cobalt. The limit of detectability for each element was approximately 0.02 percent (200 ppm). Line scans were made for both elements across the width of the slot liner starting at the discoloration. Equipment and procedures used were as described in the bore seal braze analysis. The scanning speed was 10 microns per minute. Acceleration voltage was 30 kV and the specimen current was 0.025 microamperes. The detectable limit calculation was based upon background measurements taken on a pure aluminum oxide sample with the spectrometer set for nickel and cobalt. Neither element was detected anywhere in the slot liner by this method.

X-ray Diffraction Analyses of Boron Nitride Fiber Cement. - Boron nitride fiber cement samples were examined by x-ray diffraction methods. Unaged and aged samples of the fiber cement were studied for structural changes attributable to an increase

Table 9. - Comparative Semi-Quantitative Emission Spectrographic Analyses from 10,000-Hours, 1300° F Ultrahigh Vacuum Aged Stator Slot Liner and Lead Wire Feedthrough Deposits and Substrates.

SAMPLE \ CONSTITUENT	MICROGRAM LEVELS OF ELEMENTS DETECTED IN EACH DEPOSIT												
	Si	Al	Mg	B	Be	Ti	Cr	Mn	Fe	Co	Ni	Cu	Zn
Components aged in stator for 10,000 hours at 1300° F, 3 x 10^{-9} torr and 292V, 400 Hz													
1. Slot Liner, Al_2O_3, Substrate	3	(a)	1	(b) < 0.1	(b) < 0.01	0.1	(b) < 0.1	0.5	2	(b) < 0.1	(b) < 0.1	< 0.1	(b) < 0.1
2. Slot Liner, Al_2O_3, Darkened Spots	3	(a)	0.5	(b) < 0.1	< 0.01	0.1	(b) < 0.1	0.1	2	0.6	(b) < 0.1	< 0.1	(b) < 0.1
3. Feedthrough, Al_2O_3, Substrate	> 10	(a)	>10	(b) < 0.1	< 0.01	0.1	0.3	0.8	5	(b) < 0.1	0.5	< 0.1	
4. Feedthrough, Al_2O_3, Darkened Spot	5	(a)	5	(b) < 0.1	0.1	0.1	0.3	0.3	1	0.5	1	8	

(a) - Major constituent (> 10 micrograms)
(b) - Not detected. Limits of detection in micrograms are as shown following < sign.

in boric oxide (B_2O_3) content. An increase in B_2O_3 would indicate the presence of available gaseous oxygen during aging and the resultant release of nitrogen. Because of only partial crystalline structure of the samples, the diffraction lines were broad and diffuse. The powdered samples were examined using a 57.3 millimeter Debye-Scherer powder camera with CuK radiation. The results of aged and unaged stator specimen are presented in table 10. Control samples were prepared using compositions of

Table 10. - X-Ray Diffraction Identification Analyses of Boron Nitride Fiber Composite Specimens From the Stator. Unaged and Aged for 10,000 Hours at 1300° F in Ultrahigh Vacuum Plus Control Specimens.

Sample	Compounds Detected
Boron Nitride Fiber Cement Aged in Stator (10,000 hours at 1300° F, 10^{-9} torr) not in Contact with Conductor Electrical Insulation	BN Al_2O_3
Boron Nitride Fiber Cement Aged in Stator (10,000 hours at 1300° F, 10^{-9} torr) in Contact with Conductor Electrical Insulation	BN Al_2O_3
Boron Nitride Fiber Cement, Unaged	BN
Control: 90% BN + 10% B_2O_3	BN B_2O_3
Control: 50% BN + 50% B_2O_3	BN B_2O_3

10 percent boric oxide plus 90 percent boron nitride fiber and 50 percent boric oxide plus 50 percent boron nitride fiber. The results on the controls showed that boric oxide could be detected but that the detectability was poor. Review of these analytical results indicates that negligible amounts of boric oxide, if any, were produced during aging.

Electron Microprobe Analyses of Inconel-Clad Silver Conductors. - Electron microprobe analyses were performed on aged and unaged stator Inconel-clad silver conductors. The object of these analyses was to determine the possible extent of silver and chromium diffusion at the silver-Inconel interface, and the depletion of chromium from the vacuum-exposed Inconel surface. Equipment and procedures used in these analyses were as described in the section on bore seal braze analyses.

Electron microprobe scans for the diffusion investigation were made perpendicular to the cladding-silver interface for both silver and chromium. The scan speed was 10 microns per minute. The scan information was recorded on a chart recorder. Estimates were made from the charts as to the interface thickness. Pure silver and chromium standards provided signals for the hundred percent count rate and for the background count rate. In this case the background was obtained by setting the spectrometer on the silver Lα wave length and then positioning the chromium standard under the electron beam (30 kV, 0.015 microamperes). This low specimen current permitted control of the beam diameter to approximately one micron. Counts were obtained for five 100-second intervals. The reverse procedure was used for the chromium Kα background signal.

Several scans for chromium (limit of detectability was 300 to 400 ppm) were made across the entire width of the cladding and to a position approximately 40 to 50 microns inside the silver. Beyond this, spot checks for the presence of chromium were made in several places. Scans for silver (limit of detectability was 800 ppm) were started 40 to 50 microns from the interface inside the silver and continued 50 to 60 microns into the Inconel. Beyond this range, spot checks for silver were made in several areas in the cladding. Electron microprobe traces of the silver-Inconel interfaces for silver Lα in both the aged and unaged stator conductors are shown in figure 32. No differences can be discerned when comparing the aged specimen with the unaged specimen. In both cases the interfaces seem to be identical. The silver Lα signal decreased from 100 percent silver to background over a distance of 16 microns (approximately 0.0006 inch). When monitoring the chromium Kα signal, the silver level decreased from 100 percent to background over a distance of approximately 10 microns. The actual values of 11 and 9 microns shown in the chromium Kα scans of figure 32 are not significantly different because of the inherent accuracy of the microprobe system at one micron beam diameter. Silver could not be detected above this level more than five microns from the end of the area

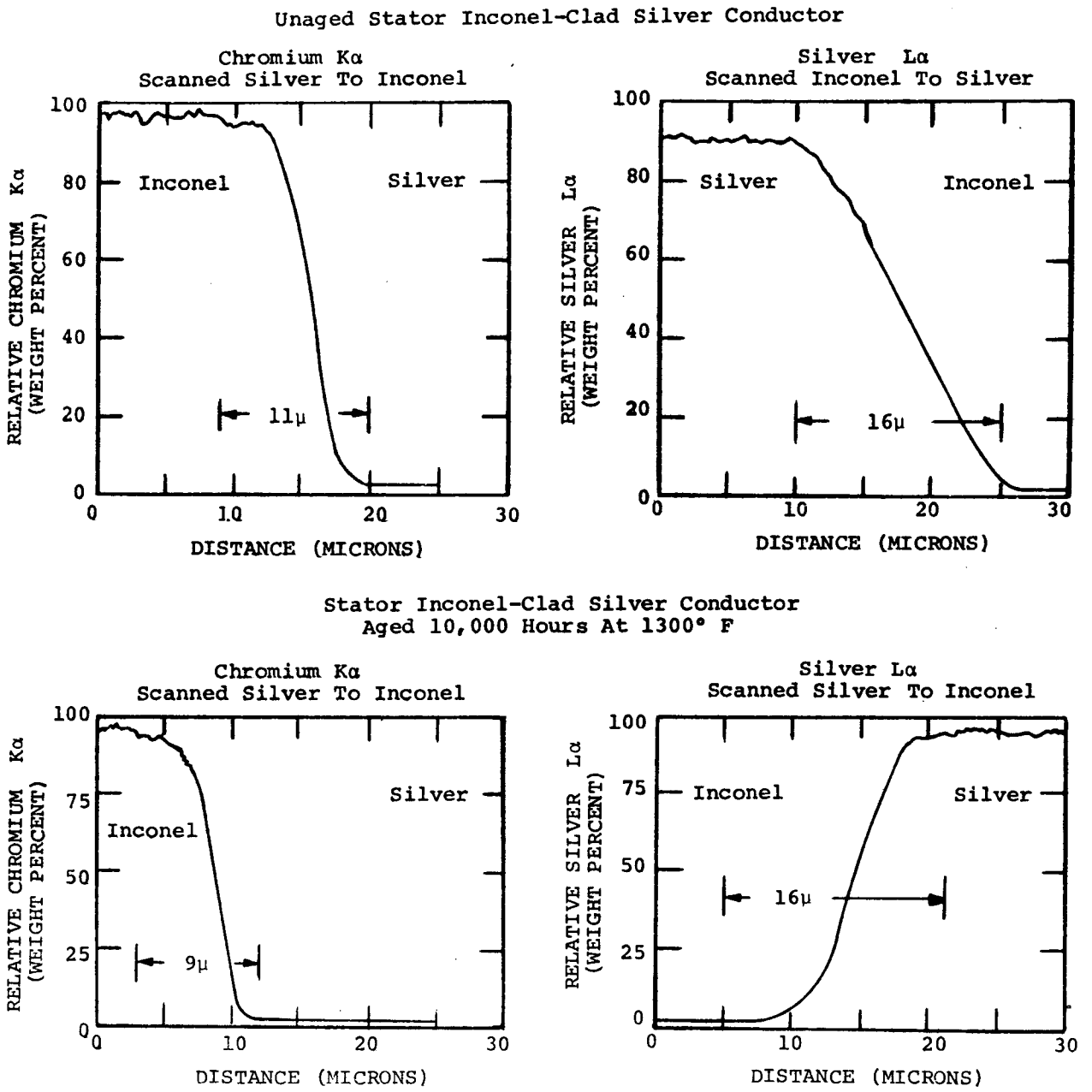

Figure 32. - Electron Microprobe Scans For Silver and Chromium in Aged (10,000 Hours at 1300° F Ultrahigh Vacuum) and Unaged Stator Inconel-Clad Silver Conductors.

indicated as being the interface. Silver could not be detected anywhere in the Inconel cladding nor could chromium be detected in the silver.

A check was made for possible chromium depletion from the outside of the aged Inconel specimen. A chromium scan was made from the silver interface across the width of the cladding. There was some indication that the chromium content might have decreased from 14 percent to 13 percent in the last 10 microns, but due to edge effects (rounding the specimen in polishing), this is very difficult to confirm. The beam size was reset to a smaller (nearer one micron) diameter and the edge area was rerun. There was even less evidence of any chromium depletion at the vacuum-exposed edge when the smaller beam was used. Figure 33 gives two charts showing these two scans.

Metallographic Examinations of Inconel-Clad Silver Conductors. - Metallographic examinations were performed on unaged and aged Inconel-clad silver stator conductors from both end turn and slot. Figure 34 is representative of aged conductor from both end turn and slot. No differences were detected between the silver or the Inconel microstructures of the two aged specimens. Figure 35 is a photomicrograph of unaged conductor. A comparison of aged and unaged conductors showed considerably larger grains in the aged Inconel and somewhat larger grains in the aged silver. Grain growth found was considered normal for the aging conditions. There was no evidence of diffusion of silver or chromium in either aged conductor specimen.

Visual Examination of Stator Magnetic Lamination Stack After Sectioning. - After disassembly of the high-temperature stator following 1300° F endurance testing in ultrahigh vacuum (in the 10^{-9} torr range), the magnetic stack was sectioned for examination. The electron beam weldments around the stack perimeter (see figure 1) were intact. The weld material was removed by grinding to permit separation of the 0.008-inch thick iron-27% cobalt laminations. There was slight adhesion between adjacent laminations in random locations. Lamination surfaces showed a grayed matte finish except for a narrow, intermittent stain pattern. This stain pattern was attributed to a hydrocarbon residue (machining lubricant used during O.D. grinding of the welded stack) that remained after ultrasonic degreasing of the compressed stack. Degreasing had been performed prior to final assembly of the stator. Simple bend tests revealed the laminations to be brittle.

Specimens were removed for magnetic testing, metallurgical examinations, microhardness surveys, and interstitial analyses. At the time of stator fabrication, magnetic laminations were randomly selected for comparative tests of material in the un-

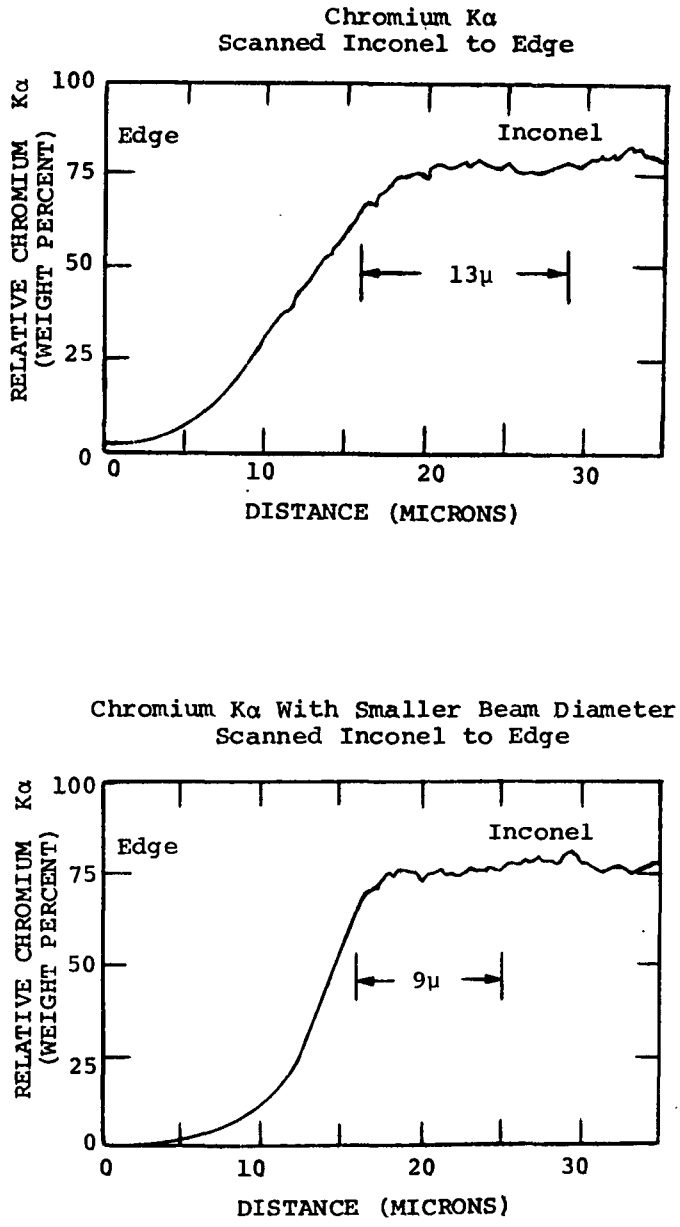

Figure 33. - Electron Microprobe Scans For Chromium in Inconel From Aged (10,000 Hours at 1300° F Ultrahigh Vacuum) Stator Conductor Specimen.

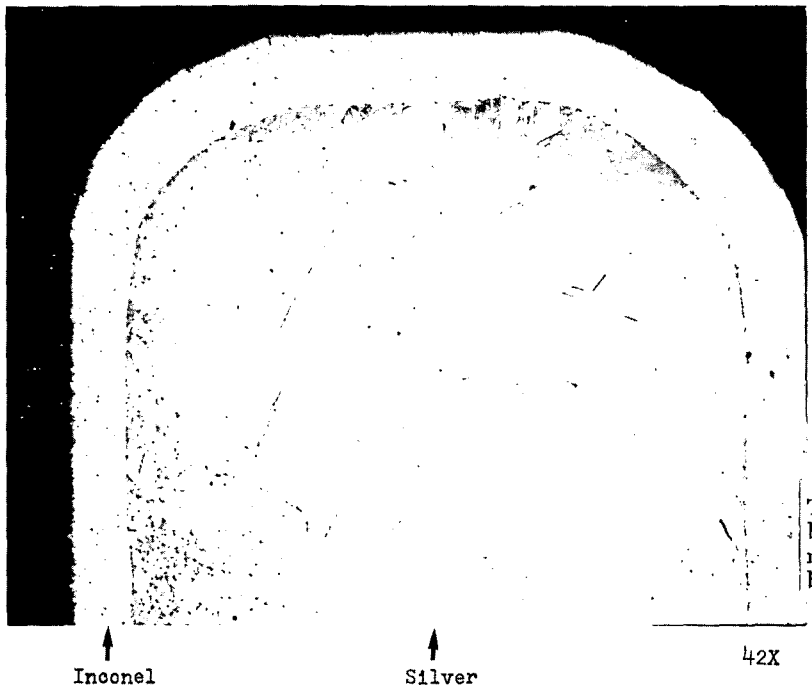

This page is reproduced at the back of the report by a different reproduction method to provide better detail.

Figure 34. - Photomicrograph of Unaged Stator Conductor (42X)

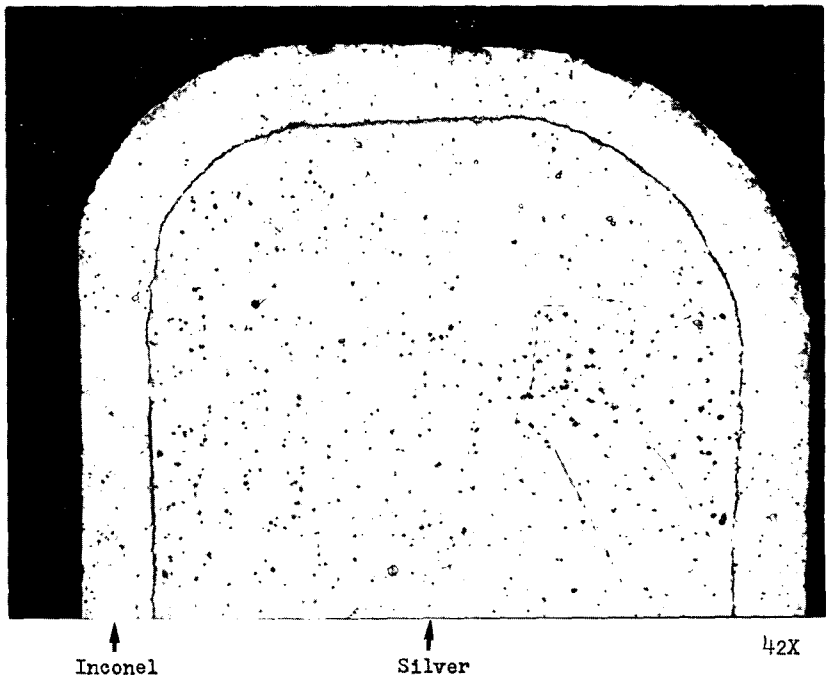

Figure 35. - Photomicrograph of Conductor From Stator Slot After 10,000-Hour, 1300° F 10^{-9} Torr Pressure Exposure. (42X)

aged condition are presented along with those obtained on laminations removed from the stator after 10,000-hour thermal-vacuum testing.

Coercive Force Determinations on Stator Laminations. - Coercive force was used to indicate changes in magnetic quality as brought about by changes in alloy structure during prolonged high-temperature vacuum aging. These changes in structure can be beneficial to magnetic quality, including those of relief of internal strains, purification, and magnetic annealing effect; or detrimental, such as the effect of oxide particles originating from internal oxidation. Beneficial effects prevailed during aging. Table 11 shows the coercive force value of aged and unaged lamination samples. It should be noted that the cutting of coercive force test samples from both aged and unaged material induced internal strains which in turn increased the coercive force. As a result, the coercive force values

Table 11. - Magnetic Properties (Coercive Force)[a] of Magnetic Materials From High Temperature Stator Unaged and After 1300° F Endurance Testing at a Pressure in the 10^{-9} Torr Range.

Description of Specimen	Specimen Condition	Room Temperature Coercive Force H_c (oersteds)
Iron-27% Cobalt Stator Laminations, 0.008-Inch Thick	Unaged Lamination	2.4
Iron-27% Cobalt Stator Laminations, 0.008-Inch Thick	After 10,000-hour stator endurance test at 1300° F and pressure in the 10^{-9} torr range	1.62

(a) Coercive force measurements were made using a precision Coercive Force Meter manufactured by the Institute Förster, Reutlingen, West Germany. Accuracy of all measurements was ±2 percent.

shown for all specimens are 20 to 40 percent higher than they were before cutting. In any case, the coercive force values are a strong indication that the magnetic quality had improved during high temperature vacuum aging.

Lower coercive force was created by the exposure of the material at high temperatures to magnetic fields induced by the current passing through the magnetizing windings during endurance testing of the stator. The effect of annealing treatments on the coercive force values of iron-cobalt alloys, for fast-cooled specimens and those exposed to magnetic annealing, are reported in reference 9. Similar improvements in coercive force values were observed in iron-27% cobalt laminations exposed to a magnetic field at 1400° F during a preceding materials study (ref. 1, pp. 171-176). Although no magnetization curves were determined in this program (most sample geometries would not lend themselves to accurate magnetization tests), the data reported in reference 10 indicate that annealing in the presence of a magnetic field at temperatures above 1392° F (700° C) brings about rectangular magnetization curves both at temperature and at room temperature after high temperature exposure. In the temperature range 1472° to 1652° F (800° to 900° C), the magnetic annealing effect becomes particularly pronounced. Similar magnetic effects were observed in tests of iron-27% cobalt performed on both laminated and solid rings in the previously mentioned NASA Materials Program (ref. 1), except that magnetic testing was not carried out at temperatures above 1400° F (760° C).

Coercive force measurements as well as data from the technical literature show, therefore, that prolonged high-temperature vacuum exposure results in no harmful effects to the magnetic quality of the iron-27% cobalt material. If the exposure temperature is sufficiently high, the magnetic quality can be improved considerably by the magnetic annealing effect.

Interstitial Analyses of Magnetic Materials. - Interstitial analysis results for unaged iron-27% cobalt laminations and specimens from the endurance tested stator are shown in table 12. Since the presence of alumina interlaminar insulation on one surface of the aged stator lamination affects the apparent lamination oxygen level, two values are shown for oxygen. One sample (245 ppm) reflects the oxygen content in the central cross sectional area of the lamination. The second value (1370 ppm) includes oxygen available from the plasma arc sprayed alumina; the oxygen level of the aged lamination increased considerably. Nitrogen content also increased after aging but to a lesser degree. Apparent sources for both were occluded and adsorbed air on the plasma arc sprayed alumina surface. Carbon content of the aged lamination was one-half that of the unaged lamination. During thermal aging, oxygen was available to form carbon monoxide which evolved, thus depleting carbon in the aged specimen.

Table 12. - Interstitial Content[a] of Iron-27% Magnetic Materials Before and After Endurance Testing in a Stator at 1300° F for 10,000 Hours and a Pressure in the 10^{-9} Torr Range.

Description of Specimen	Specimen Condition	Interstitial Content (ppm)		
		Oxygen	Nitrogen	Carbon
Iron-27% Cobalt Stator Lamination, 0.008-Inch Thick	Unaged Lamination	61	39	111
Iron-27% Cobalt Stator Lamination, 0.008-Inch Thick	After 10,000-Hour Stator Test at 1300° F and Pressure in the 10^{-9} torr Range	245[b] 1370[c]	70	55

(a) All analyses were made by the Westinghouse R & D Center. Oxygen by vacuum fusion; nitrogen by modified Kjeldahl. Carbon by combustion. Accuracies are as follows:

Oxygen at 20ppm ±10%
at 100ppm ±4%

Carbon at 20ppm ±10%
at 50ppm ±6%
at 250ppm ±3%

Nitrogen at 30 to 100 ppm ±5%

(b) Bulk sample analysis from central portion of lamination.
(c) Analysis included oxygen available from plasma arc sprayed alumina surface.

Metallographic Examinations and Microhardness Surveys of Magnetic Materials. - An investigation of the microstructure was carried out and the results were correlated with microhardness tests and bend ductility observations. These data show that high temperature vacuum exposure brought about internal oxidation of the outer layers of laminations as well as intergranular brittleness. The samples tested here were as brittle as the phosphate-coated laminated core which had successfully passed a vibration test (ref. 5, p. 167).

Internal oxidation occurred by oxygen diffusion from the laminations surface through grain boundaries and into the grains; this produced a network of oxide inclusions. Figure 36 shows this structure. The inclusion network increased the hardness (table 13) in the material layers close to the surface and prevented further grain growth. The grains in the center layers of the aged samples grew to three to five times their original size. This grain growth, however, was conducive to interlaminar brittleness because grain boundaries contain oxygen, the relative concentration of which increases with the reduction in the length of grain boundary network (grain growth). This mechanism applies to both thin laminations and thick sections except that grain growth was more pronounced in laminations because the surface area to volume ratio was larger in the case of laminations.

I 0.001 inch

ASTM Grain Size: 8

200 X

(a)

This page is reproduced at the back of the report by a different reproduction method to provide better detail.

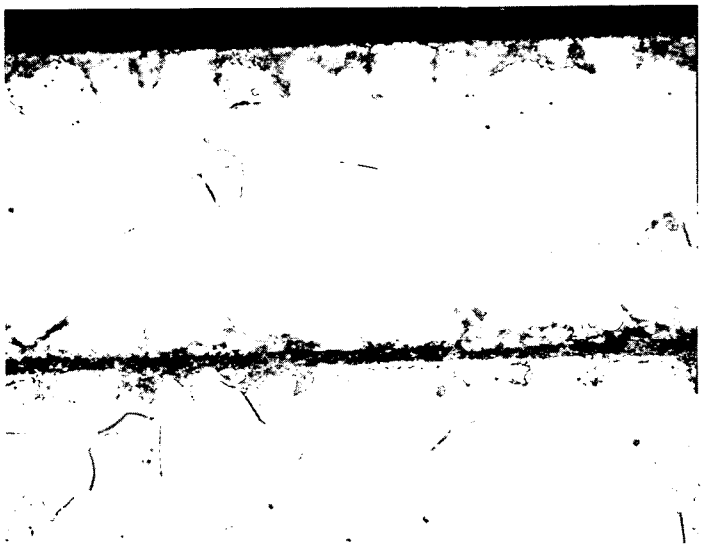

Second Phase Penetration into Lamination Surface

ASTM Grain Size: 4 - 5

I 0.001 inch

200 X

(b)

Figure 36. - Photomicrographs of Iron-27% Cobalt Magnetic Laminations Used in the High Temperature Stator Before and After Thermal Aging for 10,000 Hours at 1300° F and a Pressure in the 10^{-9} Torr Range.

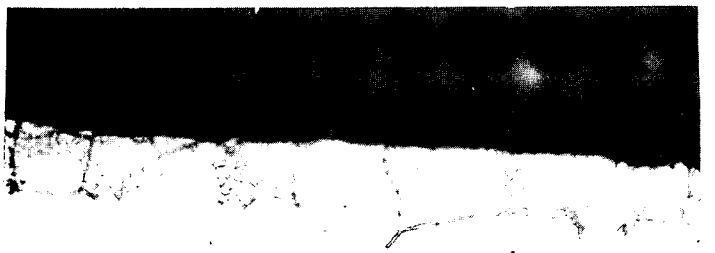

Second Phase

ASTM Grain Size: 4 - 5

0.001 inch

500 X

(c)

This page is reproduced at the back of the report by a different reproduction method to provide better detail.

(a) Unaged iron-27% cobalt stator lamination with plasma arc sprayed alumina applied, 200 X.

Etchant: $50HNO_3$, $45CH_3COOH$, $5H_2O$.

(b) Iron-27% cobalt stator laminations with plasma arc sprayed interlaminar insulation after 10,000 hours aging at 1300° F, unetched, 200 X.

(c) Iron-27% cobalt stator laminations with plasma arc sprayed interlaminar insulation after 10,000 hours aging at 1300° F, unetched, 500 X.

NOTE: Micrograph shows oxide penetration into lamination surface and grain growth within the lamination. Grain structure revealed by relief polishing.

Figure 36. - Continued.

Table 13. - Knoop Hardness of Magnetic Laminations From the High Temperature Stator Before and After Thermal Endurance Testing at a Pressure in the 10^{-9} Torr Range.

Description of Specimen	Specimen Condition	Microhardness[a] Knoop (25 g)			Remarks
		Edge	Center	Edge	
Iron-27% Cobalt Stator Laminations 0.008-Inch Thick	Unaged Lamination	270	256	---	Ductile in bending
Iron-27% Cobalt Stator Lamination, 0.008-Inch Thick	After 10,000-hour stator test at 1300° F and a pressure in the 10^{-9} torr range	328	318	322	Brittle in bending

(a) Each value shown is the average of five test indentations.

Furthermore, the original grain size of the thick sections is three to five times greater than that of laminations and does not increase much during high temperature exposure.

The unexposed (cold-rolled, hot-worked, or annealed) laminations as well as thick sections were ductile. The brittleness in the aged specimens was brought about because the oxide films on the lamination or thick section surfaces (produced during heat treatment or plasma spraying) diffused continually into the material during the long term thermal vacuum testing of the component. One way to minimize this internal oxidation is to limit the outer surface oxides. This is not an easy task considering that any high-temperature treatment in a normal "protective atmosphere" (except ultrahigh vacuum) would leave an oxide film (probably a complex iron-cobalt oxide) on the surface.

Interlaminar Insulation. - Interlaminar insulation consisted of particles of alumina (99.995% Al_2O_3) plasma-arc sprayed onto stator laminations. Interlaminar insulation resistance tests were performed on both unaged and aged stator laminations. The unaged specimen was a representative lamination taken from the group coated for this stator. The aged specimens were taken from the stator during disassembly. Tests were conducted in the manner described in reference 2 using a weighted 1/4-inch-diameter flat electrode. Initial attempts to measure interlaminar insulation resistances of both aged and unaged specimens were

unsuccessful because the resistances were below the 0.1 ohm sensitivity of the test instrument.[10] Electrode loading was subsequently reduced and measurements again made, but with the same results. Visual inspection of specimen surfaces revealed the following differences:

	Coated Side	Uncoated Side
Unaged:	Matte, metallic appearance scattered iridescence due to heat treatment. Roughened, abrasive to the touch.	Moderately bright metallic appearance with similar iridescence. Smooth to the touch.
Aged:	Gray matte with irregular dark stain pattern. Laminations embrittled and stuck together. Abrasive to the touch.	Similar to the coated side except smoother to the touch even in the stained areas.

Interlaminar insulation resistance was very low both before and after aging for 10,000 hours at 1300° F in an ultrahigh vacuum.

Examination of Mechanical Function Parts. - Mechanical function parts consisted of the housing and retaining ring made of iron-27% cobalt magnetic material, and the end bell and bore seal pedestal made of a nickel base alloy (see figures 1 and 15 and table 1). These parts were given visual examinations. No evidence of unacceptable change was noted. There were no deposits or discolorations unique to these parts.

[10]Measurements were made with a Voltohmist WV77E.

EVALUATION, RELATIVE TO AGING, OF BORE SEAL CAPSULE AND STATOR MATERIALS

Each major material used in the bore seal capsule and stator was evaluated on the basis of detectable changes caused by the 10,000-hour, 1300° F exposure. Evaluations were based on comparisons of information from the previously discussed tests analyses, and examinations of aged and unaged materials. Any material changes found were investigated to determine their cause. Causes were related to either thermal aging per se, or to thermal aging at interfaces. Evaluations of materials relative to their performance in the bore seal capsule and stator are given in the paragraph on Materials Evaluation Relative to Component Functional Performance in this section.

Bore Seal Capsule Materials

The bore seal capsule consisted of 99.8 percent beryllia joined to columbium-1% zirconium with a 60Zr-25V-15Cb active metal braze. Inside the capsule was high purity potassium. Materials interfaces consisted of the braze with both beryllia and columbium-1% zirconium. The environment consisted of 10^{-9} torr range gas pressure on the outside of the bore seal capsule and approximately nine psia potassium vapor on the inside of the capsule. Evaluation of the bore seal capsule materials relative to aging in specific environments are given in the following paragraphs.

Deposits found on the outside (see table 4) and inside of the bore seal capsule did not contribute to the performance or degradation of the bore seal capsule.

Beryllia Ceramic. - The bore seal 99.8 percent beryllia ceramic was not affected by the 10,000-hour, 1300° F exposure nor by the potassium and vacuum (10^{-9} torr range) environments. Table 6 lists flexural strengths for three groups of specimens. Each group had a different side (relative to the potassium) in tension. There was no significant difference in average flexural strength between the three groups indicating that there was no penetrating effect due to either potassium or vacuum exposure. Table 6 also gives flexural strengths of unaged material. A comparison of aged and unaged material strengths shows no significant difference between the two groups. The 99.8% BeO ceramic cylinders used in fabricating the four-inch diameter bore seal capsule for this program had shown indications of surface porosity (ref. 6). Micrographs (ref. 6, figs. 39 and 40) of the beryllia ceramic obtained prior to endurance testing did not indicate an abnormal bulk porosity for this grade of beryllia ceramic.

After 10,000 hours exposure to potassium, the beryllia ceramic retained its flexural strength and the microstructure appeared unchanged. However, trace elements shown in the potassium analysis (see table 5) after 10,000-hour, 1300° F exposure indicate that the possibility of an extremely slow reaction of potassium with trace elements in the beryllia ceramic cannot be disregarded. As noted previously, the appearance of the trace elements in potassium may have occurred by selective reaction with less stable oxides in the ceramic or the indirect reaction with active metal brazing by-products. The twenty-two parts-per-million increase in beryllium content of the bore seal capsule potassium (see table 5) is not considered the result of a beryllia corrosion problem. The probable sequence for beryllium transfer from the bore seal capsule beryllia into the potassium is as follows: (1) less than 100 micrograms of beryllia was reduced to beryllium at the beryllia-braze alloy interface during active metal brazing, (2) this beryllium vaporized and was deposited on the bore seal capsule interior, and (3) the evaporated beryllium was dissolved in potassium during aging. The detection of oxygen in the braze (see figures 23, 24, 25, and 26) tends to substantiate the belief that beryllia was reduced during brazing.

Columbium-1% Zirconium. - The columbium-1% zirconium in the bore seal capsule was essentially unaffected by the 10,000-hour, 1300° F exposures to vacuum (10^{-9} torr range) and potassium. The minor increase of columbium in the bore seal potassium, (21 parts-per-million, see table 5), apparently from the columbium-1% zirconium, is a relatively insigificant amount. It should be noted that several trace elements found in the potassium (table 5) were also present in trace quantities in the columbium-1% zirconium (table C-2, ref. 6). Metallographic examination showed no changes in structure due to either the potassium or the vacuum aging environments.

Braze Alloy and Brazed Joint Interfaces. - The 60Zr-25V-15Cb active metal braze appeared unaffected by the 10,000-hour, 1300° F aging and the exposure to vacuum (10^{-9} torr range) and potassium environments. The lack of increase of braze alloy constituents in bore seal capsule potassium confirms the resistance of the alloy to potassium. Microscopic examinations revealed no penetration by potassium. Electron microprobe analyses confirmed that each probed joint had a different composition, and that there was a general lack of homogeneity (see figures 23, 24, 25, and 26). The lack of homogeneity in the braze and the gradation in braze structures (less homogeneous in the bottom seals - more homogeneous in the top seals) probably occurred during brazing and is thought to be a function of brazing time and temperature. The top brazes probably experienced the lowest brazing temperature and/or was at brazing temperature for less time when compared with the bottom brazes.

Microscopic examinations of the braze alloy interfaces (see figures 27 and 29) revealed good wetting of the metal by the braze. Electron microprobe analyses revealed that columbium from the metal end member had diffused into the braze alloy during brazing. Interfaces between the braze alloy and both the columbium-1% zirconium and the beryllia showed no degradation or effects caused by the 10,000 hours aging at 1300° F.

Stator Materials

The stator consisted of iron-27% cobalt alloy magnetic laminations, Inconel-clad silver electrical conductors, and both flexible and rigid electrical insulations. Associated with the stator were mechanical function parts of either iron-27% cobalt alloy or a nickel base super alloy. These materials were aged at 1300° F for 10,000 hours in a 10^{-9} torr pressure range environment. Each material was evaluated on the basis of any changes caused by the thermal vacuum aging, and also any changes caused by interfaces with other materials. Evaluations of stator materials relative to aging in specific environments follow.

Evaluation of Stator Magnetic Laminations. - Coercive force measurements indicated that the magnetic quality of the iron-27% cobalt laminated stack improved slightly after the 10,000 hour aging at 1300° F in a pressure in the 10^{-9} torr range (see table 11). This improved magnetic performance resulted from a magnetic annealing effect that was created by the ac magnetic field induced in the windings during the exposure at elevated temperatures.

Information from metallurgical examinations, microhardness determinations, interstitial analyses, and brittleness observations revealed changes in the metallurgical structure and mechanical properties of the stator magnetic materials due to thermal vacuum aging. The metallurgical structure revealed substantial grain growth (3 to 5 times original size in the center of the lamination) after thermal aging (see figure 36). Knoop hardness increased from approximately 270 in the unaged to 328 in the aged material (see table 13). Grain growth at the edge of the aged lamination was limited by the oxide inclusion network formed by oxides diffusing along the grain boundaries from the lamination surface. Adherent surface oxides present after lamination and stator processing are the apparent source of the second phase oxygen. As a result of the oxides, the aged iron-27% cobalt laminations were very brittle. Oxides in the grain boundaries of the iron-27% cobalt alloy lower the cohesive strength of the material and cause intergranular embrittlement. Interstitial analyses of stator laminations indicated a depletion

of carbon, an increase in nitrogen level, and a significant increase in oxygen after thermal-vacuum aging (see table 12).

Inconel-clad Silver Conductors. - Inconel-clad silver conductors (0.090 in. x 0.144 in.) were evaluated after comparing information on aged and unaged specimens. No changes due to aging could be detected by visual examination. Electrical resistance values determined before, during, and after aging (see table 3 and figure 6) also showed no change due to aging. Metallographic examinations revealed that grain growth had taken place in both the Inconel and silver (see figures 34 and 35) of the aged material. This grain growth is considered normal for the aging conditions. No diffusion of silver into Inconel or chromium (from the Inconel) into silver could be detected by a comparative examination of aged and unaged microstructures (see figures 34 and 35) or electron microprobe analyses (see figure 32). Also, no depletion of chromium from the vacuum exposed Inconel surface could be detected by either metallographic examination or electron microprobe analysis (see figure 33). No detrimental change due to aging could be found in the Inconel-clad silver conductors.

Electrical Insulation. - Stator electrical conductor insulation was evaluated after studying information from visual and microscopic examinations and from spectrographic analyses of aged and unaged specimens. The basic "S" glass fibers were not apparently attacked further by the glass-ceramic matrix of the Anadur composition during the thermal aging of 10,000 hours at 1300° F as may be observed by comparing figure 30 and figure 31. The glass fibers were fractured throughout the insulation structure after the firing which was required for preparation of the insulation system for the life test operation. Some fraying was exhibited before the aging began, especially at the end turns of the stator coils. This condition of fractured fibers was not worse after aging than before. The exposed surfaces of the Anadur "S" insulation was darkened to a dull gray color, but where covered with other components of the system, the original white color was maintained. No mechanical or electrical performance problem related to surface condition was noted. The chemistry of the Anadur "S" insulation exhibited minor increases in calcium, beryllium, chromium, manganese, and cobalt and similar magnitude of decreases in zinc and sodium. The change in manganese content may be attributed to a migration from the solid refractory insulation materials to the conductor insulation. The solid insulation bodies displayed a reduction in manganese quantity in the surface region compared to that of the interior substrate. The migration may have been caused by a solvent or fluxing effect of the glass frit component of Anadur "S" insulation on the ceramic body. The adhesion of the insulation to the conductor surface was only fair at the start of

aging and was somewhat reduced at the conclusion of the test. The ac current leakage and the dc insulation performances of the insulation system including all insulation components displayed improvement throughout the duration of the aging period. Thus the electrical performance of the insulation system was better at the completion of the exposure than initially.

Rigid Electrical Insulation. - The rigid electrical insulation components used in the stator were evaluated after studying of information from visual and microscopic examinations and from spectrographic analyses of unaged and aged specimens. Boron nitride fiber cement retained its physical integrity, but its adhesion to the adjacent insulations was very poor and its outer surface was darkened. Spectrographic results revealed a general increase in the elements detected in the original specimen. The discolored regions contained high quantities of chromium, manganese, and iron. It is interesting that beryllium and cobalt were not detected in the boron nitride fiber cement although the adjoining Anadur "S" insulation exhibited notable increases in the levels of these elements. These differences probably can be attributed to the presence of a glassy matrix in the Anadur "S" conductor insulation and its absence in the fiber cement. The glass, being held during the aging at a temperature approaching its softening range, was more active in an ionic mode. The rigid insulation components were high purity aluminum oxide ceramic bodies. They all exhibited the anticipated high mechanical and electrical stability. The changes were visual, consisting of discolored spots. The nature of the discolorations were varied including black, brown, orange, green, and blue. The discolored zones yielded higher than original levels of cobalt, nickel, and copper. The ceramic surfaces, both white and colored, were lower in manganese content than their respective substrates. As noted previously, the Anadur "S" conductor insulation displayed increases in manganese values which has been attributed to the activity of the glass matrix at the aging temperature. At scattered locations on the sides and bottoms of the slot liners, numerous dark spots had formed. The larger spots, measuring about 1/32-inch in diameter, extended completely through the 0.020-inch wall of the part. No deleterious effects upon electrical or mechanical operation were noted. No mechanism or identification of source for these abnormalities has been established.

Mechanical Function Parts. - No changes due to aging could be found by visual examination of the mechanical function parts i.e., housing and retaining ring of iron-27% cobalt alloy, and end bells and bore seal pedestal of nickel base super alloy. See table 1.

MATERIALS EVALUATION RELATIVE TO COMPONENT FUNCTIONAL PERFORMANCE

Each material was evaluated on the basis of its contribution to the functional performance of the bore seal capsule or the stator. The following summarized these evaluations.

Bore Seal Capsule

The bore seal capsule maintained its leak tightness containing potassium for 10,000 hours at 1300° F. Evaluation of bore seal capsule materials (beryllia, columbium-1% zirconium, and braze alloy) revealed no penetrating effects due to either potassium exposure or low pressure exposure (10^{-9} torr range). The absence of deterioration in either the functional performance or in the bore seal capsule materials indicates that this bore seal capsule could function for a much longer period of time at 1300° F in the ultrahigh vacuum.

Stator

The stator performed with no degradation for 10,000 hours at 1300° F at a 10^{-9} torr range pressure environment. Inconel-clad silver electrical conductors did not change in electrical conductivity. Magnetic laminations showed improved magnetic performance (lower coercive force) after the endurance test. The electrical insulation system consisted of both "flexible" (glass fibers in a matrix of fused glass and oxides) and rigid insulation (high alumina slot liners, wedges, and spacers). Electrical insulation system performance improved (electrical leakage decreased and dielectric strength increased) during exposure. Functional and materials performance indicate that this stator was capable of operating for a much longer period of time at 1300° F in an ultrahigh vacuum.

SECTION III

TRANSFORMER AND SOLENOIDS

BACKGROUND AND CONSTRUCTION OF TRANSFORMER AND SOLENOIDS

A transformer and two solenoids were endurance-tested for 5000 hours at 1300° F in high vacuum on a previous program (ref. 5). Design, test details, and test results have been reported in reference 5. Cutaway views of the transformer and solenoids are shown in figures 37 and 38 respectively. Materials summaries for transformer and solenoids are given in tables 14 and 15 respectively.

During the course of the 5000-hour endurance test the transformer primary (high voltage) winding suffered a failure after 244 hours at 1300° F. At the time of failure, it was believed that the winding shorted turn-to-turn resulting in an open winding after failure. Preliminary analysis was that the failure resulted from abrasion of the glass conductor insulation between two adjacent turns, and was caused by mechanical forces generated between the high and low voltage windings in the energized transformer. This analysis remained to be verified by post-test investigation. After failure, the test was continued with 600 volts ac applied across each winding to ground, to investigate the effects of long term voltage stress on insulation performance.

One solenoid was continuously energized during the test except as required for taking weekly electrical performance readings. The second solenoid was intermittently energized during the test period for weekly electrical performance readings. The energized solenoids supported a 3.0 pound weight during the test exposure period.

After approximately 984 hours of endurance testing, the continuously energized solenoid insulation system performance indicated that the conductor was grounded either somewhere along the lead or inside the solenoid winding. However, the solenoid continued to actuate and remain energized with the previously applied winding voltage and current.

The continuously energized solenoid performance continued until approximately the 4899th hour of the endurance test. At that time a second circuit to ground was affected and the solenoid could no longer be energized. Solenoid lead-to-lead resistance, measured outside the chamber, was in the order of 0.02 ohms. After completion of the 5000-hour test, the test chamber was placed on room ambient temperature standby. An ultra-high vacuum environment was maintained inside the chamber pending

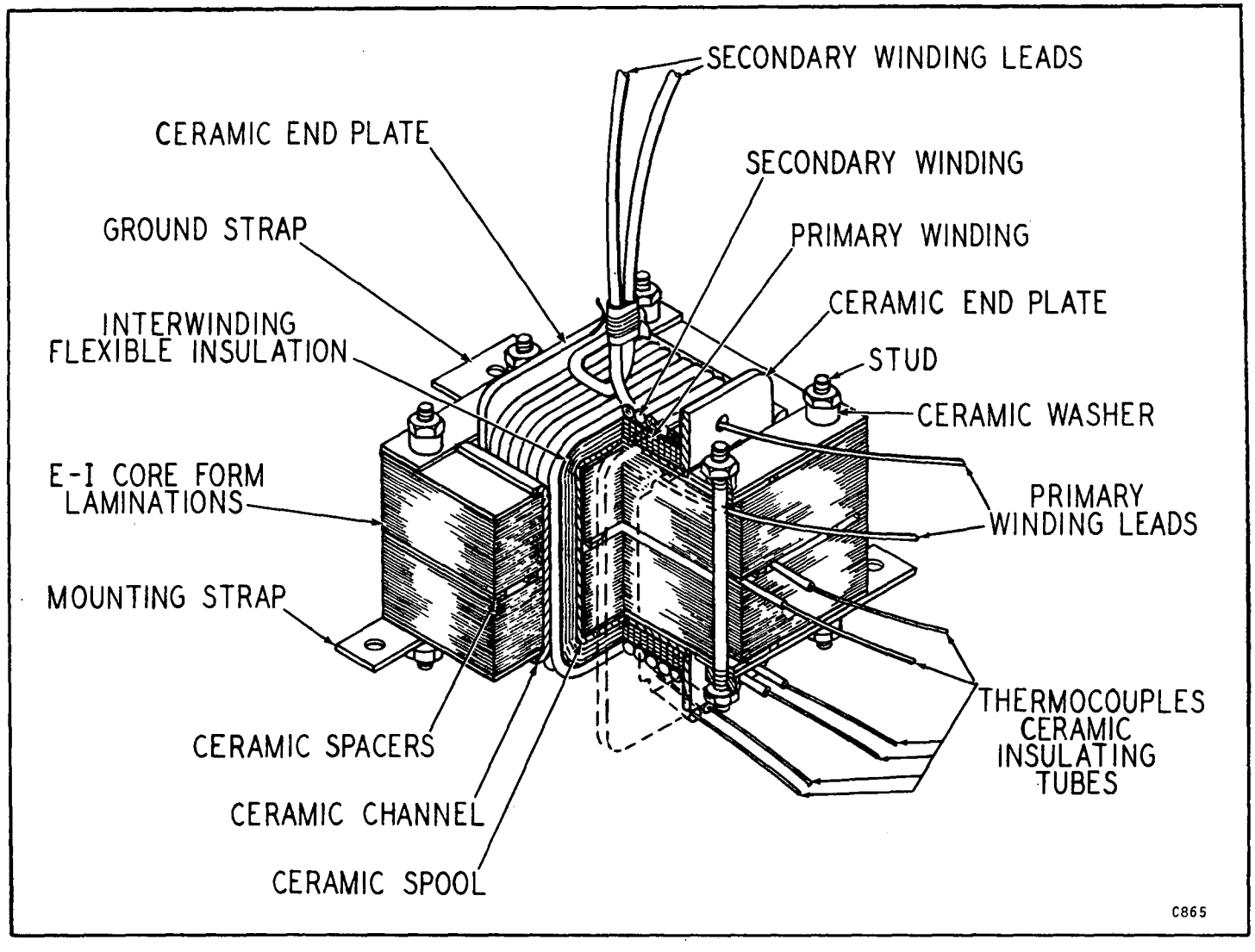

Figure 37. - Cutaway View of Transformer

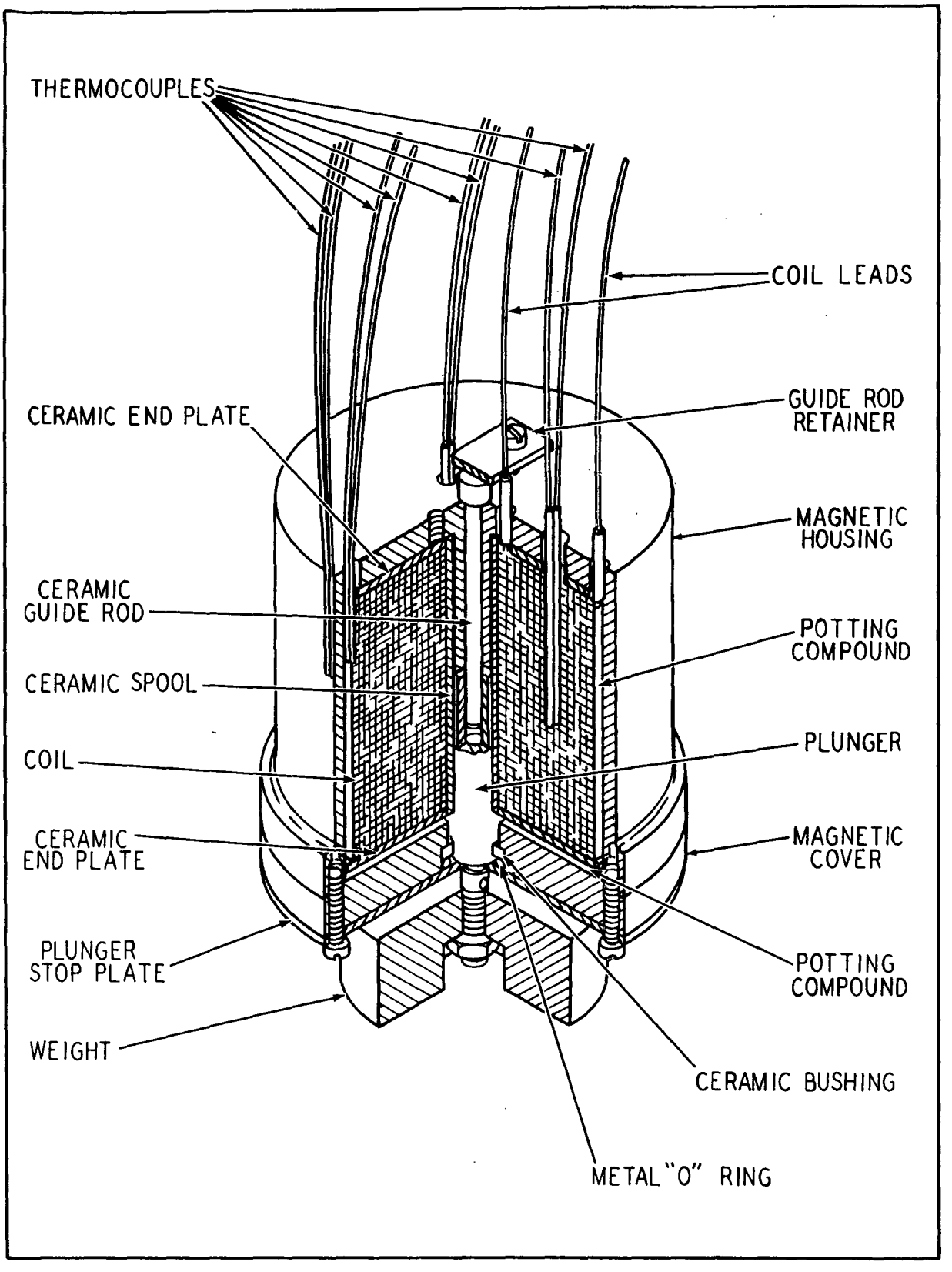

Figure 38. - Cutaway View of Solenoid.

Table 14. - Transformer - Magnetic, Insulation and Conductor Materials Summary

Part	Material	Reference For Additional Information
Laminations	Iron-27% Cobalt Sheet[a], 0.008-Inch Thick	Reference 1
Interlaminar Insulation	Plasma-arc sprayed Al_2O_3[b] (99.995%)	Reference 1
Coil Spool	Al_2O_3 (99.5%)	Reference 2
Coil End Plates	Al_2O_3 (99.5%)	
Coil Channels	Al_2O_3 (99.5%)	
Thermocouple Insulators	Al_2O_3 (99%)	Reference 2
Stud Spacer	Al_2O_3 (99%)	
Lamination Spacer	Al_2O_3 (99%)	
Flexible Insulation	Boron nitride fiber mat	
Conductor Insulation	Glass fiber double serving overcoated with a proprietary oxide-loaded silicone wire enamel[c].	Reference 2
Potting Compound	Boron nitride chopped fiber cement	
Conductors - Wire Sizes #20 and #7 AWG	Inconel-Clad Silver - (28% Inconel 600 Cross-Sectional Area)	Reference 2
Lamination Support Plates	Nickel Base Super Alloy[d]	
Hardware	Nickel Base Super Alloy[d]	
Thermocouples	Inconel 600 Sheath - Platinel II Wire System	

(a) - Hiperco 27 Alloy supplied by Westinghouse Electric Corp., Blairsville, Pa.
(b) - Linde A supplied by Linde Division, Union Carbide Corp., East Chicago, Ind.
(c) - Anadur "S" supplied by Anaconda Wire and Cable Co., Muskegon, Mich.
(d) - Hastelloy B manufactured by the Stellite Division of Union Carbide Corp., Kokomo, Ind.

Table 15. - Solenoid - Magnetic, Insulation and Conductor Materials Summary

Part	Material	Reference For Additional Information
Housing	Iron-27% Cobalt Forging[a]	Reference 1
End Bell	Iron-27% Cobalt Forging[a]	
Plunger	Iron-27% Cobalt Forging[a]	
Plunger Bushing	Al_2O_3 (99.5%)	Reference 2
Plunger Guide Rod	Al_2O_3 (99.5%)	
Coil End Plates	Al_2O_3 (99.5%)	
Coil Spool	Al_2O_3 (99%)	Reference 2
Coil Lead Insulators	Al_2O_3 (99%)	
Thermocouple Insulators	Al_2O_3 (99%)	
Conductor Insulation	Glass fiber double serving overcoated with a proprietary oxide-loaded silicone wire enamel.[b]	Reference 2
Potting Compound	Boron nitride chopped fiber cement	
Conductors - Wire Size #20 AWG	Inconel 600-Clad Silver - (28% Inconel 600 Cross-Sectional Area)	Reference 2
End Plates, Stop Plate, Hardware	Nickel Base Super Alloy[c]	
Weight	Tungsten Base Heavy Alloy[d]	
Thermocouples	Inconel 600 Sheath - Platinel II Wire System	
Metal "O" Ring	321 Stainless Steel	

(a) - Hiperco 27 Alloy supplied by Westinghouse Electric Corp., Blairsville, Pa.
(b) - Anadur "S" supplied by Anaconda Wire and Cable Co., Muskegon, Mich.
(c) - Hastelloy B manufactured by the Stellite Division of Union Carbide Corp., Kokomo, Ind.
(d) - Mallory 1000 manufactured by R.P. Mallory Co. Inc., Indianapolis, Ind.

completion of the second 5000 hours of stator endurance testing at 1300° F.

POST 5000-HOUR ENDURANCE TEST PROCEDURES, TESTS, EXAMINATIONS, AND ANALYSES OF TRANSFORMER AND SOLENOIDS

Final electrical performance readings were taken with the test chamber still under an ultrahigh vacuum environment (3.0×10^{-10} torr) for comparison with values obtained during the 9700-hour standby period. Conductor resistance values in the transformer secondary (low voltage) winding and unenergized solenoid winding remained unchanged during the room temperature standby period. Transformer primary winding and energized solenoid conductor resistance could not be measured for reasons described earlier. Measurable insulation performance values in the three components also remained unchanged during the standby period.

After measurements were completed, the test chamber was raised to ambient pressure using dry nitrogen as the cover gas, and the top cover was removed. Figure 39 is a photograph of the top of the test chamber after cover removal. Thermocouples were brought through the top heat shields in groups of eight. Transformer and solenoid leads are as noted on the photograph. Inspection showed that both lead wires to the energized solenoid were grounded to the top chamber heat shield. The hollow aluminum tubes which were used to insulate the leads as they passed through the heat shields had slipped down, one at a time, until each lead became grounded to the chamber. After the insulators were pulled back into position, the solenoid functioned normally, repeating pre-test bench test values for conductor resistance and insulation performance. Voltage and current values required to pick up and hold the plunger and weight also repeated pre-test bench test values. Thus, the energized solenoid did not suffer an internal failure. The problem was caused by chamber installation procedure and the vibrations that occurred in the test area.

Figure 40 is a view of the chamber with the top heat shields removed. The transformer and two solenoids are shown in position on the model support fixture. Figure 41 is another view of the solenoids with the transformer removed from the chamber. The generally clean condition of the test chamber can be noted by the reflections inside the heating element and on the outside of the outer heat shield. Figure 42 shows the test chamber with the solenoids and support fixture removed.

This page is reproduced at the back of the report by a different reproduction method to provide better detail.

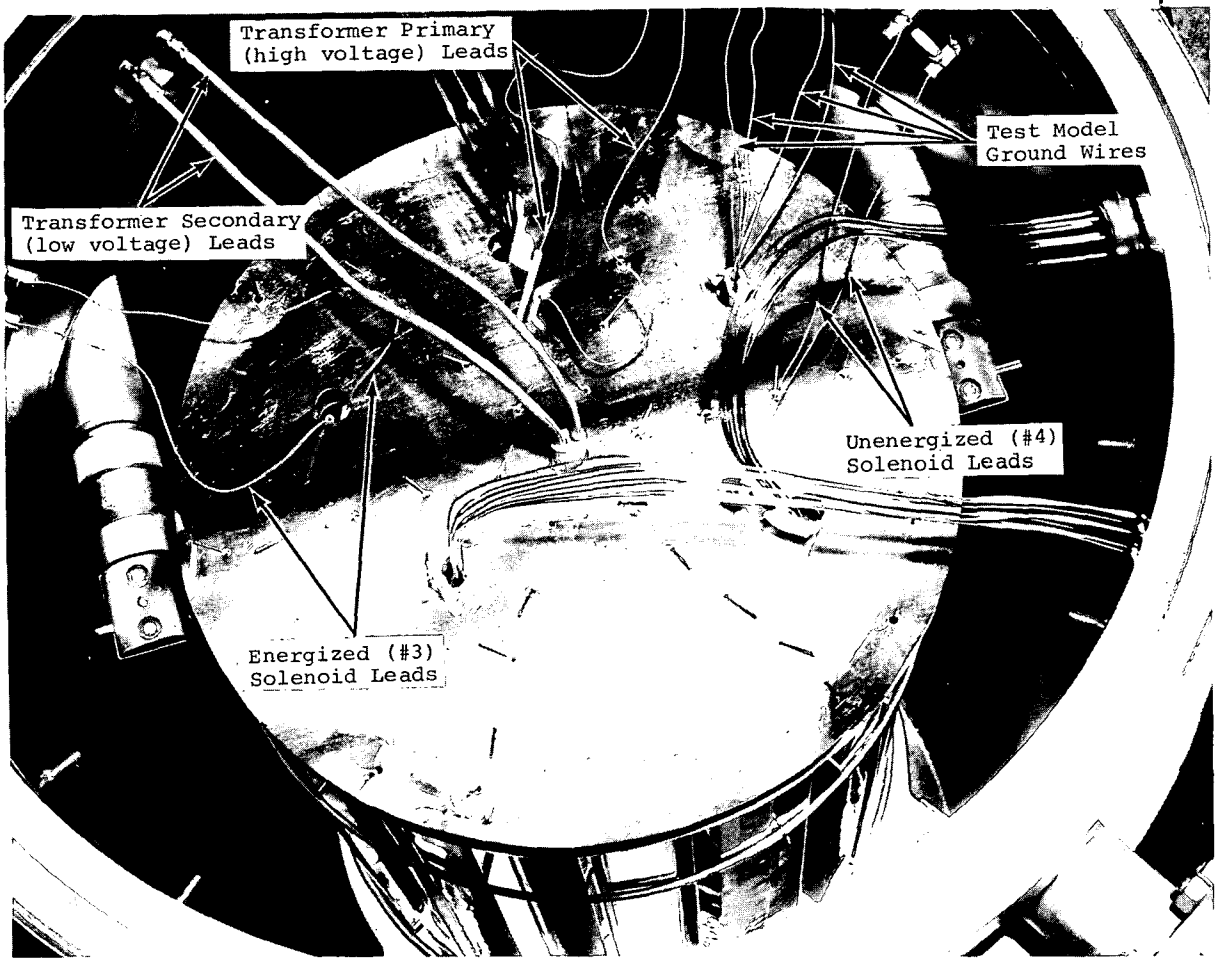

Figure 39. - Transformer and Solenoid Test Chamber with Top Removed After Thermal Vacuum Testing.

This page is reproduced at the back of the report by a different reproduction method to provide better detail.

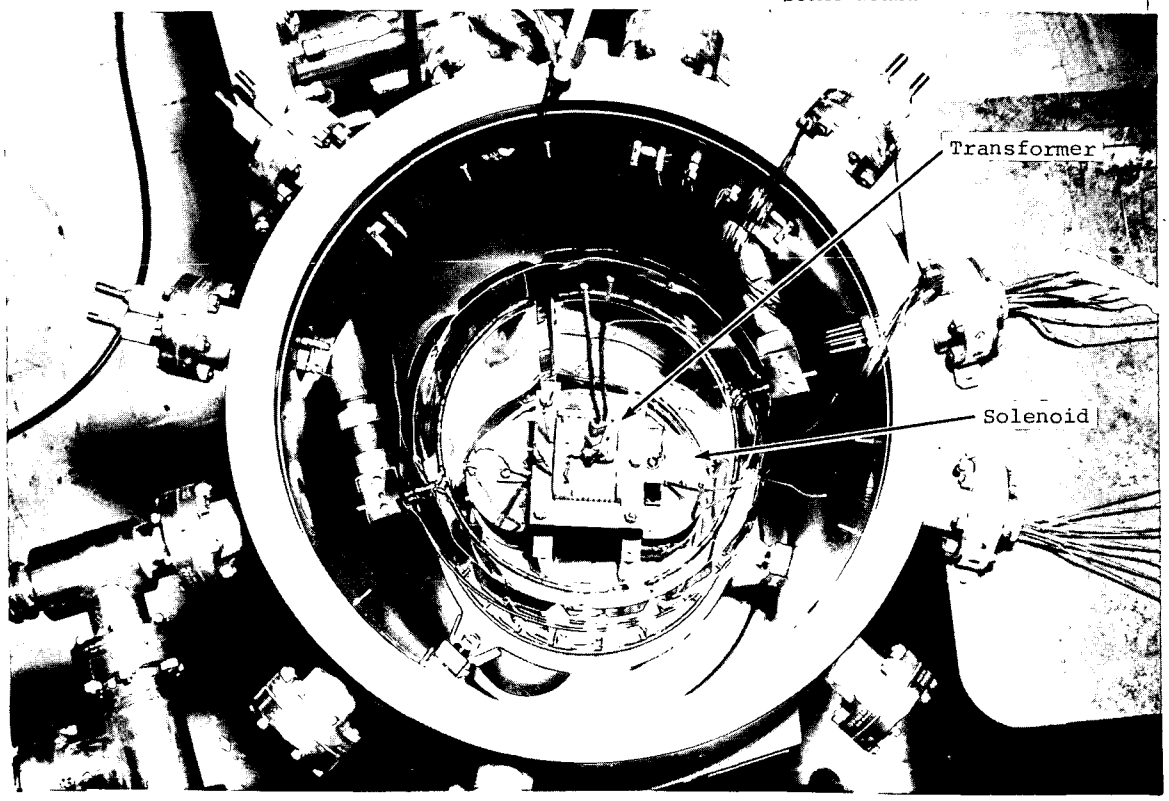

Figure 40. - Photograph of the Transformer and Two Solenoids in the Test Chamber With Top Heat Shields Removed After Thermal Vacuum Testing.

This page is reproduced at the back of the report by a different reproduction method to provide better detail.

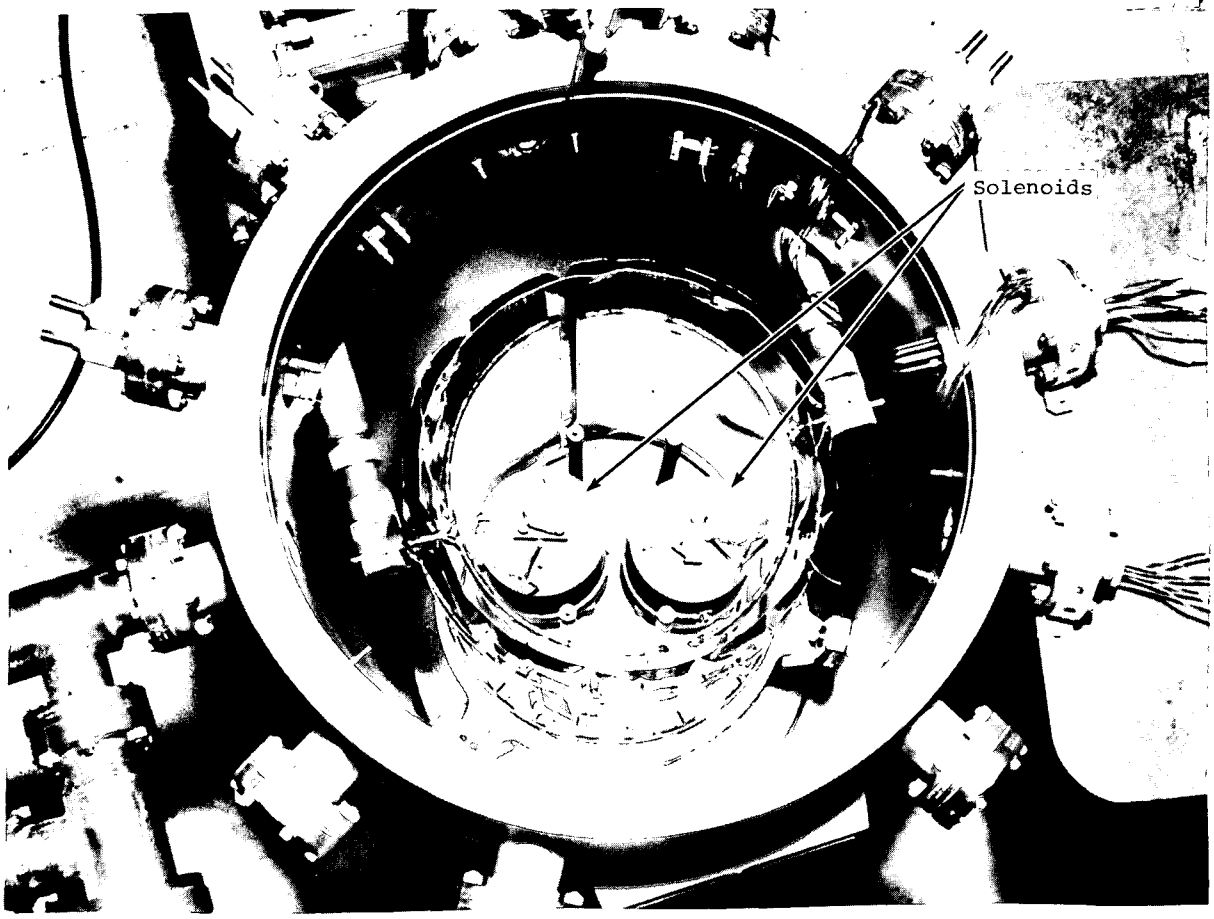

Figure 41. - Photograph Showing the Two Solenoids in the Test Chamber After Thermal Vacuum Testing. Transformer Has Been Removed.

This page is reproduced at the back of the report by a different reproduction method to provide better detail.

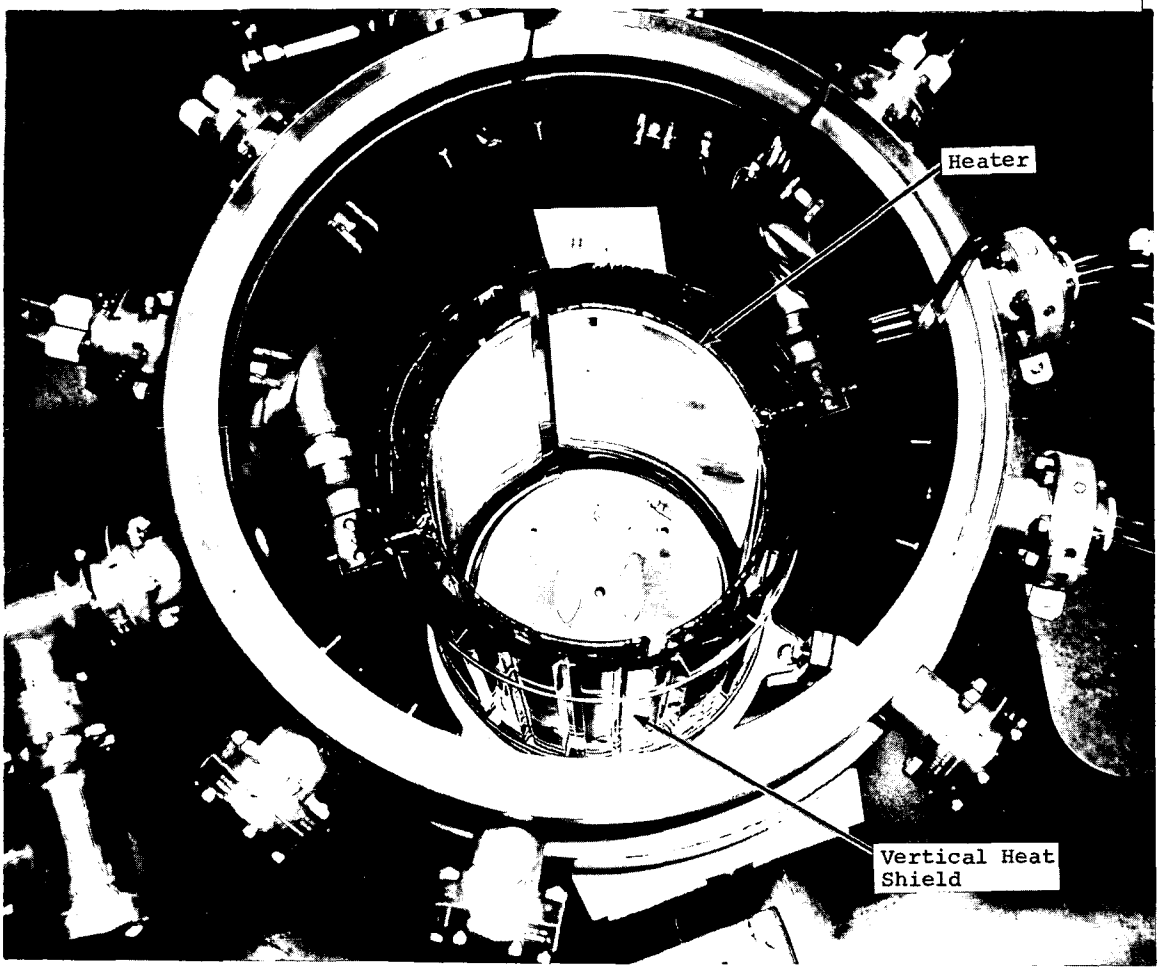

Figure 42. - Photograph of the Interior of the Test Chamber After Thermal Vacuum Testing. Transformer and Two Solenoids Have Been Removed.

Figure 43 is a photograph of the transformer, solenoids and support fixture. The powdery material seen on the flat surfaces is loose conductor insulation which was disturbed when dry nitrogen was admitted to bring chamber pressure up to ambient pressure. The weight from the continuously energized solenoid is also displayed in the photograph.

Transformer

Electrical Tests and Data. - Table 16 gives the transformer endurance test and post-endurance test electrical performance data at room temperature and ambient pressure. The primary (high voltage) winding had shorted after 244 hours of endurance test at 1300° F. The result of the short was a separation within the winding, which is the reason for the extremely high post-endurance test conductor resistance. The secondary winding (low voltage) did not show a change in resistance as a result of the endurance test. The dc insulation showed improvement for each winding-to-ground reading as a result of the endurance test, in a manner similar to the stator performance improvement (see Section II, Evaluation of Stator Electrical and Bore Seal Capsule Functional Performance After 10,000-Hour, 1300° F Simulated Space Endurance Testing, Stator Electrical Performance paragraph). Insulation resistance between the two windings was reduced 50 percent probably as a result of the primary winding failure. The insulation system ac leakage current showed an increase in post-test values, but the level was still quite low.

Visual Examination. - Visual examination showed all exterior surfaces to be discolored. The normally white insulation and bright metal surfaces had a dull gray appearance, due to the deposition of evaporated materials. The ceramic spool end plates had a pattern of deposits indicating line-of-sight deposition.

Disassembly and Failure Analysis. - When bench testing had been completed, the transformer and two solenoids were disassembled for materials analysis. One portion of the transformer disassembly procedure was to investigate a primary (high voltage) winding failure which has occurred early in the 1300° F hot-spot endurance test. After approximately 244 hours of endurance testing, the primary winding had developed a turn-to-turn short circuit that resulted in the formation of an open circuit within the winding. At the time of failure, the transformer primary winding was carrying 1.86 amps at 600 volts ac and the secondary (low voltage) winding was carrying 20.8 amps at 32 volts ac. The transformer primary winding consisted of five layers (174 turns) of No. 20 AWG (0.032-inch diameter) Inconel-clad silver wire formed around a rectangular cross section alumina coil form or spool. Boron nitride fiber flexible sheet insulation approxi-

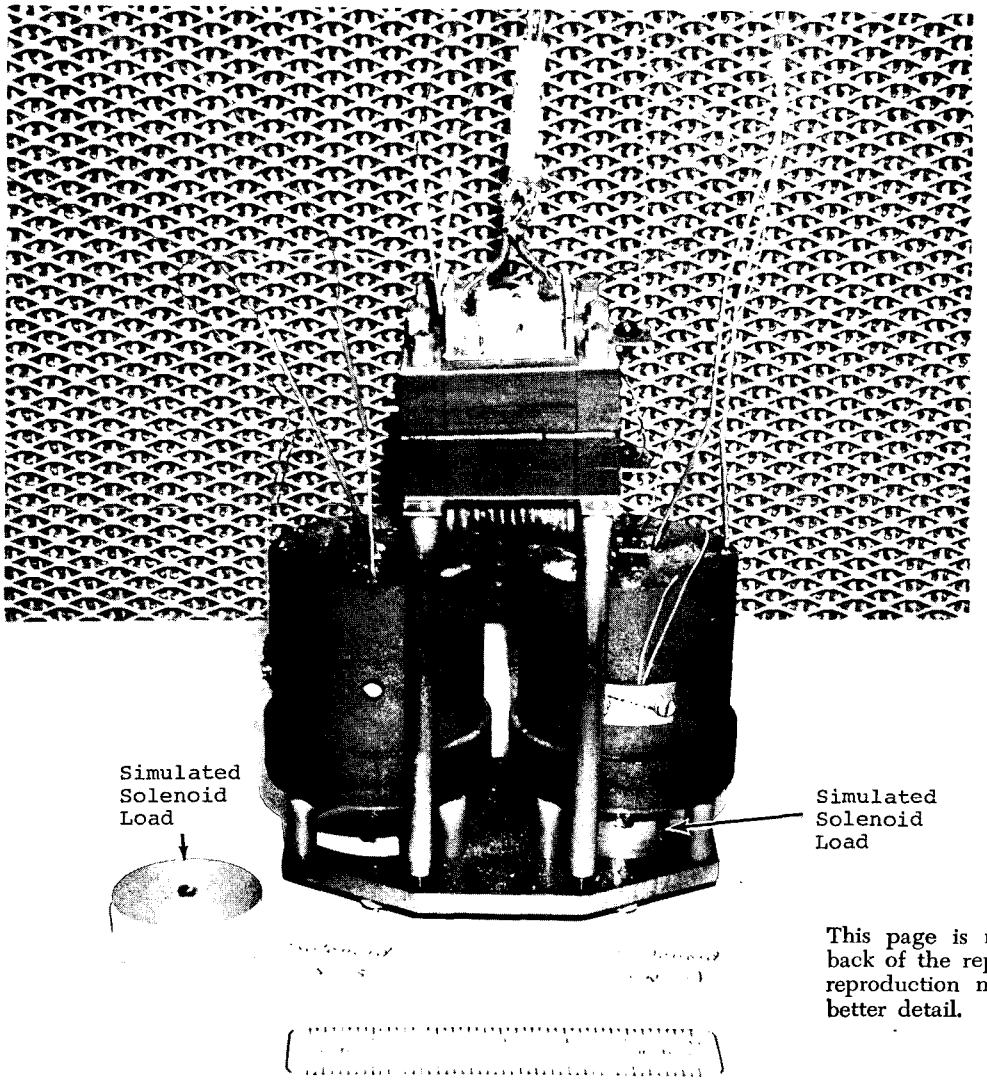

This page is reproduced at the back of the report by a different reproduction method to provide better detail.

Figure 43. - Photograph of the Transformer and Two Solenoids After Thermal-Vacuum Testing.

Table 16. - Comparison of Transformer Room Temperature Bench Test Electrical Data Taken Before and After a 5000-Hour Thermal Vacuum Exposure.

MEASUREMENT	TRANSFORMER WINDING (a)	BEFORE ENDURANCE TEST		AFTER ENDURANCE TEST	
		OHMS	TEMPERATURE (°F)	OHMS	TEMPERATURE (°F)
Conductor Resistance	Primary(b)	1.7640	72	3×10^9	78
	Secondary	0.0080	72	0.00805	78
		MEGOHMS @ 500 Vdc	TEMPERATURE (°F)	MEGOHMS @ 500 Vdc	TEMPERATURE (°F)
DC Insulation Resistance	Primary to Secondary(b)	7×10^4	72	3.5×10^4	78
	Primary to Ground	1.45×10^4	72	4.3×10^4	78
	Secondary to Ground	5.5×10^4	72	8.0×10^4	78
		MICROAMPS @ 500 Vac	TEMPERATURE (°F)	MICROAMPS @ 500 Vac	TEMPERATURE (°F)
AC Leakage Current	Primary to Secondary(b)	< 1	72	14	78
	Primary to Ground	< 1	72	9	78
	Secondary to Ground	< 1	72	9	78

(a) Transformer windings are designated as primary (high voltage) and secondary (low voltage) for winding conductor resistance measurements.

(b) Primary (high voltage) winding failed after 244 hours at test temperature (1300°F hot spot).

mately 0.010-inch thick was installed between each pair of layers. The secondary winding consisted of a single layer (10 turns) of No. 7 AWG (0.144-inch diameter) Inconel-clad silver wire formed around the outside of the primary winding and separated from it by approximately 0.040-inch of flexible boron nitride sheet insulation. The magnetic stack consisted of 0.008-inch-thick E and I laminations of iron-27% cobalt alloy.

After removal of the laminations from the transformer assembly, the combined windings and alumina spool were visually inspected for evidence of failure. No failure indications were noted. Both windings were then separated from the alumina spool. A small metallic stain was noted along one of the rounded corners that joined the four flat sides making up the rectangular cross-section alumina coil form. Inspection of the primary winding showed a hole, roughly circular and approximately 5/16-inch in diameter, where the innermost two winding layers had been perforated and the resulting loose ends fused together around the hole. This hole was located in a position corresponding to the location of the stain. The primary and secondary windings were separated for further investigation. There was no evidence of an induced failure reaction in the secondary winding or in the outer layer of the primary winding.

The primary winding was unwound, one layer at a time, starting with the outer layer. No signs of winding failure were evident until two layers had been removed. The third layer conductor insulation had a very small black stain overlying the failed spot. The third conductor layer was unwound and when the stained spot was reached, the conductor turn passing through the stain area was found to be completely separated. This explains the open circuit even though most of the failed area adjacent turns ends were fused together. Figure 44 shows the fourth layer conductors from the failure region looking into the transformer. Figure 45 shows the fifth layer in the foreground and behind it the fourth layer. There is a larger void region in the fifth layer than in the fourth layer.

Examination and Analysis of Magnetic Materials. - After 5000 hours of endurance testing of the transformer in ultrahigh vacuum, the stack of iron-27% cobalt magnetic laminations was disassembled for examination. Adjacent laminations adhered to each other and the laminations were brittle. A typical pair of adhering laminations as well as separated laminations were subjected to metallographic examinations. Other laminations were selected for magnetic testing, microhardness surveys, and analysis for carbon. Test and analyses results are included in tables 17, 18 and 19. Unaged, but processed, transformer laminations are compared with laminations from the transformer after the elevated temperature 5000-hour test at a pressure in the 10^{-9} torr range.

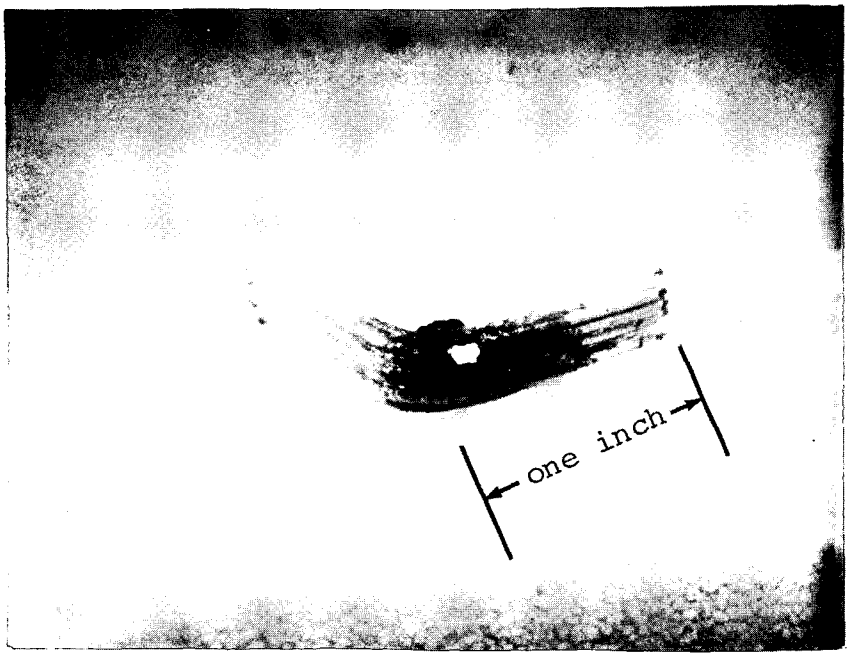

Figure 44. - View, After Disassembly, of the Failure Region in the 1300° F Transformer, Primary Winding, Fourth Layer from the Outside.

This page is reproduced at the back of the report by a different reproduction method to provide better detail.

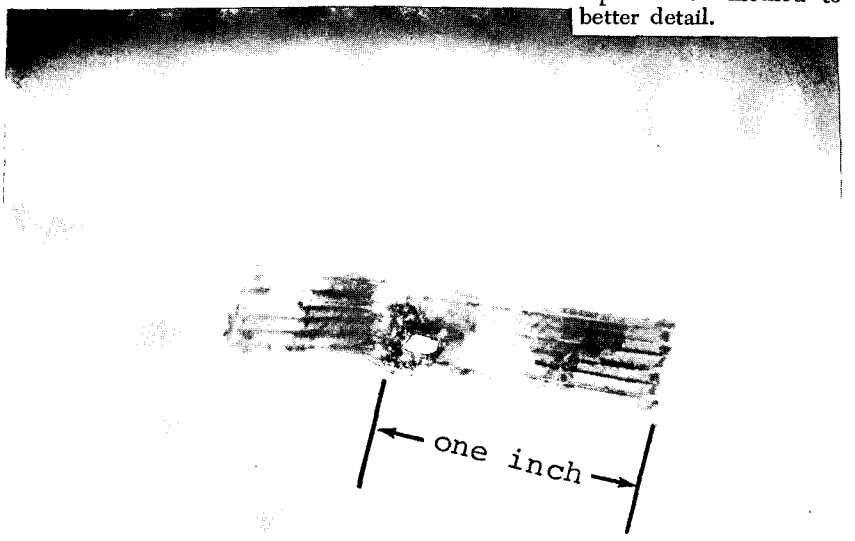

Figure 45. - View, After Disassembly, of the Failure Region in the 1300° F Transformer, Primary Winding, Fifth Layer from the Outside in the Foreground.

Table 17. - Magnetic Properties (Coercive Force)[a] of Magnetic Materials Unaged and From High Temperature Transformer and After 1300° F, 5000-Hour Endurance Testing at a Pressure in the 10^{-9} Torr Range.

Description of Specimen	Specimen Condition	Room Temperature Coercive Force H_c (oersteds)
Iron-27% Cobalt Transformer Laminations, 0.008-Inch Thick	Unaged lamination, with plasma arc sprayed alumina interlaminar insulation	1.64
Iron-27% Cobalt Transformer Laminations, 0.008-Inch Thick. Laminations from Center of the Transformer.	After 5000-hour transformer exposure test at 1300° F[b] and a pressure in the 10^{-9} torr range	1.80
Iron-27% Cobalt Transformer Laminations, 0.008-Inch Thick. Laminations from Outside Area of the Transformer.	After 5000-hour transformer test at 1300° F and a pressure in the 10^{-9} torr range	1.82

(a) Coercive force measurements were made using a precision Coercive Force Meter manufactured by the Institute Förster, Reutlingen, West Germany. Accuracy of all measurements was ±2 percent.

(b) Transformer was energized for 244 hours. After this time, the temperature decreased to 1170° F.

Table 18. - Interstitial Carbon Content[a] of Iron-27% Magnetic Materials Before and After Endurance Testing in a Transformer at 1300°F for 5000 Hours and a Pressure in the 10^{-9} Torr Range.

Description of Specimen	Specimen Condition	Interstitial Content of Carbon (ppm)
Iron-27% Cobalt Transformer Lamination, 0.008-Inch Thick	Unaged Lamination	99
Iron-27% Cobalt Transformer Lamination 0.008-Inch Thick	After 5000-Hour transformer test at 1300° F at a pressure in the 10^{-9} torr range	18

(a) All analyses were made by the Westinghouse R & D Center. Carbon by combustion. Accuracies are as follows:

Carbon at	20ppm	± 10%
at	50ppm	± 6%
at	250ppm	± 3%

Coercive force was used to indicate changes in magnetic quality of the alloy as a result of high temperature vacuum aging. Coercive force values of two aged samples of "I" lamination were each slightly higher than that of the unaged sample (table 17). These slightly higher values may be attributed to strains induced when disassembling adhering specimens. The 244 hours of magnetic field exposure at 1300° F starting the 5000 hours of thermal aging did not produce a detectable residual magnetic annealing effect. The temperature of the transformer after 244 hours stabilized at 1190° F for the remainder of the 5000-hour exposure test.

Results of carbon analyses for the unaged transformer laminations and those aged for 5000 hours are shown in table 18. Carbon content decreased from 99 ppm to 18 ppm. As indicated

Table 19. - Knoop Hardness of Magnetic Laminations From the High Temperature Transformer Before and After Thermal Endurance Testing at a Pressure in the 10^{-9} Torr Range.

Description of Specimen	Specimen Condition	Microhardness[a] Knoop (25 gm)			Remarks
		Edge	Center	Edge	
Iron-27% Cobalt Transformer Lamination, 0.008-Inch Thick	Unaged Lamination with Plasma Arc Sprayed Alumina	258	229	224	Ductile in Bending
Iron-27% Cobalt Transformer Laminations, 0.008-Inch Thick. Laminations from Center of the Transformer.	After 5000-hour transformer test at 1300° F and a pressure in the 10^{-9} torr range	320	241	362	Brittle in Bending
Iron-27% Cobalt Transformer Laminations, 0.008-Inch Thick. Laminations from the Outside Area of the Transformer.	After 5000-hour transformer test at 1300° F and a pressure in the 10^{-9} torr range	337	269	411	Brittle in Bending

(a) Each value shown is the average of five test indentations.

in the case of the stator laminations, depletion occurred by reaction of oxygen with carbon with subsequent evolution of carbon monoxide.

Transformer/lamination microstructure was examined. Typical micrographs are shown in figure 46. Oxide penetration appears pronounced on both sides in the aged (5000 hours) transformer lamination; in fact it was greater than that which occurred in the stator laminations that had been aged for a longer period. There was a three-to-five fold increase in grain size in the center portion of the aged transformer lamination over that in the unaged specimen (see figure 46(b) and 46(d)). However, it should be noted that grain growth near the lamination surface was minimal. The oxide had diffused rapidly along the grain boundaries near the lamination surface, thus inhibiting grain growth in this area. Bulk diffusion proceeded at a slower rate.

A pair of bonded laminations is shown in figure 46(c). Surface oxide had bridged the spacing between laminations resulting in laminations adhering to each other.

Microhardness surveys revealed increased hardness across the lamination (table 19) with more significant increases near the lamination surface. The microstructure revealed indications of grain boundary brittleness. However, the increase in brittleness is not critical in this static application of iron-cobalt magnetic laminations.

Interlaminar Insulation. - The laminations of the transformer core were strongly adhered over most of their contacting surfaces. As noted above, the electrical steel was embrittled. These two conditions prevented an evaluation of electrical properties of the interlaminar insulation itself.

Metallurgical Examinations of Conductors. - Specimens of aged and unaged transformer primary and secondary Inconel-clad silver conductors were examined and compared. Unaged secondary conductor microstructure is shown in figure 47 and that of aged secondary conductor is shown in figure 48. The aged silver had a larger grain size than that of unaged silver as would be expected from thermal aging. Inconel in the unaged conditions had a uniform small grain structure while that in the aged condition had a thermal aging induced duplex structure; that is, areas of large and small grains. Small voids were observed at or near the Inconel-silver interface and are shown in figure 49. Voids appear to be the result of cladding defects, (e.g. surface contamination at the interface of the composite which prevented bonding) and not the result of aging or silver melting. No voids were observed in the unaged specimen.

Microstructures of transformer primary conductors are shown unaged in figure 50 and as aged in figure 51. Grain growth due to thermal aging occurred in both the silver and the Inconel. Grain growth was as expected and was similar to that found in the aged secondary conductor. No evidence of voids was found in either aged or unaged primary conductor specimen.

Boron Nitride Paper Insulation. - Boron nitride paper insulation specimens taken from the aged transformer were unchanged in visual appearance except in the immediate region of the electrical fault where severe damage was evident. The paper in the non-faulted area was white, flexible and retained its normal handling characteristics. Table 20 shows the results of X-ray diffraction analysis of unaged and aged boron nitride paper. No boron oxide (B_2O_3) was detected by this technique. Table 21

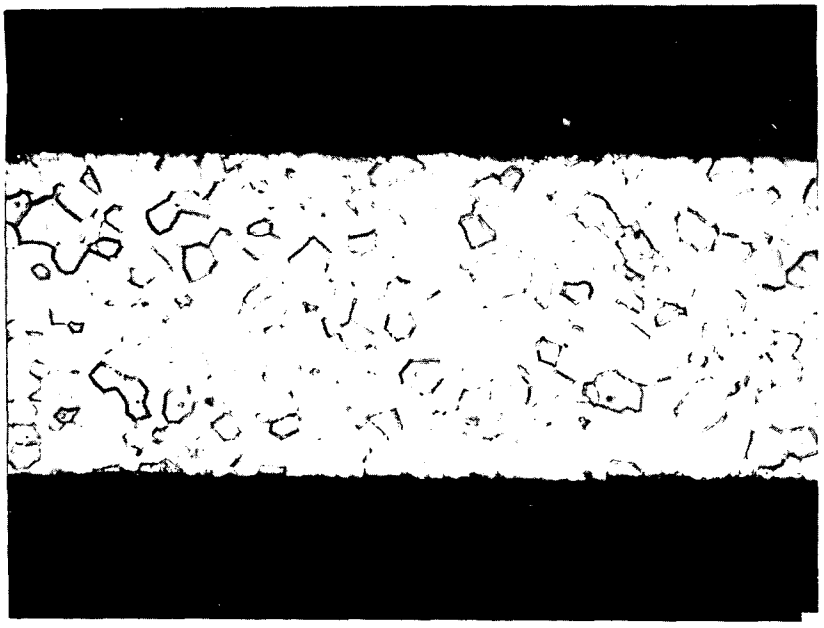

200 X

(a)

500 X

(b)

Figure 46. - Photomicrographs of Iron-27% Cobalt Magnetic Laminations from the Transformer Before and After Thermal Aging for 5000 Hours at a Pressure in the 10^{-9} Torr Range.

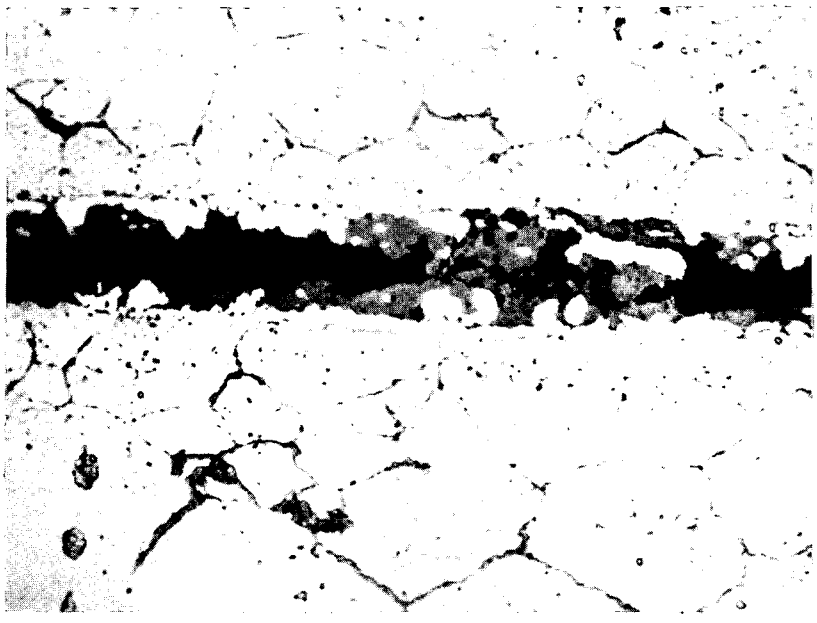

(c)

This page is reproduced at the back of the report by a different reproduction method to provide better detail.

(a) Unaged iron-27% cobalt transformer lamination with plasma arc sprayed alumina interlaminar insulation (99.99+% Al_2O_3) applied, 200X.

Etchant: $50HNO_3$, $45CH_3$, COOH, $5H_2O$

(b) Unaged iron-27% cobalt transformer lamination with plasma arc sprayed alumina interlaminar insulation applied, 500 X.

(c) Iron-27% cobalt laminations with plasma arc sprayed interlaminar insulation applied, after 5000 hours aging at 1300° F, unetched, 1000X. Note area of "cold-weld" - area between laminations bridged by oxide caused adherence of adjacent laminations.

(d) See next page.

Figure 46. - Continued.

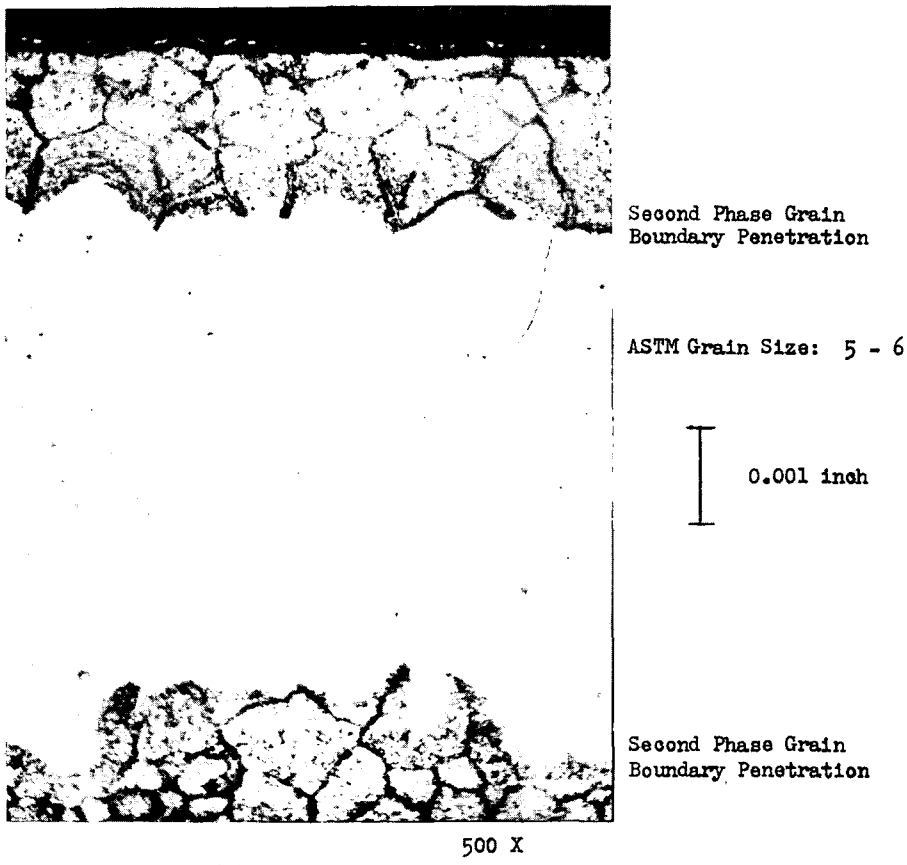

(d)

This page is reproduced at the back of the report by a different reproduction method to provide better detail.

(d) Iron-27% cobalt transformer lamination with plasma arc sprayed alumina interlaminar insulation applied, after 5000-hour thermal aging, unetched, 500X.

NOTE: Grain structure revealed by relief polishing.

Figure 46. - Photomicrographs of Iron-27% Cobalt Magnetic Laminations from the Transformer Before and After Thermal Aging for 5000 Hours at a Pressure in the 10^{-9} Torr Range. (Concluded)

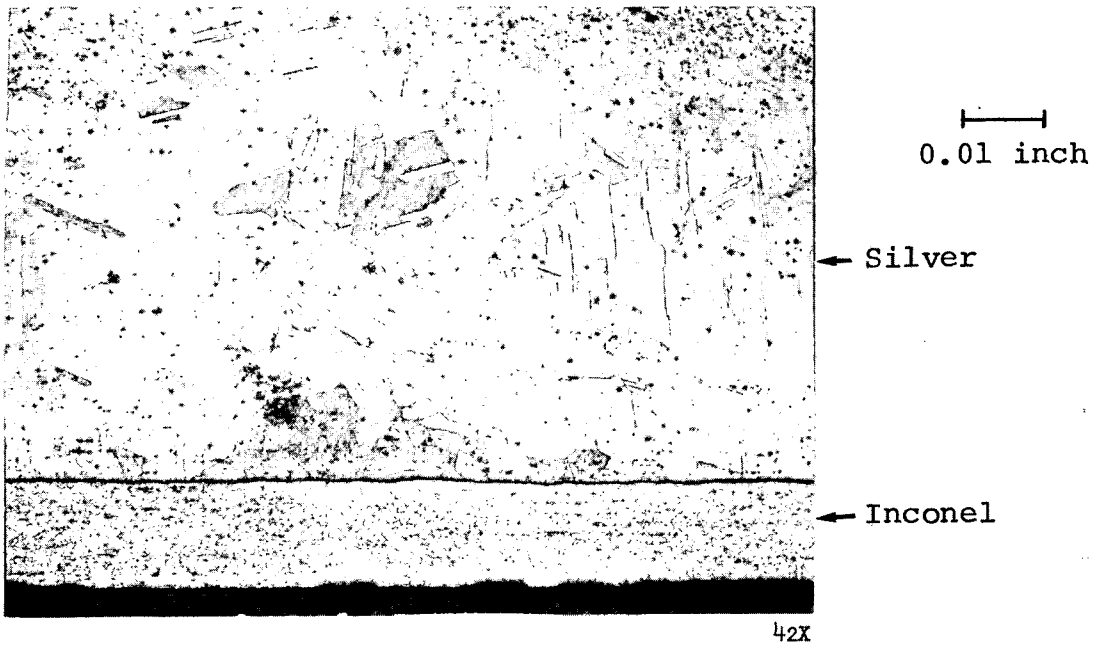

Figure 47. - Photomicrograph of Longitudinal Section of Unaged Transformer Secondary Conductor (42X)

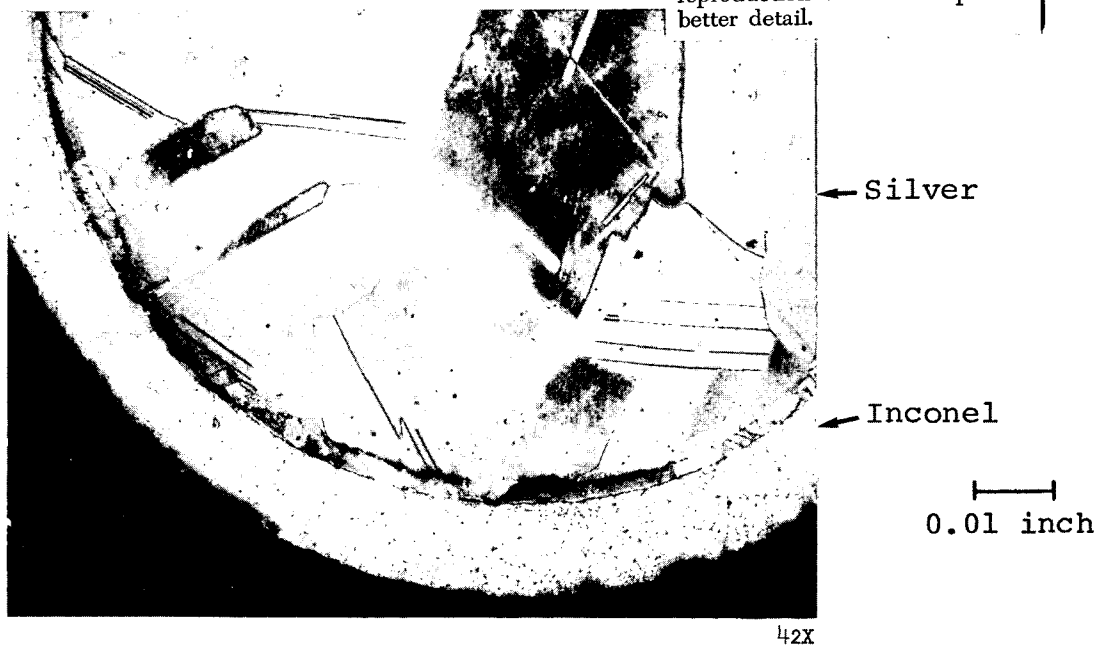

Figure 48. - Photomicrograph of Transverse Section of Transformer Secondary Conductor After 5000-Hour Thermal-Vacuum Exposure (42X)

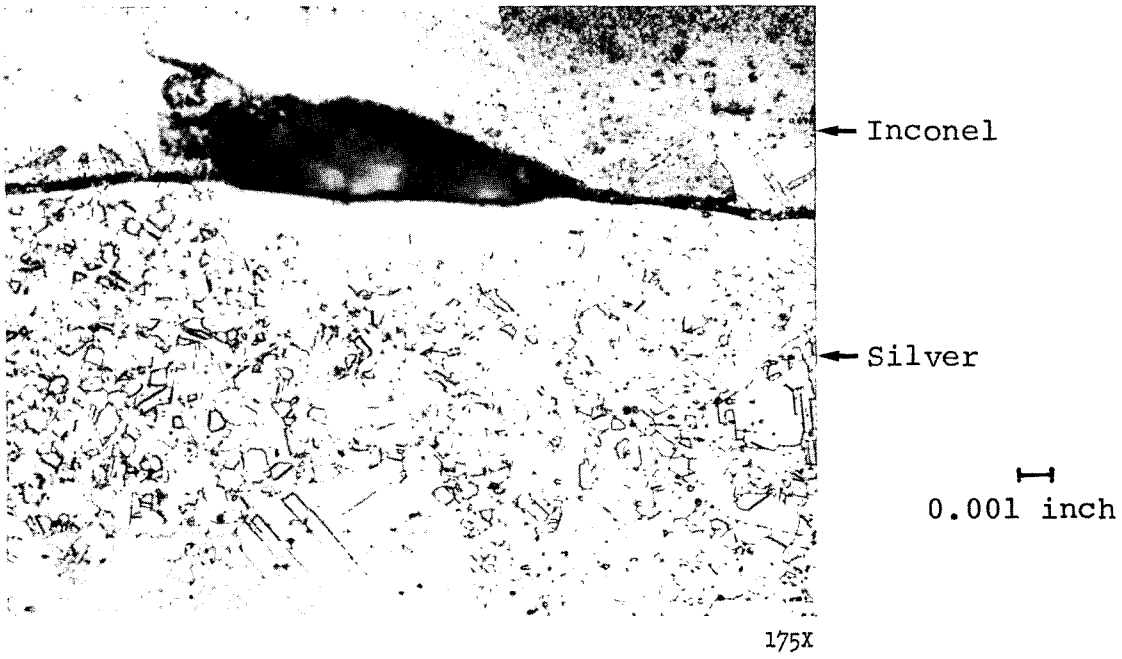

Figure 49. - Photomicrograph of Transverse Section of Transformer Secondary Conductor After 5000-Hour Thermal-Vacuum Exposure (175X)

This page is reproduced at the back of the report by a different reproduction method to provide better detail.

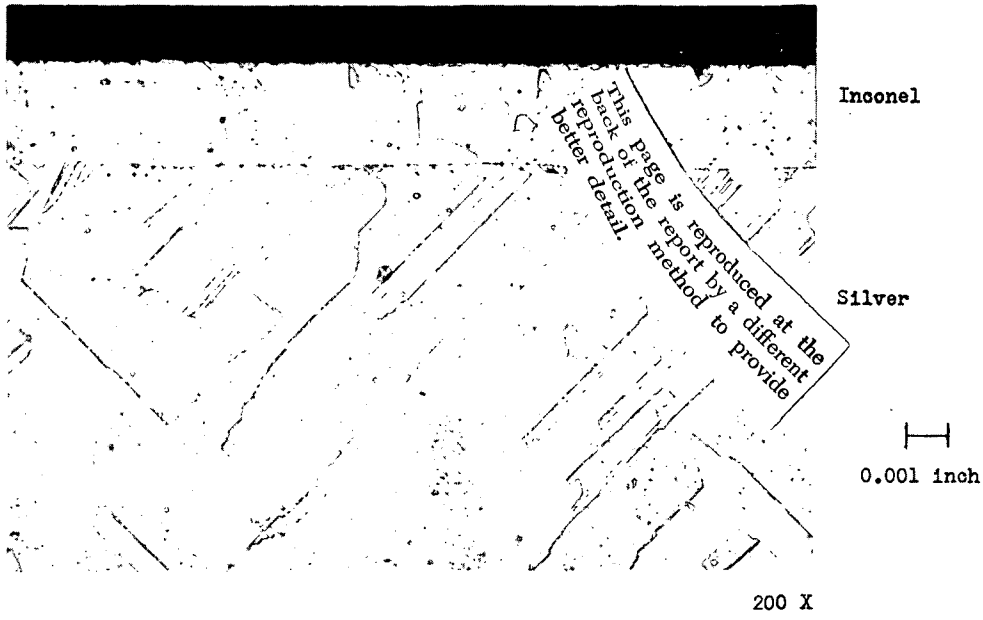

Figure 50. - Photomicrograph of Longitudinal Section of Transformer Primary Conductor After 5000-Hour Thermal-Vacuum Exposure. (200X)

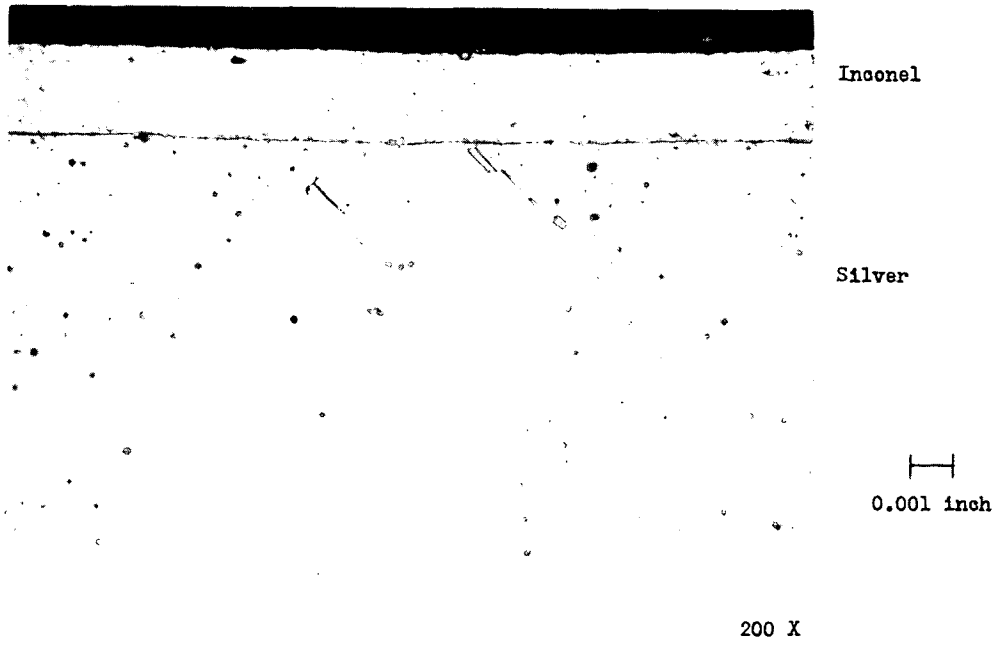

Figure 51. - Photomicrograph of Longitudinal Section of Unaged Transformer Primary and Solenoid Conductor. (200X)

Table 20. - X-Ray Diffraction Identification Analyses of Transformer Boron Nitride Fiber Composite Specimens Unaged and Aged for 10,000 hours at 1300° F in Ultrahigh Vacuum plus Control Specimens.

Sample	Compounds Detected
Boron Nitride Paper, Unaged	BN
Boron Nitride Paper, Aged in Transformer for 5000 Hours at 1300° F, 10^{-9} torr	BN
Control: 90% BN + 10% B_2O_3	BN, B_2O_3
Control: 50% BN + 50% B_2O_3	BN, B_2O_3

presents data on electrical performance in vacuum for unaged and aged specimens taken from the test transformer during the post aging evaluation disassembly. These data indicate no reduction in useful electrical properties attributable to the 5000-hour thermal-vacuum aging. Dissipation factor and resistance values improved slightly during the aging. The test specimen used for the aged values reported in table 21 was subjected to 4000 volts dc at 1400°F in the test assembly without insulation breakdown. This is equivalent to an electrical strength greater than 250 volts per mil.

Microscopic Examination of Conductor Electrical Insulation. - The electrical insulation on the aged transformer primary conductors which were fused together at the fault had lost nearly all adhesion to the metal surface. The interface was blackened and the insulation near the fault was fused, end glazed, losing

Table 21. - Electrical Performance of Boron Nitride Paper Insulation Unaged and Aged in Transformer For 5000 Hours at 1300° F and 10^{-9} Torr.

Temperature (°F)	Test Conditions: 0.016-Inch Thick Paper Between One-Inch Diameter, Flat Electrodes With 230 Grams Total Load at 10^{-6} Torr.					
	Power Factor (Percent at 10 kHz)		Dissipation Factor (tan δ)		Resistance (Ohms at 100 Vdc)	
	Unaged	Aged	Unaged	Aged	Unaged	Aged
60	--	8.24	--	0.0004	--	9×10^{9}
565	6.7	8.32	0.001	0.0006	7×10^{13}	5×10^{13}
910	6.81	8.34	0.01	0.0029	2×10^{11}	2×10^{10}
980	6.9	8.37	0.03	0.0057	2×10^{10}	9×10^{10}
1200	6.8	8.54	0.06	0.0252	3×10^{7}	3×10^{9}
1400	9.2	10.39	0.77	0.0284	2×10^{6}	6×10^{7}

the normal fibrous appearance as shown in figure 31. The insulation of the primary and secondary conductors in non-faulted areas appeared white, fibrous, and showed normal adhesion to the conductor surface. Metallographic specimens of aged conductor insulation are shown in figure 30.

Chemical Analysis of Conductor Electrical Insulation. - Samples of conductor electrical insulation aged on the transformer were removed from the primary and secondary windings and analyzed by the same techniques that are described in Section II, Evaluation, Relative to Aging, of Bore Seal Capsule and Stator Materials paragraph. These results are presented in table 22. Most levels of the sixteen elements investigated were unchanged by the aging. However, the chromium level was increased in the primary winding specimen. Analysis of the secondary winding insulation did not reveal any similar increase. Reductions of copper and zinc levels were noted in both windings. Only the primary winding showed a reduction in sodium. These changes are similar to those reported for the stator conductor insulation.

Ceramic Coil Form Deposits Analysis. - Two types of deposits were noted on the aluminum oxide coil form after disassembly. One was orange and the other was very dark, approaching black. Analyses of the substrate and the deposits are given in table 23. The orange specimen showed increases in the amounts of chromium, iron, cobalt, and nickel. The analysis of the dark deposit was similar to the orange but with much greater iron content plus increases in manganese and copper over that of the substrate. It is probable that the two discolored areas represent two stages in a single contamination process. The source may have been an assembly contact point where the magnetic laminations rubbed against the abrasive aluminum oxide coil form. These uncontrolled and inconsistent contacts would develop nonuniform deposits which would age unevenly. The performance of the insulation component at the rated voltage of this device would not be degraded by this condition.

Solenoids

Electrical Tests and Data. - Table 24 compares pre-test and post-endurance test room ambient environment electrical performance data for the two solenoids. Post-test conductor resistance values were within experimental accuracy of pre-test values when post-test values were corrected for temperature. The dc insulation resistance showed improvement as a result of the outgassing which occurred during the endurance test. The change in ac leakage current before and after the endurance test was considered insignificant, as the smallest scale division on the meter is two microamperes on a 100 microampere scale.

Table 22. - Composition of Transformer Conductor Insulation Unaged and Aged.

CONSTITUENT / SAMPLE	PERCENT															
	Si	Al	Mg	B	Na	Ca	Be	Ti	Cr	Mn	Fe	Co	Ni	Cu	Zn	Ag
Unaged Transformer Standard	27(a)	13(a)	2.4(a)	1	0.5	5	<0.001	0.05	0.01	(b) <0.01	0.5	(b) < 0.02	0.05	0.06	0.3	0.01
Unaged Solenoid Standard	>10	>10	>10	1	0.5	5	<0.001	0.05	< 0.01	(b) <0.01	0.2	(b) < 0.02	0.1	0.04	0.2	0.1
Aged in Transformer (Primary Winding) 5000 Hours at 1300° F, 10^{-9} torr Range	>10	>10	>10	1	0.2	5	<0.001	0.05	0.05	< 0.01	0.5	(b) < 0.02	0.01	0.02	0.05	< 0.01
Aged in Transformer (Secondary Winding) 5000 Hours at 1300° F, 10^{-9} torr Range	>10	>10	>10	1	0.5	5	<0.001	0.05	< 0.01	0.01	0.5	(b) < 0.02	0.02	0.02	0.1	(b) < 0.01

(a) - Quantitative wet chemical analysis. All other analyses are semiquantitative spectrographic.
(b) - Not detected. Limits of detection are as shown after < sign.

Table 23. - Comparative Analyses of Deposits and Substrates From Transformer Coil Form By Quantitative Emission Spectrographic Methods.

SAMPLE \ CONSTITUENT	MICROGRAM LEVELS OF ELEMENTS DETECTED IN EACH DEPOSIT											
	Si	Al	Mg	B	Be	Ti	Cr	Mn	Fe	Co	Ni	Cu
Components aged in transformer for 5000 hours at 1300° F, 3×10^{-9} torr												
1. Coil Form, Al_2O_3, Substrate	5	(a)	5	(b) < 0.1	(b) < 0.01	(b) < 0.1	(b) < 0.1	0.1	2	(b) < 0.1	(b) < 0.1	< 0.1
2. Coil Form, Al_2O_3, With Orange Deposit	3	(a)	0.5	(b) < 0.1	(b) < 0.01	< 0.1	0.6	< 0.1	5	2	0.5	0.1
3. Coil Form, Al_2O_3, With Dark Deposit	5	(a)	1	(b) < 0.1	(b) < 0.1	0.5	0.6	1	> 10	2	1	5

(a) - Major constituent (> 10 micrograms).
(b) - Not detected. Limits of detection in micrograms are as shown following < sign.

Table 24. - Comparison of Solenoid Room Temperature Bench Test Electrical Data Taken Before and After a 5000-Hour Endurance Test in Ultrahigh Vacuum with a 1300° F Hot-Spot Temperature.

MEASUREMENT[a]	SOLENOID ENERGIZED	BEFORE ENDURANCE TEST			AFTER ENDURANCE TEST		
		OHMS		TEMPERATURE (°F)	OHMS		TEMPERATURE (°F)
Conductor Resistance	Continuously	12.05		72	12.53		78
	Intermittently	11.65		72	12.05		78
		MEGOHMS @ 500 Vdc		TEMPERATURE (°F)	MEGOHMS @ 500 Vdc		TEMPERATURE (°F)
DC Insulation Resistance	Continuously	$4x10^4$		72	$8.0x10^4$		78
	Intermittently	$1.05x10^4$		72	$7.0x10^4$		78
		MICROAMPS @ 500 Vac		TEMPERATURE (°F)	MICROAMPS @ 500 Vac		TEMPERATURE (°F)
AC Leakage Current	Continuously	1		72	2.0		78
	Intermittently	1		72	2.0		78
		VOLTS DC	AMPS DC	TEMPERATURE (°F)	VOLTS DC	AMPS DC	TEMPERATURE (°F)
Load Performance							
Minimum Pickup	Continuously	5.0	0.4	72	4.9	0.38	78
Minimum Pickup	Intermittently	4.8	0.395	72	6.0	0.46	78
Minimum Hold	Continuously	0.6	0.05	72	0.6	0.05	78
Minimum Hold	Intermittently	0.8	0.07	72	0.7	0.06	78

(a) In a single-winding component, measurements can only be made within the winding (conductor resistance, volts, amps) or from winding to ground.

The continuously energized solenoid did not show a notable change in minimum pick-up and holding voltage and current as a result of the endurance test. The intermittently energized solenoid showed an increase in pick-up voltage and current and a decrease in minimum holding voltage and current. The sliding bearing surfaces for the plunger are 99.5 percent pure alumina. It is believed that, as a result of periodically energizing the plunger to obtain performance data, the relative surface smoothness between the plunger and ceramic bearing surfaces decreased. An increase in friction would cause higher pick-up values and lower minimum hold values.

Visual Examination. - Visual examinations showed all external surfaces were discolored to varying shades of gray (as compared with the unaged solenoids) except for the tungsten base heavy alloy weight which remained bright. The windings of the continuously energized solenoid were inspected after the housing and end bell parts were removed. The boron nitride compound on the coil windings was partially blackened and green-gray. A thermocouple insulating tube made of alumina was blackened with small areas of tan discoloration.

Examination and Analysis of Magnetic Materials. - As in the case of the high temperature stator and transformer, the continuously and intermittently energized solenoids were disassembled following thermal vacuum endurance testing. The two solenoids had been subjected to different exposure conditions. The continuously energized solenoid was energized (except for weekly tests) during the first 4899 hours of exposure with its hot spot temperature at 1300° F. During the remaining 101 hours the solenoid was unenergized at a uniform temperature of 1170° F. The intermittently energized solenoid had been subjected to a 5000-hour test at 1190° F and pressure in 10^{-9} torr range. Intermittent testing for brief periods was used to verify operability.

After disassembly, the magnetic end bell and plunger (both fabricated from iron-27% cobalt alloy forgings) were examined. For details of construction, see figure 38. The housing of both solenoids had darkened considerably; a yellow scale was evident on the exterior of the intermittently energized solenoid and a gray scale was apparent on the continuously energized solenoid. The plungers from both solenoids had darkened slightly during testing.

The forged iron-27% cobalt bar from which the solenoid parts were fabricated had been retained for comparison of properties in the unaged condition. As in the case of the high temperature stator and transformer, coercive force was used to

indicate changes in the magnetic quality of the materials resulting from thermal-vacuum aging. Table 25 shows that the coercive force of the iron-27% cobalt plunger from the continuously energized solenoid decreased from 2.1 oersteds to 0.54 oersteds. The decrease in coercive force resulted from magnetic annealing of iron-27% cobalt (refs. 1, 9, and 10). This effect was created by the magnetic field induced in the solenoid plunger by the current passing through the magnetizing windings during 4899 hours of the 5000-hour test at 1300° F. The end bell was affected to a smaller degree by magnetic annealing (1.9 oersteds after aging) because of the relatively lower flux density (fewer effective lines of flux per unit area in the larger end bell). The coercive force of the plunger from the intermittently energized solenoid was 1.26 oersteds after aging. This solenoid plunger had been energized intermittently during a 5000-hour exposure at 1050° F and a 5000-hour exposure at 1190° F. In all cases, the lower coercive force values are a strong indication that the magnetic quality of the magnetic material improved during thermal-vacuum testing.

Interstitial analysis results for the the unaged iron-27% cobalt forged bar and for a specimen from the continuously energized solenoid are presented in table 26. There was a slight change (from 75 ppm to 67 ppm) in oxygen content of the solenoid end bell after 5000 hours at 1300° F and a pressure in the 10^{-9} torr range. The difference, however, is within the range of analytical accuracy for oxygen at the indicated level. The oxygen levels shown for these thick sections are more representative of the bulk oxygen content than that shown for thin lamination specimens reported previously. The surface area to volume ratio of the former is much smaller than the latter, contributing less surface oxygen to the overall content in the solid sections. The nitrogen content of the iron-27% cobalt unaged forging and the end bell from the continuously energized solenoid are also shown in table 26. Nitrogen analyses were performed on an aged specimen which was proximate to boron nitride fiber cement insulation and another specimen that had not been in contact with boron nitride insulation. These samples, as well as the unaged sample, showed nitrogen levels of less than 5 ppm. Therefore, interstitial analyses of the iron-27% cobalt solenoid end bell specimen showed no evidence of reaction with nitrogen from the boron nitride fiber cement insulation.

The microstructure of sections from solenoid end bells and plungers were examined and compared with a specimen from the unaged iron-27% cobalt forged bar. Representative microstructures are shown in figures 52 and 53. Some grain growth is evident in the iron-27% cobalt plunger (figure 52(c)) from the continuously energized solenoid, number 3, (aged 5000 hours at

Table 25. - Magnetic Property (Coercive Force)[a] of Magnetic Materials From High Temperature Solenoids Before and After Thermal Vacuum Aging at a Pressure in the 10^{-9} Torr Range.

Description of Specimen	Specimen Condition	Room Temperature Coercive Force H_c (oersteds)
Iron-27% Cobalt Solenoid Forging	Unaged forging	2.10
Iron-27% Cobalt End Bell Forging from Continuously Energized Solenoid	After 5000-hour solenoid exposure test at 1300° F and a pressure in the 10^{-9} torr range	1.90
Iron-27% Cobalt Plunger Forging from Continuously Energized Solenoid	After 5000-hour solenoid exposure test at 1300° F[b] and a pressure in the 10^{-9} torr range	0.54
Iron-27% Cobalt Plunger Forging from Intermittently Energized Solenoid	After 5000-hour solenoid exposure test at 1100° F and a 5000-hour test at 1300° F[c] and a pressure in the 10^{-9} torr range	1.26

(a) Coercive force measurements were made using a precision Coercive Force Meter manufactured by the Institute Förster, Reutlingen, West Germany. Accuracy of all measurements was ±2 percent.

(b) Continuously energized solenoid was energized for 4899 hours. After this time, the temperature decreased to 1260° F.

(c) The intermittently energized solenoid plunger was energized once each week during 5000 hours exposure at 1050° F and 5000 hours exposure at 1190° F.

Table 26. - Interstitial Content[a] of Iron-27% Cobalt Magnetic Materials Before and After 5000-Hour Thermal Vacuum Aging in the Continuously Energized Solenoid at a Pressure in the 10^{-9} Torr Range.

Description of Specimen	Specimen Condition	Interstitial Content (ppm)	
		Oxygen	Nitrogen
Iron-27% Cobalt Forged Bar	Unaged Forging	75	< 5
Iron-27% Cobalt End Bell from Forging for Continuously Energized Solenoid	After 5000-Hour Solenoid Test at a 1300° F at a Pressure in the 10^{-9} torr Range	67	< 5[b] < 5[c]

(a) All analyses were made by the Westinghouse R & D Center. Oxygen by vacuum fusion; nitrogen by modified Kjeldahl. Accuracies are as follows:

Oxygen at 20ppm ± 10% at 100ppm ± 4% Nitrogen at 30-100ppm ± 5%

(b) Sample for analysis taken from area proximate to boron nitride insulation.

(c) Sample for analysis taken from area away from boron nitride insulation.

1300° F as compared to the unaged forging (figure 52(a)). The plunger specimen from the intermittently energized solenoid, number 4, (aged 5000 hours at 1050° F and 5000 hours at 1190° F) exhibits still larger grain size (see figure 52(b)). There is evidence of a slight penetration by a second phase at the surface of the specimen shown in figure 52(b). This second phase is probably iron oxide.

Results of long term contact between boron nitride fiber cement and iron-27% cobalt iron are exhibited in figure 53(b). At a magnification of 700X, a slight second phase penetration along the grain boundaries may be noted in the part of end bell that had been in contact with boron nitride cement insulation during the 5000-hour test at 1300° F. The diffusing phase may be a

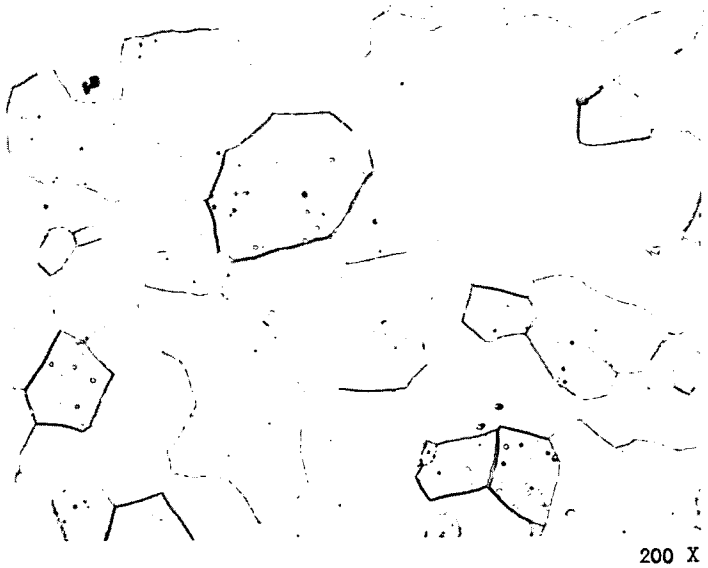

ASTM Grain Size: 6 - 7

0.001 inch

200 X

(a)

This page is reproduced at the back of the report by a different reproduction method to provide better detail.

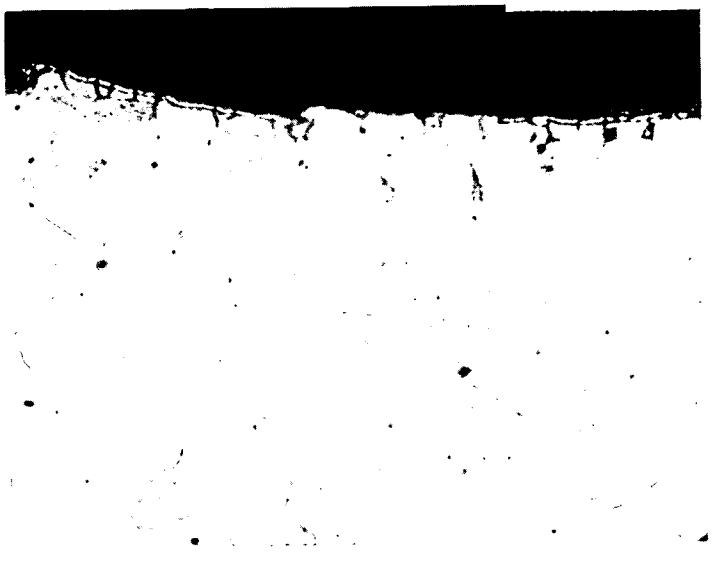

Second Phase Penetration

ASTM Grain Size: 4 - 5

0.001 inch

200 X

(b)

Figure 52. - Photomicrographs of Forged Iron-27% Cobalt Magnetic Alloy from Solenoids Before and After 5000-Hour Thermal-Vacuum Exposure. (200X)

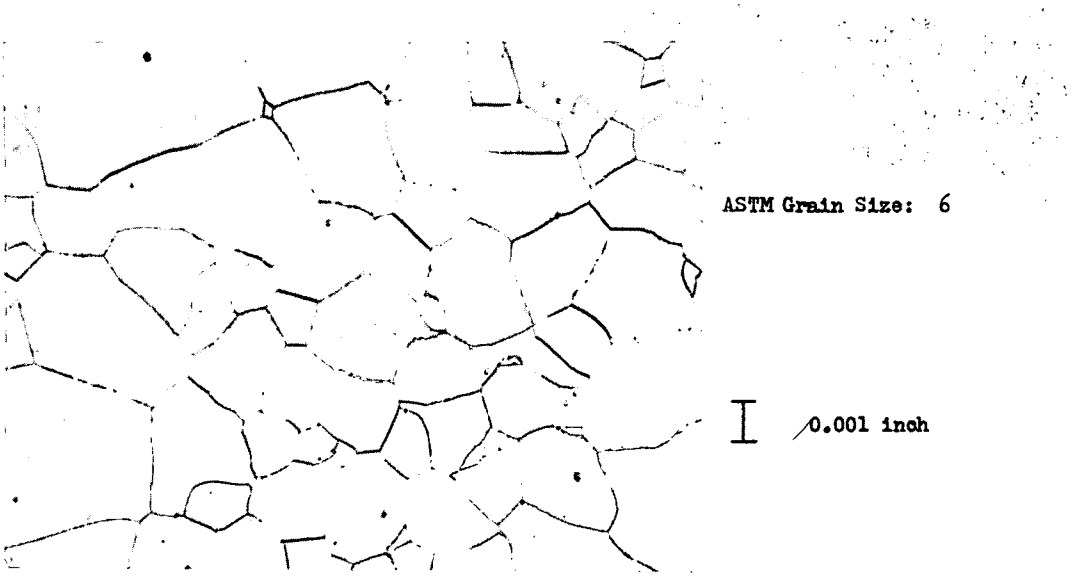

(c)

This page is reproduced at the back of the report by a different reproduction method to provide better detail.

(a) Unaged iron-27% cobalt forging, 200 X.

Etchant: $50HNO_3$, $45CH_3COOH$, $5H_2O$

(b) Iron-27% cobalt forged plunger from solenoid No. 4 after aging 5000 hours at 1100° F and 5000 hours at 1300° F. Solenoid intermittently energized, 200 X.

Etchant: $50HNO_3$, $45CH_3COOH$, $5H_2O$

(c) Iron-27% cobalt forged plunger from solenoid No. 3 after aging 5000 hours at 1300° F, 200 X.

Etchant: $50HNO_3$, $45CH_3COOH$, $5H_2O$

Figure 52. - Continued.

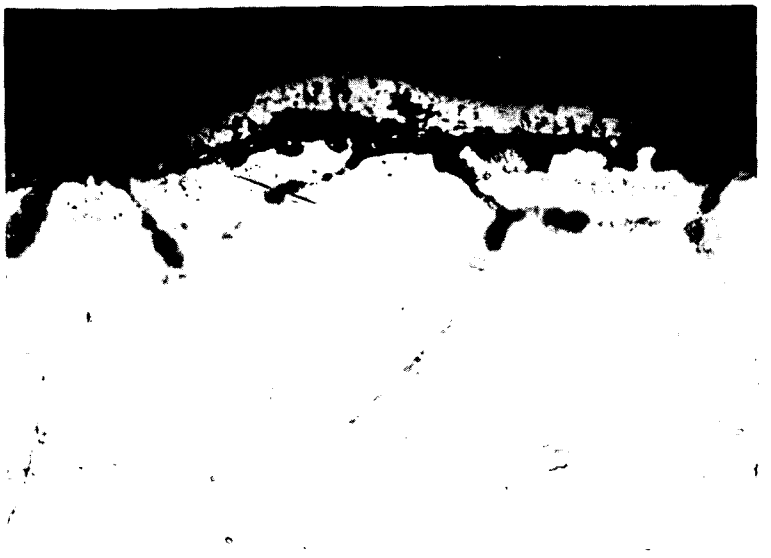

(a)

This page is reproduced at the back of the report by a different reproduction method to provide better detail.

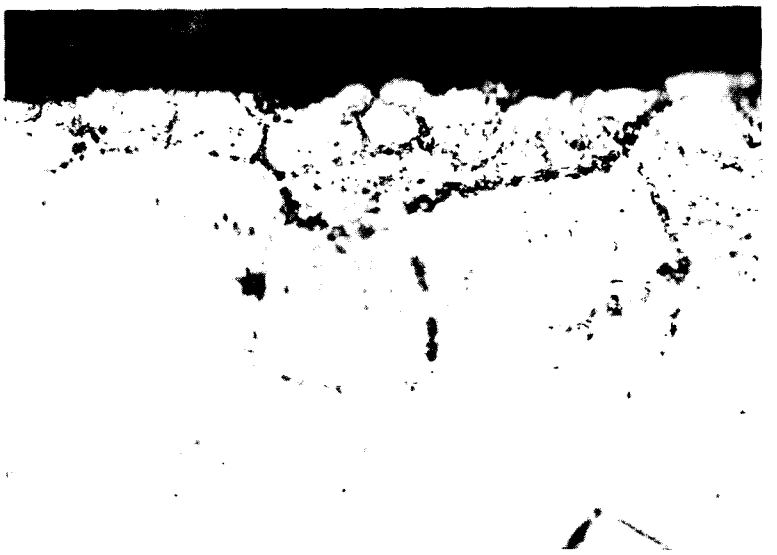

(b)

Figure 53. - Photomicrograph of Thermally Aged Iron-27% Cobalt End Bells From Solenoid No. 3 Showing Second Phase Penetration Near Boron Nitride Fiber Cement Insulation. (700X unetched)

boride. Figure 53(a) representing an outer bell surface, shows little evidence of second phase penetration. An oxide layer may be seen on the end bell surface.

Simple impact tests indicated that both the iron-27% cobalt end bell and plunger were brittle after long term aging. However, samples from these thick sections of forged iron-27% cobalt were not as brittle as the iron-27% cobalt laminations that had undergone aging in the stator and transformer magnetic stacks.

Metallographic Examinations of Electrical Conductors. - Metallographic examinations were performed on Inconel-clad silver conductors, unaged and from each solenoid. The solenoid conductor is the same as that used for the transformer primary. Microstructure of the unaged material is shown in figure 51. Microstructure of the conductor from the intermittently energized solenoid is shown in figure 54. Grain growth occurred in both the Inconel and the silver during aging, as was to be expected. Large random voids in the silver are seen in figure 54. Particles of silver may be seen adhering to Inconel cladding. It is probable that the silver was molten at some time after the beginning of the cladding process (such as in strand annealing between drawing operations). The random distribution of the voids indicates a short time in the molten state (incipient melting) as there was insufficient time for the voids to coalesce. No voids were detected in the unaged conductor (figure 51).

Figure 55 shows the microstructure of one lead from the exposure chamber electrical feedthrough to the continuously energized solenoid. A comparison of this microstructure and that of the unaged conductor, figure 51, shows that considerable grain growth occurred in the Inconel cladding during aging. Some grains on the aged Inconel extend the full thickness of the cladding. This indicates exposure to a very high localized temperature which probably occurred when the leads were short circuited through a heat shield at the 4899-hour point of the 5000-hour exposure test. There is evidence of a shallow surface depletion concentrated at the grain boundaries of the vacuum exposed Inconel surface. This depletion may have been caused by thermal etching during the high temperature caused by the short circuit.

Conductor Electrical Insulation Analysis. - Spectrographic analyses were conducted on both aged and unaged specimens of inorganic conductor electrical insulation from the high temperature solenoids. The solenoid conductor is the same as that used in the transformer primary winding. The purposes of the analyses were to (1) identify extraneous elements present in deposits or discolorations noted after aging, (2) estimate

This page is reproduced at the back of the report by a different reproduction method to provide better detail.

Figure 54. - Photomicrograph of the Electrical Conductor of the Intermittently Energized Solenoid After 5000-Hour Thermal-Vacuum Exposure. (200X)

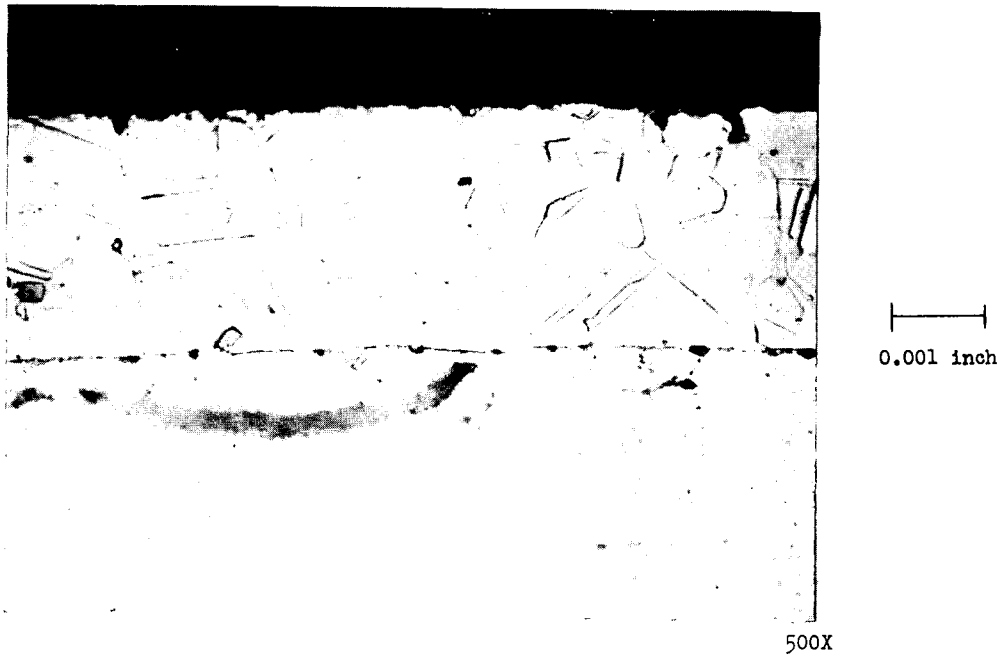

Figure 55. - Photomicrograph of an Electrical Lead of a Continuously Energized Solenoid After 5000-Hour Thermal-Vacuum Exposure. (500X)

relative amounts of extraneous materials, and (3) note changes in the elemental constituents of the conductor insulation. The semiquantitative analytical technique was the same as that described for the stator conductor insulation in section II of this report.

The results of spectrographic analyses for aged conductor insulation specimens from the two solenoids (continuously energized and intermittently energized) are compared with unaged conductor insulation in table 27. Also included is the analysis of an aged conductor insulation specimen which had been adjacent to boron nitride compound in the continuously energized solenoid.

A study of the analytical results reveals depletion in the zinc content of all aged specimens (intermittently and continuously energized as well as insulation covered with boron nitride cement). Zinc content was reduced from 0.2 to 0.1 percent in the aged specimens. A depletion of silver content is also indicated. The silver content of unaged insulation was shown to be 0.1 percent. After thermal aging the silver content of the conductor insulation was less than 0.01 percent in two specimens. The third specimen which had been covered with boron nitride insulation showed a silver content of 0.07 percent. The presence of even trace amounts of silver in unaged insulation covering the Inconel-clad silver solenoid conductor is puzzling. It is possible that silver from cut conductor ends was mechanically transferred or deposited on areas of the conductor in reeling and de-reeling during the application of insulation or during the cure and bake-out of insulation prior to use in the device. Depletion of silver and zinc after aging is attributed to evaporation at 1300° F in vacuum. No deleterious effects on the insulation performance would be expected from the depletion of silver or zinc. The copper content of inorganic solenoid conductor insulation also shows a decrease after aging; again a smaller decrease (0.04 to 0.02%) in the specimen covered with boron nitride cement than in the case of aged insulation which was not covered with boron nitride cement (0.04 to 0.01%). Nickel was the other element that showed a change and it followed a depletion pattern similar to that of copper.

Boron Nitride Fiber Cement. - After disassembly of the continuously energized solenoid, the boron nitride fiber cement on the conductor coil appeared darkened. The boron nitride cement that had adhered to the alumina end plate appeared green in areas where it had been in contact with the magnetic housing. Samples of the boron nitride cement were subjected to x-ray diffraction analyses and semiquantitative spectrographic analyses. Analytical results are shown in tables 28 and 29. The discolored areas in the boron nitride cement exhibited high manganese and

Table 27. - Composition of Solenoid Conductor Electrical Insulation Unaged and Aged.

CONSTITUENT / SAMPLE	PERCENT															
	Si	Al	Mg	B	Na	Ca	Be	Ti	Cr	Mn	Fe	Co	Ni	Cu	Zn	Ag
Unaged Transformer Standard	27[a]	13[a]	2.4[a]	1	0.5	5	<0.001	0.05	0.01	(b) <0.01	0.5	(b) <0.02	0.05	0.06	0.3	0.01
Unaged Solenoid Standard	>10	>10	>10	1	0.5	5	<0.001	0.05	<0.01	(b) <0.01	0.2	(b) <0.02	0.1	0.04	0.2	0.1
Aged in Solenoid (Intermittently Energized) 5000 Hours at 1300° F, 10^{-9} torr Range	>10	>10	>10	1	0.5	5	<0.001	0.05	0.05	<0.01	0.2	(b) <0.02	0.02	<0.01	0.1	<0.01
Aged in Solenoid (Continuously Energized) 5000 Hours at 1300° F, 10^{-9} torr Range and 28V DC	>10	>10	>10	1	0.5	5	<0.001	0.05	0.05	<0.01	0.5	(b) <0.02	0.02	0.01	0.1	<0.01
Aged in Solenoid With Boron Nitride Compound (Continuously Energized) 5000 Hours at 1300° F, 10^{-9} torr Range and 28 V DC	>10	>10	>10	1	0.5	5	0.001	0.05	0.05	0.01	0.5	(b) <0.02	0.05	0.02	0.1	0.07

(a) - Quantitative wet chemical analysis. All other analyses are semiquantitative spectrographic.
(b) - Not detected. Limits of detection are as shown after < sign.

Table 28. - X-Ray Diffraction Identification Analysis of Solenoid Boron Nitride Fiber Composite Specimens Unaged and Aged for 10,000 Hours at 1300° F in Ultrahigh Vacuum plus Control Specimens.

Sample	Compounds Detected
Boron Nitride Fiber Cement, Unaged	BN
Boron Nitride Fiber Cement Aged in Continuously Energized Solenoid for 5000 Hours at 1300° F, 10^{-9} torr, and 28 V D-C	BN Al_2O_3
Control: 90% BN + 10% B_2O_3	BN B_2O_3
Control: 50% BN + 50% B_2O_3	BN B_2O_3

magnesium contents. The dark area had increased in chromium content to a greater degree than the green area, but the latter contained more iron. The source of magnesium appears to be the conductor insulation; the source of other elements was the iron-cobalt magnetic alloy. Again long term interaction between adjacent materials resulted in visible discoloration but did not affect functional performance. It should be noted that boron oxide was not detected in the aged specimens of boron nitride fiber cement. If boron oxide had formed as a reaction product, electrical performance would have degraded.

The results of analytical tests conducted on a similar boron nitride insulation (boron nitride paper insulation) also indicated the absence of boron oxide after thermal-vacuum aging. Electrical tests performed on the boron nitride paper insulation

Table 29. - Comparative Analyses of Deposits and Substrates For Energized Solenoid By Semiquantitative Emission Spectrographic Methods.

SAMPLE \ CONSTITUENT	MICROGRAM LEVELS OF ELEMENTS DETECTED IN EACH DEPOSIT												
	Si	Al	Mg	B	Be	Ti	Cr	Mn	Fe	Co	Ni	Cu	Zn
Components aged in continuously energized solenoid for 5000 hours at 1300° F, 3 x 10^{-9} torr and 28V d-c													
1. Plate, Al_2O_3, Substrate	3	(a)	5	(b) < 0.1	(b) < 0.01	0.1	(b) < 0.1	< 0.1	1	(b) < 0.1	(b) < 0.1	< 0.1	(b) < 0.1
2. Plate, Al_2O_3, Gray Deposit	0.5	(a)	0.5	(b) < 0.1	(b) < 0.01	0.1	(b) < 0.1	0.1	5	0.5	(b) < 0.1	< 0.1	(b) < 0.1
3. Plate, Al_2O_3, Green Deposit	0.5	(a)	0.5	(b) < 0.1	(b) < 0.01	0.1	(b) < 0.1	0.2	5	0.5	(b) < 0.1	< 0.1	(b) < 0.1
4. Thermocouple Tube, Al_2O_3, Substrate	10	(a)	3	(b) < 0.1	(b) < 0.01	0.1	0.2	2.0	2.0	(b) < 0.1	1	0.03	< 0.1
5. Thermocouple Tube, Al_2O_3, Black Deposit	0.1	3	< 0.1	(b) < 0.1	(b) < 0.01	0.1	0.1	0.1	0.6	0.5	(b) < 0.1	0.03	< 0.1
6. Boron Nitride Fiber Cement. Unaged	2	> 10	0.8	(a)	(c)	0.5	(b) < 0.1	0.2	1	(b) < 0.1	0.3	0.5	(c)
7. Boron Nitride Fiber Cement Aged, remained white	> 10	(a)	> 10	(a)	(b) < 0.01	0.1	0.2	0.8	5	(b) < 0.1	1	1	5
8. Boron Nitride Fiber Cement, Aged, Black Deposit	8	(a)	10	(a)	(b) < 0.01	0.1	2	3	1	(b) < 0.1	1	0.2	< 0.1
9. Boron Nitride Fiber Cement, Aged, Green Deposit	2	> 10	0.6	(a)	(c)	0.2	(b) < 0.1	5	> 10	(b) < 0.1	0.3	0.5	(c)
10. Black Scale From Fe 27 Co End Bell	1	> 10	0.3	1	(c)	0.5	(b) < 0.1	8	> 10	10	1	0.5	(c)

(a) - Major constituent (> 10 micrograms).
(b) - Not detected. Limits of detection in micrograms are as shown following < sign.
(c) - Not detected.

after thermal vacuum aging verified its electrical stability (see table 21). Although no electrical tests were performed on the boron nitride fiber cement, post-test analyses imply that no appreciable degradation occurred.

Examination and Analyses of Ceramic Parts. - After thermal-vacuum testing for 5000 hours, two high-temperature solenoids were disassembled and examined. The ceramic (99.5% alumina) end plate from the continuously energized solenoid showed a green deposit on the surface adjacent to the iron-cobalt magnetic housing. The alumina end plate surface adjacent to the windings showed a thin gray deposit on the periphery exposed to the solenoid atmosphere, but remained white in areas that had been in contact with conductor insulation and boron nitride cement. The thermocouple insulating tubes revealed gray and black deposits on the outer surface where they exited the end plate.

Results of semiquantitative chemical analyses of representative areas from these deposits are shown in table 29. The green deposit on the alumina end plate consisted primarily of iron with small amounts of cobalt and manganese. Other constituents were common to those in the substrate. The source for all major extraneous elements was the iron-27% cobalt magnetic material adjacent to the alumina; these elements were transferred by evaporation and diffusion. The same extraneous elements were present in the gray deposit. However, less manganese was found in the gray deposit than in the green deposit adjacent to the iron cobalt alloy. The method of transfer of the gray deposit was by evaporation. Cobalt was the primary element in the colored area of the thermocouple tube insulation. Although the extraneous deposits were apparent upon visual examination of the ceramic parts, functional performance was not impaired. Nor was the functional performance of the donor material (iron-cobalt magnetic alloy) impaired after 5,000 hour thermal-vacuum testing.

Construction Material Examinations. - Solenoid construction materials were given visual examinations. The stop plate from the continuously energized solenoid and unaged material were subjected to metallographic examinations and were compared. Figures 56 and 57 show microstructures of the unaged and aged materials respectively. The unaged material has the normal annealed face centered cubic structure while the aged material exhibits a face centered tetragonal structure probably mixed with a close packed hexagonal structure. However to verify this, electron diffraction studies will be necessary. Visual examination of the solenoid weights revealed no degradation occurred in thermal aging. No degradation was found in the examination of the 321 stainless steel O-ring.

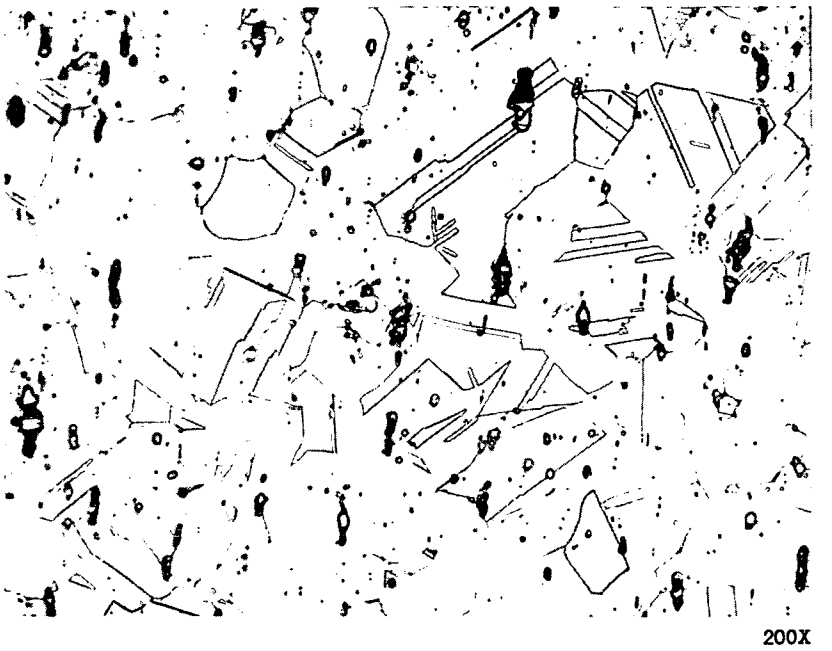

Figure 56. - Photomicrograph of Unaged Solenoid Stop Plate Material. (200X)

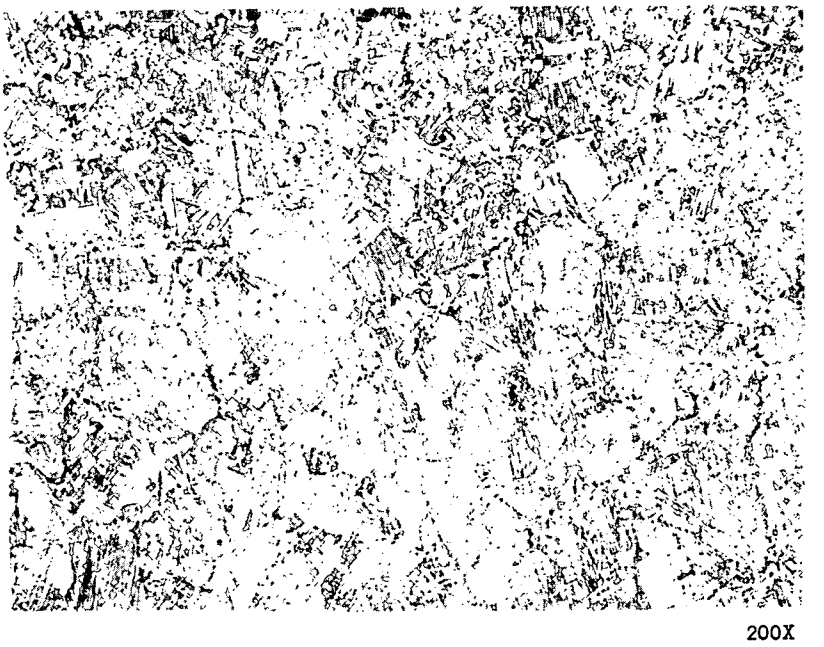

Figure 57. - Photomicrograph of Solenoid Stop Plate Material After 5000-Hour Thermal-Vacuum Exposure. (200X)

EVALUATION OF TRANSFORMER AND SOLENOID ELECTRICAL AND MECHANICAL PERFORMANCE

Electrical performance of the transformer and solenoids before and during the 5000-hour exposure were given in reference 4. Evaluations of devices electrical performances, based on the aforementioned information and information obtained on this program, follow.

Transformer

The transformer performed normally for 244 hours at 1300° F hot-spot temperature in a 10^{-9} torr range environment before a failure occurred. The failure was probably a turn-to-turn short circuit in the primary (high voltage) winding, caused either by abrasion of conductor electrical insulation due to mechanical forces generated by opposing magnetic fields in the primary and secondary windings or electrical conduction through silver that may have escaped through the Inconel cladding. Attempts to clear the short circuit by applying 600 volts ac across the fault resulted in vaporizing and melting a portion of the primary windings thus increasing the resistance. Table 16 gives room temperature bench test resistance values of conductors and insulation before and after the exposure test. Secondary conductor electrical resistance did not change due to aging. The dc insulation resistance showed improvement for each winding-to-ground as a result of exposure. The probable cause for this improvement, as in the case of the stator, was outgassing of the insulation. Winding-to-winding dc insulation resistance decreased to one-half of its initial value, probably as a result of vaporized material associated with the failure of the primary winding. Insulation system ac leakage showed an increase in post-endurance-test values, but the level remained low.

Continuously Energized Solenoid

The continuously energized solenoid performed without degradation through 4899 hours of the 5000-hour endurance test at 1300° F in a 10^{-9} torr range environment, but showed minor conductor resistance increase in a comparison of data taken before exposure with that taken after exposure (see table 24). The inability to operate this solenoid during the last 101 hours at high temperature was caused by a short circuit between the external leads and was not related to the device. The dc insulation resistance showed improvement, due to outgassing, during the exposure and was higher after exposure than before. The

insulation system ac leakage current was higher in post-test values, but the change of approximately one-to-two microamperes was considered insignificant as the smallest scale division was two microamperes on the 100 microamperes full scale meter. No significant change in minimum pickup and holding voltage and current was found to result from the endurance test.

Intermittently Energized Solenoid

The intermittently energized solenoid functioned throughout the 5000-hour thermal endurance test in a 10^{-9} torr range environment. Solenoid pickup and voltage and current increased and minimum holding voltage and current decreased throughout the test. Sliding bearing surfaces of the plunger (used in an intermittently energized solenoid at 1100° F previously (ref. 4)) were coated with plasma-arc sprayed alumina (99.5%) and mated with a stationary solid ceramic bearing. The probable cause for change in both pickup and minimum hold voltages and currents was a decrease in relative smoothness of mating bearing surfaces (an increase in friction) caused by the periodic use. An increase in friction would cause the higher pickup and lower minimum hold voltages and currents (see table 24). The dc insulation resistance improved (increased), due to outgassing, during the exposure and was higher after the exposure than before. The insulation system ac leakage current was higher in post-test values, but the change of approximately one-to-two microamperes was considered insignificant as the smallest scale division was two microamperes on the 100 microamperes full scale meter.

EVALUATION, RELATIVE TO AGING, OF TRANSFORMER AND SOLENOIDS MATERIALS

Each major material used in the transformer and solenoids was evaluated on the basis of any changes caused by the thermal-vacuum aging. Evaluations were based on comparisons of information from the previously discussed tests, analyses, and examinations of aged and unaged materials. Any changes found were investigated to determine their cause. Causes were related to either thermal aging or to thermal aging at interfaces. Evaluations of materials relative to their performance in the transformer and solenoids are given in the Materials Evaluations Relative to Transformer and Solenoids Functional Performance part of this section.

Transformer Materials

The transformer materials included iron-27% cobalt E and I magnetic laminations, primary and secondary electrical conductors of Inconel-clad silver with glass fiber insulation, flexible boron nitride paper insulation between winding layers, and coil form parts of alumina (see table 14 and figure 37). Transformer materials were aged in ultrahigh vacuum (10^{-9} torr range) for 244 hours at 1300° F hot-spot temperature and 4756 hours at 1170° F. The transformer was electrically energized during the 244 hours. Evaluations of transformer materials relative to aging in specific environments are given in the following paragraphs.

Evaluation of Transformer Magnetic Laminations. - The magnetic quality of iron-27% cobalt laminations showed essentially no change after 5000 hours thermal aging at pressure in the 10^{-9} torr range. Coercive values were not changed (within the limits of accuracy) after aging. Although this seems contrary to the results obtained with the same material on the high temperature stator, it should be noted that the transformer was energized (400 Hz magnetic field) for only the first 244 hours of the 5000-hour thermal exposure. The transformer temperature decreased from 1300° F (while energized) to 1170° F after the winding failure occurred. Therefore, this component was thermally aged but was not subjected to the magnetic annealing effect experienced by the stator.

Grain size in the aged transformer laminations was three to five times that of the unaged laminations.

Definite second phase penetration (approximately 0.0015 inch) occurred at the lamination surfaces during aging. As in the case of stator laminations, thin surface oxide layers that formed during processing are believed to the source of the penetrating second phase. Knoop hardness near the surface increased from 240 in the unaged lamination to 360 in the aged lamination. The laminations were very brittle after aging; this resulted from the reduction in grain boundary cohesive strength.

Electrical Conductors. - Inconel-clad (28 area percent) silver conductors for the transformer primary (0.032 in. diam.) and secondary (0.144 in. diam.) were evaluated after comparing information on aged and unaged specimens. Electrical resistance values for the secondary conductor showed no change due to aging (see table 16). No comparison of primary resistance values could be made because of the open circuit in this winding after 244 hours at 1300° F hot-spot temperature. Metallurgical examinations of both primary and secondary conductor specimens revealed

that grain growth in both silver and Inconel had taken place during aging (see figures 47, 48, 50, and 51). This grain growth is considered normal for the aging conditions. Voids between the silver core and Inconel cladding were found in the transverse section of the transformer secondary (see figure 49). These voids do not appear to be related to aging. No detrimental change due to aging could be found in the transformer primary or secondary electrical conductors.

The open circuit in the primary may have been initiated by an undetected defect in the Inconel cladding. A defect would allow silver to migrate into the conductor insulation thus causing current leakage. The current leakage would in turn accelerate the migration of silver leading to electrical breakdown.

Conductor Electrical Insulation. - Failure of the primary winding after 244 hours of test exposure prevented full aging and evaluation of the electrical conductor insulation. The secondary winding maintained electrical strength and insulation resistance throughout the subsequent aging to a total of 5000 hours. One mode of failure in the primary could have been caused by motion of the primary windings relative to their own turns and layers. The processing of Anadur "S" conductor insulation after winding produces a reduction in overall insulated conductor diameter which in turn causes a loosening of the winding layers. Alternating current operation of these windings generates a small but continuous relative motion of the many turns. This constant motion could abrade the hard fibrous conductor insulation and permit the layers of windings to move closer together and finally experience electrical breakdown. The conductor insulation is apparently chemically stable but constraint to avoid abrasion may be necessary.

Boron Nitride Paper Insulation. - Review of x-ray diffraction results and electrical testing of boron nitride paper insulation indicates that this material composition performs well in hard vacuum at elevated temperature. The data is presented in tables 20 and 21. The physical handling characteristics were also retained throughout the 1300° F exposure.

Rigid Electrical Insulation. - The rigid electrical insulation displayed no apparent degradation. Surface discolorations which formed during the test exposure were found to be nondetrimental. The aluminum oxide bodies performed satisfactorily during 5000 hours of exposure at 1300° F and 1170° F in a 10^{-9} torr environment.

Solenoids - Materials

Two solenoids were subjected to thermal-vacuum aging. Materials in each solenoid included a housing, end bell, and plunger of iron-27% cobalt alloy magnetic material, glass fiber insulated Inconel clad silver electrical conductor, and flexible boron nitride paper insulation between layers of conductor (see figure 38 and table 15). One solenoid was energized continuously (except for periodic measurements) for 4899 hours at 1300° F hot-spot temperature and then aged unenergized for 101 hours at 1170° F. The other transformer was operated intermittently for short periods of time during a 5000-hour aging at 1190° F. Evaluations of materials (relative to aging) from each solenoid are listed by material in the following paragraphs.

Evaluation of Solenoid Magnetic Materials

The effect of aging in the presence of an induced dc magnetic field is quite apparent on specimens obtained from the forged iron-27% cobalt alloys used in the two high-temperature solenoids. Magnetic quality, as indicated by coercive force measurements, definitely improved after aging. The coercive force value of the plunger removed from the continuously energized solenoid decreased 75 percent (to one-fourth its original value) after 4899 hours at 1300° F in the dc magnetic field. The plunger from the intermittently energized solenoid had been aged for 5000 hours at 1050° F as well as 5000 hours at 1190° F and was energized only intermittently (weekly for short periods). This solenoid plunger showed a decrease (improvement) of 40 percent in coercive force. A specimen from the end bell in the continuously energized solenoid which had been subjected to a weaker effective magnetic field during aging improved slightly with respect to magnetic quality.

Thermal aging for 5000 hours produced slight grain growth in the forged iron-27% cobalt magnetic material. It was not as pronounced as that produced in the cold-rolled laminations in the stator or transformers.

Second phase surface penetration of oxides was negligible. There appeared to be a slight reaction with boron nitride fiber-cement insulation at contact areas but the extent of this also was negligible. Although simple impact tests showed the aged material to be somewhat brittle, the specimens from thick iron-27% cobalt sections were much more ductile than were the laminations.

Electrical Conductors. - Inconel-clad silver conductors from the two solenoids were evaluated after comparing information

on aged and unaged specimens. These conductors were from the same material as that used in the transformer primary. No degradation in electrical conductivity was detected in the conductor from either the continuously or intermittently energized solenoids. Metallographic examinations of unaged and aged solenoid conductors revealed the expected grain growth in the silver and Inconel of the intermittently energized solenoid (see figures 51 and 54). Unusual grain growth (both Inconel and silver) in a lead from the continuously energized solenoid is thought to have resulted from heating of the lead at the time of the lead short circuit; and therefore is not a result of normal aging. The thermal etching of the Inconel cladding of this lead (see figure 55) probably also occurred during short circuit heating. No detrimental change due to aging could be found in the Inconel clad silver conductors from the solenoids.

Electrical Conductor Insulation. - The electrical insulation covering the electrical conductors of the continuously energized solenoid and the intermittently energized solenoid performed well throughout the 5000-hour aging at 1300° F and 10^{-9} torr. There were no apparent differences between performances of the insulation in the two units attributable to the conductor electrical insulation.

Rigid Electrical Insulation. - The rigid electrical insulation composed of aluminum oxide used in the solenoids performed satisfactorily and was compatible with other materials of the devices. The greatest change noted was the formation of discolored spots. These discolored areas have been attributed to sublimation of the iron-cobalt magnetic alloy and condensation upon the insulator surface.

MATERIALS EVALUATIONS RELATIVE TO TRANSFORMER AND SOLENOIDS FUNCTIONAL PERFORMANCE

Each transformer and solenoid material was evaluated on the basis of its contribution to functional performance of its respective device. The following summarizes these evaluations.

Transformer

The transformer functioned with no detected degradation for 244 hours at 1300° F hot-spot temperature in a 10^{-9} torr range environment. A turn-to-turn short circuit is believed to have developed in the primary winding at 244 hours into the test. This short circuit may have been the effect of abraded conductor electrical insulation resulting from relative movement between conductors caused by opposing magnetic fields in the

primary and secondary windings. Another possible cause for the failure may have been an undetected defect in the Inconel cladding which permitted silver to migrate through the conductor insulation layers leading to electrical breakdown.

Attempts to clear the short circuit in the primary winding effected melting of the faulted winding resulting in an open circuit in the primary winding. The effect of these changes was to initiate a new aging condition. Neither of the Inconel-clad silver conductors degraded in electrical conductivity during the first 244 hours of transformer thermal-vacuum testing and the secondary did not degrade during the total 5000 hours. Primary and secondary conductor electrical insulation and coil form ceramic insulation performance was stable after the primary winding was melted. The boron nitride paper insulation separating the windings improved in dissipation factor and resistance during the 5000 hours. Magnetic laminations showed slightly higher coercive force after aging than before aging (see table 17). This difference is considered insignificant because of its small value and the fact that the laminations were strained during disassembly (because they were bonded together).

SECTION IV

OVERALL ELECTRICAL DEVICE MATERIALS EVALUATIONS

Electrical device materials from the transformer, solenoids and stator were evaluated on the basis of their stability with respect to time under thermal and vacuum aging conditions. Evaluations were made on the basis of correlations between and among tests, analyses, and examinations of unaged materials and those subjected to various exposure temperatures for various times. Several of the materials were exposed to only one set of test conditions. Overall evaluations of these materials were given in section II and section III and will not be repeated here. The following headings list materials by major type or function with either overall evaluations given or references to where, in this report, overall evaluations are given.

EVALUATION OF MAGNETIC MATERIALS

Iron-27% cobalt magnetic material was utilized on this program for high temperature electrical components in the form of sheet laminations and parts machined from forged bars.

After thermal-vacuum testing described previously in this report, specimens were removed from the high temperature devices for magnetic testing, metallurgical examinations, microhardness surveys and interstitial analyses. Results from tests are shown in tables 30, 31, and 32. Test results from processed, but unaged materials, are presented in the tables for comparison. Details of fabrication and processing are reported in reference 5.

Coercive force measurements were used to indicate changes in the magnetic quality of the iron-27% cobalt alloy brought about by prolonged high temperature vacuum aging. Table 30 shows that the greatest decrease in coercive force (improvement in magnetic quality) appeared in the forged dc solenoid plungers after 5000-hour testing at 1300° F at a pressure in the 10^{-9} torr range. Solenoid end bell material decreased slightly in coercive force value. A smaller degree of magnetic quality improvement was observed in the stator laminations after 10,000-hour vacuum aging at 1300° F. The improvement in quality is attributed to a magnetic annealing effect created by exposure of the material to a magnetic field at elevated temperatures. The coercive force of the transformer laminations showed a slight increase after 5000 hours vacuum aging at 1190° F. It should be noted that this

Table 30. - Magnetic Property (Coercive Force)[a] of Magnetic Materials from High Temperature Stator, Transformer and Solenoids Before and After 1300° F Endurance Testing at a Pressure in the 10^{-9} torr Range.

Description of Specimen	Specimen Condition	Room Temperature Coercive Force H_c (oersteds)
Iron-27% Cobalt Stator Laminations 0.008-Inch Thick	Unaged lamination	2.4
Iron-27% Cobalt Stator Laminations, 0.008-Inch Thick	After 10,000-hour stator endurance test[b] at 1300° F and pressure in the 10^{-9} torr range	1.62
Iron-27% Cobalt Transformer Laminations, 0.008-Inch Thick	Unaged lamination (with plasma arc sprayed alumina (inter-laminar insulation)	1.64
Iron-27% Cobalt Transformer Laminations 0.008-Inch Thick. Laminations from Center of the Transformer	After 5000-hour transformer exposure test at 1300° F[c] and a pressure in the 10^{-9} torr range	1.80
Iron-27% Cobalt Transformer Laminations, 0.008-Inch Thick. Laminations from outside area of the Transformer	After 5000-hour transformer test at 1300° F and a pressure in the 10^{-9} torr range	1.82
Iron-27% Cobalt Solenoid Forging	Unaged forging	2.10
Iron-27% Cobalt End Bell Forging from Continuously Energized Solenoid	After 5000-hour solenoid exposure test at 1300° F and a pressure in the 10^{-9} torr range	1.90
Iron-27% Cobalt Plunger Forging from Continuously Energized Solenoid	After 5000-hour solenoid exposure test at 1300° F[d] and a pressure in the 10^{-9} torr range	0.54
Iron-27% Cobalt Plunger Forging from Intermittently Energized Solenoid	After 5000-hour solenoid exposure test at 1100° F and a 5000 hours at 1300° F[e] and a pressure in the 10^{-9} torr range	1.26

(a) Coercive force measurements were made using a precision Coercive Force Meter manufactured by the Institute Forster, Reutlingen, West Germany. Accuracy of all measurements was ± 2 percent.

(b) Stator was energized during the entire 10,000-hour exposure.

(c) Transformer was energized for 244 hours. After this time the temperature decreased to 1170° F.

(d) Continuously energized solenoid was energized for 4899 hours. After this time the temperature decreased to 1260° F.

(e) The intermittently energized solenoid was energized once each week during the second exposure and the temperature was 1190° F.

Table 31. - Knoop Hardness of Magnetic Laminations from the High Temperature Stator and Transformer Before and After Thermal Endurance Testing at a Pressure in the 10^{-9} Torr Range.

Description of Specimen	Specimen Condition	Microhardness[a] Knoop (25 gm)			Remarks
		Edge	Center	Edge	
Iron-27% Cobalt Stator Laminations, 0.008-Inch Thick	Unaged Lamination	270	256	---	Ductile in Bending
Iron-27% Cobalt Stator Lamination, 0.008-Inch Thick	After 10,000-hour stator test at 1300° F and a pressure in the 10^{-9} torr range	328	318	318	Brittle in Bending
Iron-27% Cobalt Transformer Lamination, 0.008-Inch Thick	Unaged Lamination with Plasma arc sprayed alumina	258	229	224	Ductile in Bending
Iron-27% Cobalt Transformer Laminations, 0.008-Inch Thick. Laminations from center of the transformer.	After 5000-hour transformer test at 1300° F and a pressure in the 10^{-9} torr range	320	241	362	Brittle in Bending
Iron-27% Cobalt Transformer Laminations, 0.008-Inch Thick. Laminations from the outside area of the transformer	After 5000-hour transformer test at 1300° F and a pressure in the 10^{-9} torr range	337	269	411	Brittle in Bending

(a) Each value shown is the average of five test indentations.

component was energized for the first 244 hours of the test, thus limiting the magnetic annealing effect. The slight increase may be attributed to internal oxidation and internal strains caused by separating adhering adjacent transformer laminations. In general, it may be noted that the magnetic quality of iron-27% cobalt alloy was improved by prolonged high temperature vacuum aging in the energized state.

Metallurgical examination of iron-27% cobalt alloys before and after endurance testing showed nearly equivalent grain growth (three to five times original size) in the stator and transformer

Table 32. - Interstitial Content[a] of Iron-27% Magnetic Materials Before and After Endurance Testing of Components at 1300° F and a Pressure in the 10^{-9} Torr Range.

Description of Specimen	Specimen Condition	Interstitial Content (ppm)		
		Oxygen	Nitrogen	Carbon
Iron-27% Cobalt Stator Laminations, 0.008-Inch Thick	Unaged Lamination	61	39	111
Iron-27% Cobalt Stator Laminations, 0.008-Inch Thick	After 10,000-hour stator test at 1300° F and pressure in the 10^{-9} torr range	245(b)	70	55
Iron-27% Cobalt Transformer Laminations, 0.008-Inch Thick	Unaged Lamination	(d)	(d)	99
Iron-27% Cobalt Transformer Laminations	After 5000-hour transformer test at 1300° F at a pressure in the 10^{-9} torr range	(d)	(d)	18
Iron-27% Cobalt Forged Bar	Unaged Forging	75	5	(d)
Iron-27% Cobalt End Bell from Forging for Continuously Energized Solenoid No. 3	After 5000-hour solenoid test at a 1300° F at a pressure in the 10^{-9} torr range	67	5(e) 5(f)	(d)

(a) All analyses were made by the Westinghouse Research & Development Center. Oxygen by vacuum fusion; nitrogen by modified Kjeldahl. Carbon by combustion. Accuracies are as follows:

Oxygen at 20ppm ± 10%
at 100ppm ± 4%

Carbon at 20ppm ± 10%
at 50ppm ± 6%
at 250ppm ± 3%

Nitrogen at 30 to 100ppm ±5%

(b) Bulk sample analysis from central portion of lamination.
(c) Analysis included oxygen available from plasma arc sprayed alumina surface.
(d) Not determined.
(e) Sample for analysis taken from area proximate to boron nitride chopped fiber cement insulation.
(f) Sample for analysis taken from area not in contact with boron nitride chopped fiber cement insulation.

laminations (stator tested 10,000 hours at 1300° F, the transformer 5000 hours at 1190° F). The forged material from the solenoid exhibited a smaller increase in grain size after testing for 5000 hours at 1190° F.

Results from interstitial analyses of stator and transformer laminations and forgings are shown in table 32. In general, the laminations exhibited a greater change in interstitial content than the forged material. There was essentially no change in oxygen or nitrogen content of the iron-27% cobalt solenoid end bell after 5000 hours testing at 1300° F. Oxygen increased approximately four fold in the stator laminations while the nitrogen content doubled after 10,000 hour testing at 1300° F. Carbon depletion was apparent in both stator and transformer laminations but was more pronounced in the latter. From these results, it appears that oxygen diffuses into the alloy and forms a second phase more rapidly than nitrogen. The oxygen source is adsorbed and occluded oxygen on the lamination surfaces and plasma arc sprayed alumina. The bulk effect is less in the case of forgings which have a larger cross section. Carbon depletion in the laminations occurred when oxygen reacted with carbon to form carbon monoxide and dioxide which subsequently evolved. A possible relationship between carbon depletion and test chamber gas content was investigated. Outgassing loads had been monitored in the test chamber by means of residual gas analysis during the endurance testing.

The residual gas analysis peaks for moisture and for nitrogen plus carbon monoxide were predominant in both stator and transformer test chambers during testing. The partial pressure for the nitrogen plus carbon monoxide peak did not exceed 1×10^{-8} torr during thermal-vacuum testing and reached a maximum at 2000 hours of test time. This was true for the nitrogen plus carbon monoxide mass number in both stator and transformer test chambers. (See figure 49, ref. 5, and table 33, page 142.)

Carbon depletion was more severe in the transformer laminations after 5000 hours testing than in the stator lamination after 10,000 hours. Since residual gas analyses shows maximum pressures for the nitrogen plus carbon monoxide peak prior to 5000 hours testing, it is likely that carbon monoxide evolution occurred early in the test period.

It should be emphasized that the magnetic materials are not the sole source for nitrogen plus carbon monoxide load in the chamber. Structural metal members and the insulation system also contributed to these gases.

Microhardness surveys of the stator and transformer magnetic laminations indicated an increase in hardness after vacuum-endurance testing. The increase in hardness was more pronounced near the lamination surfaces where second phase penetration had occurred. Transformer laminations with 5000 hours at test temperature exhibited a larger increase in surface hardness than the stator laminations that sustained 10,000 hours at the test temperature.

The second phase penetration in the laminations resulted in a reduction of cohesive strength and development of intergranular embrittlement.

In summary, it may be noted that the iron-27% cobalt alloy improved in magnetic quality after aging for 5000 or 10,000 hours in the electrically energized state in an elevated temperature, ultrahigh vacuum environment. Oxygen and nitrogen content increased while carbon content decreased. Second phase penetration and embrittlement occurred. All of these effects were more pronounced in the cold rolled and annealed thin sections (laminations) than in the forged thick section (solenoid components).

The functional performance of the components were not adversely affected by the aging effects in magnetic materials. However, the use of laminations for long-term, high temperature devices should be limited to static applications.

INCONEL-CLAD SILVER CONDUCTOR EVALUATION

Three sizes of Inconel-clad silver electrical conductors (28 volume percent cladding) were used in the test program. These were vacuum exposure tested for 5000 hours in the transformer and solenoids and for 10,000 hours in the stator. No significant degradation in electrical performance was found (see tables 3, 16 and 24). Electron microprobe analyses of silver Inconel interfaces in both unaged and stator (aged 10,000 hours at 1300° F) conductors showed no silver diffusion into the Inconel and no chromium diffusion into the silver (see figure 32). Electron microprobe scans of the Inconel vacuum interface in the aged conductor revealed no depletion of chromium (see figure 33). Microscopic examinations of conductors revealed grain growth in all normally aged conductors (see figures 34 and 35).

CONDUCTOR ELECTRICAL INSULATION EVALUATION

Conductor electrical insulation was used on all Inconel-clad silver conductors and was exposure tested for times through 10,000 hours. The insulation system consists of "S" glass (high strength-high silica) roving served on the conductors and bonded with fusible glass and refractory oxide powders. The powders were applied to the wire and serving in a silicone resin binder. After forming and placing of the conductors, the insulated conductor was fired, thus fusing the glass frit to form a rigid binder for the "S" glass serving. Conductor insulation was in contact with boron nitride paper (mat) electrical insulation (in the transformer) and boron nitride chopped fiber cement (in some areas of the solenoids and stator). In the stator, conductor insulation was in contact with rigid alumina slot liners which were adjacent to the magnetic laminations.

The electrical performance of the stator conductor electrical insulation was satisfactory in the stator, showing an improvement at the conclusion of aging. The solenoid specimens also performed well. In the transformer, however, a layer-to-layer short circuit occurred early in the aging period. While the exact cause has not been definitely established, some reflection on conductor electrical insulation is justified. It may be noted that except in the faulted region, the transformer conductor insulation was intact and appeared to be in as good condition as the stator conductor insulation. In all cases, the adhesion to the conductor was low but the microstructure of the insulation showed no detrimental changes. No incompatibility with boron nitride fiber cement nor sheet insulation nor aluminum oxide slot liners was noted. The conductor insulation used on this program is electrically and thermally stable (when protected from mechanical damage) for at least 10,000 hours at 1300° F in a 10^{-9} torr range environment.

BORON NITRIDE FIBER ELECTRICAL INSULATION EVALUATION

Boron nitride fibers were used in two forms as part of this program. The first form was a chopped fiber cement which was used in the stator and in the two solenoids. The second form was that of a flexible sheet insulation. The chopped fiber cement held together but exhibited very low adhesion to any contacting surface. External surfaces and surfaces contacting magnetic and structural alloys were discolored. Increases in the levels of chromium, manganese, nickel, and iron were noted. No electrical performance was measured because of irregular form and small amounts of the specimens.

The flexible sheet insulation was used only in the transformer where it performed satisfactorily. The material retained its mechanical strength and improved slightly in electrical properties during the aging. No compatibility problems were noted between the boron nitride sheet and other materials of the transformer. No increase in boron oxide level was noted.

RIGID ELECTRICAL INSULATION EVALUATION

The aluminum oxide rigid electrical insulation components performed in a similar fashion in all of the test assemblies. Their electrical and mechanical performance was satisfactory. Some discoloration occurred in several locations. Nearly all pieces developed small, darkly colored spots. These spots were analyzed and found to contain more cobalt, nickel, and iron than did the chromium and copper levels. Discolored spots were apparently not detrimental to electrical or mechanical performance. The variations in manganese levels were different between spots in the stator and those of the solenoids and transformer. Manganese levels in the discolored stator spots were lower than in the substrate. Visually similar spots in the solenoid and transformer had increased manganese over those of the substrates. This phenomenon has not been explained. No change in performance was noted which could be attributed to manganese.

BORE SEAL MATERIALS EVALUATIONS

The bore seal capsule consisted of 99.8 percent beryllia joined to columbium-1% zirconium with a 60Zr-25V-15Cb braze alloy. High purity potassium was inside the capsule, and the capsule exterior was exposed to a 10^{-9} torr range environment inside the stator. Bore seal capsule exposure was 10,000 hours at 1300° F. Evaluations of bore seal capsule materials is given in section II, Evaluation, Relative to Aging, of Bore Seal Capsule and Stator Materials.

SECTION V

EVALUATION OF TEST CHAMBERS

The two thermal-vacuum test chambers used on this and the previous program (NASA Contract NAS3-6465) provided satisfactory service without maintenance for nearly 20,000 hours accumulated vacuum operating time. Each chamber was of the "cold wall" construction with water cooling and included tantalum resistive heating elements and heat shields, a 500-liter-per-second sputter ion pump, a tungsten filament heated titanium sublimation pump, and associated power supplies, controls, and instrumentation. The following listing gives times, temperatures, and pressure range associated with each chamber accumulated through the opening of the chambers at the conclusion of this program.

Chamber Number 1[1]

Used for the stator and bore seal endurance tests.

Time (hours)	Temperature (°F)
5000	1100
5000	1300
4700	72 (Standby)
5000	1300
19,700[2]	

Chamber Number 2[1]

Used for the transformers and solenoids endurance tests.

Time (hours)	Temperature (°F)
5000	1100
5000	1300
9700	72 (Standby)
19,700[2]	

[1]Pressure Range for each chamber: 5.0×10^{-7} to 3.0×10^{-10} torr.

[2]Total ion pump operation.

The evaluation of satisfactory service was based on attained temperatures and pressures, examination of chamber interior after completion of thermal testing, and examination of the cooling water entrances to one chamber. Discussions of the various aspects of chamber performance follow.

The ion pumped chamber performed without fault continuously for 20,000 hours. Water in the recirculating system for cooling the jacket, feedthroughs and chamber top had been preconditioned by treatment with 25 parts-per-million of sodium phosphate. This proved to be adequate for the operational period.

Post-test examination revealed a build-up of deposits within the cooling tubes. Therefore, additional operation of the system without cooling system maintenance would be limited (perhaps 5000 hours additional). Of course, cleaning of the cooling system tubes would permit resumption of long term operation.

STATOR - BORE SEAL CHAMBER DEPOSITS

Some deposits were noted in chamber number one at the time the stator and bore seal capsule were removed following a 10,000-hour endurance test at a 1300° F hot-spot temperature. Samples of a white fibrous material were removed from the chamber interior walls and chamber vacuum feedthrough tubes. These samples were subjected to spectrochemical analysis to obtain qualitative information on the elements present. The results show the following relative quantities of elements in descending order:

Boron - Silver - Copper	(highest)
Aluminum - Nickel	(next)
Chromium	(least)

The source of the fine fibrous deposit was the boron nitride cement insulation and conductor insulation. These low density fibrous materials are friable after cure and bakeout. They were transported to the chamber wall during inert gas backfilling of the test chamber at the termination of endurance testing. Boron and alumina are present in the conductor insulation while nickel and chromium are constituents of the vacuum chamber wall. Silver and copper are present in the brazing alloy used in the cold area of the furnace to braze feedthrough terminals.

TRANSFORMER - SOLENOIDS CHAMBER DEPOSITS

Some deposits were noted in chamber number two at the time the transformer and solenoids were removed after 5000 hours of test at 1300° F. Samples of these deposits were removed from

the chamber surfaces and subjected to spectrochemical analysis to obtain qualitative information on the elements present. The results show the following relative quantities of elements in descending order:

Iron-Chromium	(highest)
Magnesium-Titanium Zinc-Aluminum	(next)
Trace Elements	(least)

The source of aluminum, magnesium and zinc was the conductor insulation. Iron and chromium were constituents of the vacuum chamber wall from which the deposits were removed. The test chamber titanium sublimation pump was the probable titanium source.

RESIDUAL GAS ANALYSES OF BOTH CHAMBERS

Data reported previously relating to the environment test chamber atmosphere have shown the water vapor level to be higher than the other gas constituents in both test chambers (see figure 11 and figures III-30 and III-49 of reference 4). Although absolute water vapor levels were very low for the major portion of the tests (partial pressures in the 10^{-9} torr range), the possibility of an external source such as chamber cooling water was investigated.

After removing the 1300° F transformer and two solenoid models, test chamber number two was closed and pumped down to take residual gas analysis (RGA) traces of the empty chamber environment. Stable ion-gage pressure was initially 3.2×10^{-8} torr at 70° F. The chamber had not been baked-out after having been opened. Chamber cooling water had been drained for this test series.

A series of nine RGA traces were recorded over a period of 350 hours. Table 33 is a summary of the behavior of the major mass peaks during this period. The units listed are the partial pressures of the various gases. Trace number one was taken shortly after the chamber had been pumped down and pressure had become stable. Water vapor was the predominant gas present. The apparent discrepancy between the water vapor partial pressure and the ion-gage pressure occurs because the ion gage is located near the bottom of the test chamber in line-of-sight with the ion pump inlet. The RGA sensing head is attached to the top of the chamber by a series of convoluted tubulations

Table 33. - Tabulation of Residual Gas Analysis Test Data From the Transformer and Solenoid Test Chamber After Removal of the Models. Units are Partial Pressures in Torr.

Trace No.	Cumulative Test Hours	Chamber Ion Gage Pressure (torr)	Partial Pressure (torr) for Major Mass to Charge Peaks						
			2 (H_2)	16 (O)	17 (OH)	18 (H_2O)	28 (N_2+CO)	40 (A)	44 (CO_2)
1. Room Temp.	0	3.2×10^{-8}	5.26×10^{-9}	9.90×10^{-9}	6.30×10^{-8}	3.06×10^{-7}	3.19×10^{-8}	7.75×10^{-10}	2.67×10^{-9}
2. Room Temp.	18	4.1×10^{-8}	2.12×10^{-9}	1.60×10^{-9}	1.28×10^{-8}	6.30×10^{-8}	1.39×10^{-8}	4.73×10^{-10}	1.51×10^{-9}
3. Heated Tubes	22	8.0×10^{-8}	7.15×10^{-9}	2.44×10^{-8}	1.85×10^{-7}	8.57×10^{-7}	3.55×10^{-8}	9.03×10^{-10}	2.27×10^{-8}
4. Heated Tubes	24	7.7×10^{-8}	1.66×10^{-8}	1.32×10^{-8}	1.12×10^{-7}	5.39×10^{-7}	4.30×10^{-8}	1.33×10^{-9}	1.56×10^{-8}
5. Room Temp.	41	4.9×10^{-8}	2.12×10^{-9}	1.25×10^{-9}	6.75×10^{-9}	3.12×10^{-8}	1.18×10^{-8}	4.73×10^{-10}	8.0×10^{-10}
6. Room Temp.	65	5.2×10^{-8}	1.86×10^{-9}	9.0×10^{-10}	6.0×10^{-9}	2.73×10^{-8}	1.12×10^{-8}	7.3×10^{-10}	4.45×10^{-10}
7. Room Temp.	209	4.8×10^{-8}	1.70×10^{-9}	6.5×10^{-10}	3.45×10^{-9}	1.58×10^{-8}	1.05×10^{-8}	7.75×10^{-10}	2.67×10^{-10}
8. Room Temp.	257	4.8×10^{-8}	1.70×10^{-9}	6.5×10^{-10}	3.55×10^{-9}	1.60×10^{-8}	1.0×10^{-8}	8.6×10^{-10}	2.67×10^{-10}
9. Room Temp.	350	4.8×10^{-8}	1.27×10^{-9}	5.0×10^{-10}	2.85×10^{-9}	1.27×10^{-8}	3.30×10^{-9}	9.9×10^{-10}	1.33×10^{-10}
10. Room Temp. Models in Chamber	-	7.8×10^{-10}	4.25×10^{-10}	1.5×10^{-10}	1.40×10^{-9}	6.63×10^{-9}	7.5×10^{-10}	Trace	Trace

and fittings (see figure 4) and has a long conductance path to the ion pump.

Trace number two, taken 18 hours after trace number one, showed a reduction in all mass peak magnitudes accompanied by an increase in ion-gage pressure. From this observation it is inferred that initially the gas analyzer was sensing gases trapped in the attaching tubulations.

Heating tapes were applied to all residual gas analyzer tabulations (fittings and convoluted tubes) and heat was applied. As the temperature reached equilibrium (estimated at 225 to 250° F), ion-gage pressure rose to 8.0×10^{-8} torr. The peak magnitudes (trace number three) for the various gases increased by factors ranging from approximately 3 to 15, indicating that various quantities of gas had been trapped in the convolutions. A second trace (number four) taken two hours later showed that the heat was driving gases from the tubulations. Trace number five was taken at a temperature of 70° F after the tubulation bakeout. Traces number six through number nine were taken after increasing time intervals, and they show a slow decrease in all peak magnitudes except argon as a function of pumping time. Trace number ten was taken when the test chamber was on standby at room temperature when the transformer and solenoids were still installed. Long term pumping had removed essentially all the argon and carbon dioxide. There were no other mass peaks showing on the RGA trace.

The residual gas analyzer and accessory tubing operate at room temperature regardless of the test chamber thermal environment. Therefore, it is probable that the gas-trapping effects of the tubulations were also present during high temperature endurance testing. There is no evidence of a leak of water vapor into the thermal-vacuum chamber.

SECTION VI

CONCLUSIONS AND RECOMMENDATIONS

CONCLUSIONS

1. A high-temperature stator and bore seal containing potassium exhibited satisfactory functional performance for 10,000 hours at 1300° F in ultrahigh vacuum.

2. Stator materials of construction, including iron-27% cobalt magnetic laminations and solid forgings, Inconel-clad silver conductor; refractory filled glass-bonded "S" glass conductor insulation and high purity alumina (>99%A_2O_3) rigid insulation, all performed without functional degradation. Improvement with aging was found in magnetic materials (lowered coercive force due to magnetic annealing) and the insulation system improved (increased dc resistance and decreased ac leakage current) with aging due to outgassing.

3. The bore seal, consisting of 99.8% beryllia ceramic brazed to columbium-1% zirconium end pieces with a 60Zr-25V-15Cb alloy, remained potassium leak tight after 10,000 hours testing at 1300° F.

4. The flexural strength of 99.8% beryllia ceramic remained unchanged after potassium exposure at 1300° F for 10,000 hours.

5. Two high-temperature solenoids performed satisfactorily after 5000 hours at 1300° F in ultrahigh vacuum.

6. Solenoid materials of construction, including iron-27% cobalt forgings, high purity (>99%Al_2O_3) alumina components, Inconel-clad silver conductor, refractory filled glass-bonded "S" glass conductor insulation, and boron nitride fiber cement, functioned satisfactorily.

7. A high-temperature transformer performed satisfactorily for 244 hours prior to a failure in the primary winding. Failure was attributed to a turn-to-turn short circuit. Possible causes for lack of electrical insulation at the failure are: (1) abrasion of insulation due to relative motion caused by opposing magnetic forces, and (2) a pin-hole in the Inconel cladding that allowed migration of silver into the insulation.

8. Iron-27% cobalt laminations, high purity (>99%Al_2O_3) alumina insulation, boron nitride fiber cement, and boron nitride fiber paper performed satisfactorily in the transformer.

9. Boron nitride fiber paper, used as insulation between winding layers, performed satisfactorily. Post aging evaluation revealed satisfactory compatibility with the fibrous conductor insulation.

10. Since the transformer experienced a fault, the long-term performance of a transformer with the designated materials system could not be assessed.

11. Two ion-pumped thermal ultrahigh vacuum chambers performed flawlessly for 19,700 hours at a pressure in the 10^{-9} torr range or lower.

12. Although a light deposit of transported material was visible on the external surfaces of all components after completion of testing in vacuum for periods as long as 10,000 hours, the performance of components was not degraded.

13. Iron-27% cobalt alloy, especially in the thin lamination form was found to be brittle after aging for 5000 or 10,000 hours at 1300° F. This brittleness is not a problem in the static applications but dynamic or highly stressed applications should be carefully considered until the mechanism of embrittlement is understood and mitigated.

14. The materials used in the high-temperature stator, solenoids and transformer exhibited low outgassing levels at 1300° F at pressures in the 10^{-9} torr range. Outgassing of the insulation system during the initial test period improved insulation performance.

RECOMMENDATIONS

1. A method of non-destructive testing of clad silver conductors should be developed and applied to reliable high temperature space electric power systems. The test method should be capable of detecting flaws including pinholes in the cladding. Detection and elimination of such flaws by 100 percent inspection of the conductor would prevent silver migration at elevated temperatures.

2. The glass-bonded fiber glass conductor insulation should be improved to enhance mechanical strength and handling characteristics and improve adherence in the cured condition.

3. An improved, high-strength potting compound is required for electrical apparatus for applications above 1000° F.

4. Thorough mechanical testing of electrical materials should be performed after long-term thermal vacuum exposure to define material limitations.

5. It is recommended that dynamic tests of a high-temperature alternator be started to determine mechanical and power characteristics under load.

APPENDIX A

EVENT FLOW SHEETS FOR POST ENDURANCE EVALUATION PLAN - HIGH TEMPERATURE STATOR, BORE SEAL, TRANSFORMER AND SOLENOIDS

A post endurance test evaluation plan was prepared during the final portion of the stator and bore seal endurance test. One objective of the plan was to organize procedures, processes, tests, analyses, and examinations (events) that were anticipated to be required to supply information necessary for the various evaluations. Event organization for this plan is given in flow sheets, figures A-1 and A-2. Following each flow sheet is an outline of events, referenced by number on the respective flow sheet.

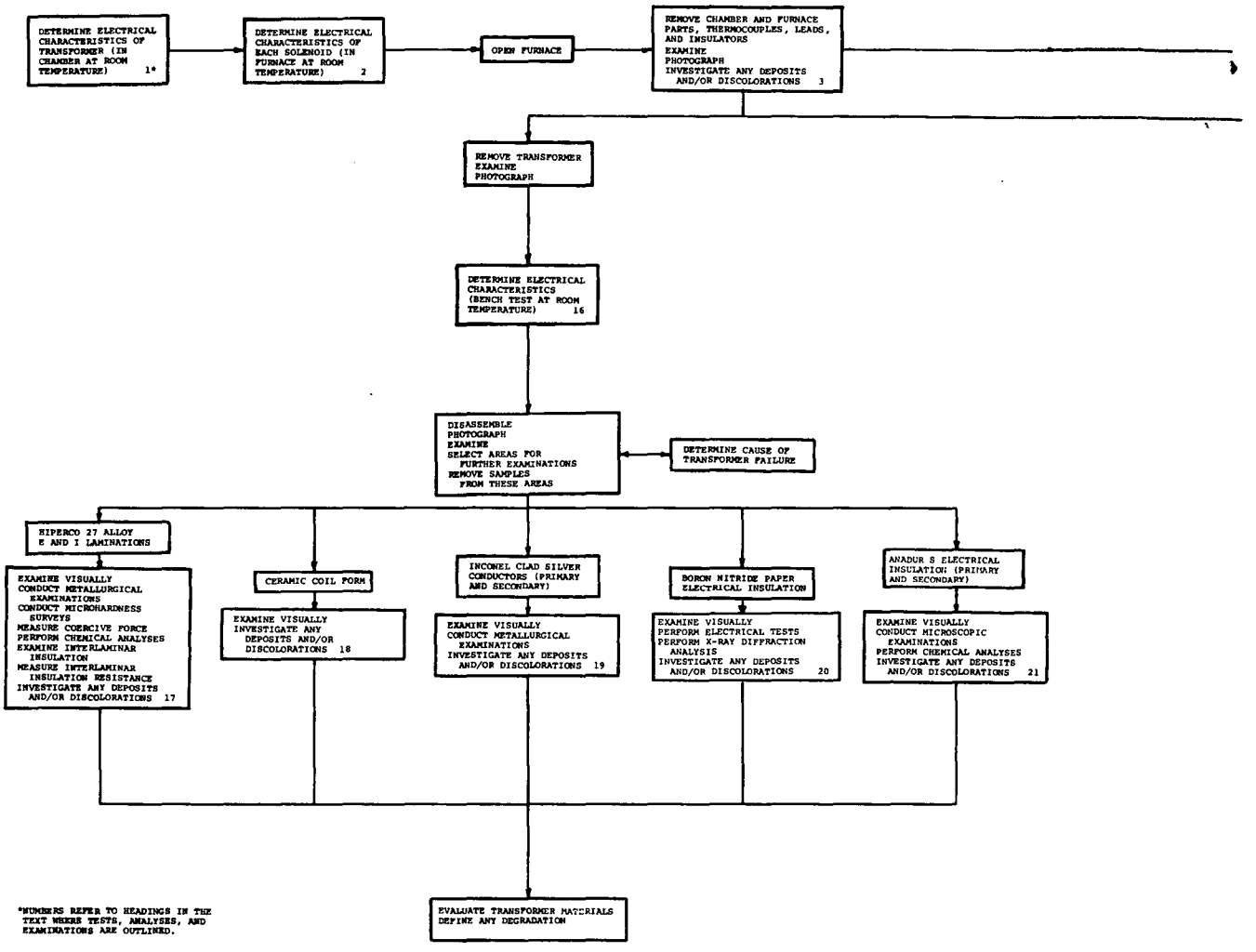

Figure A-1. - Flow Sheet For Post-Test Evaluation Events - Transformer and Solenoids

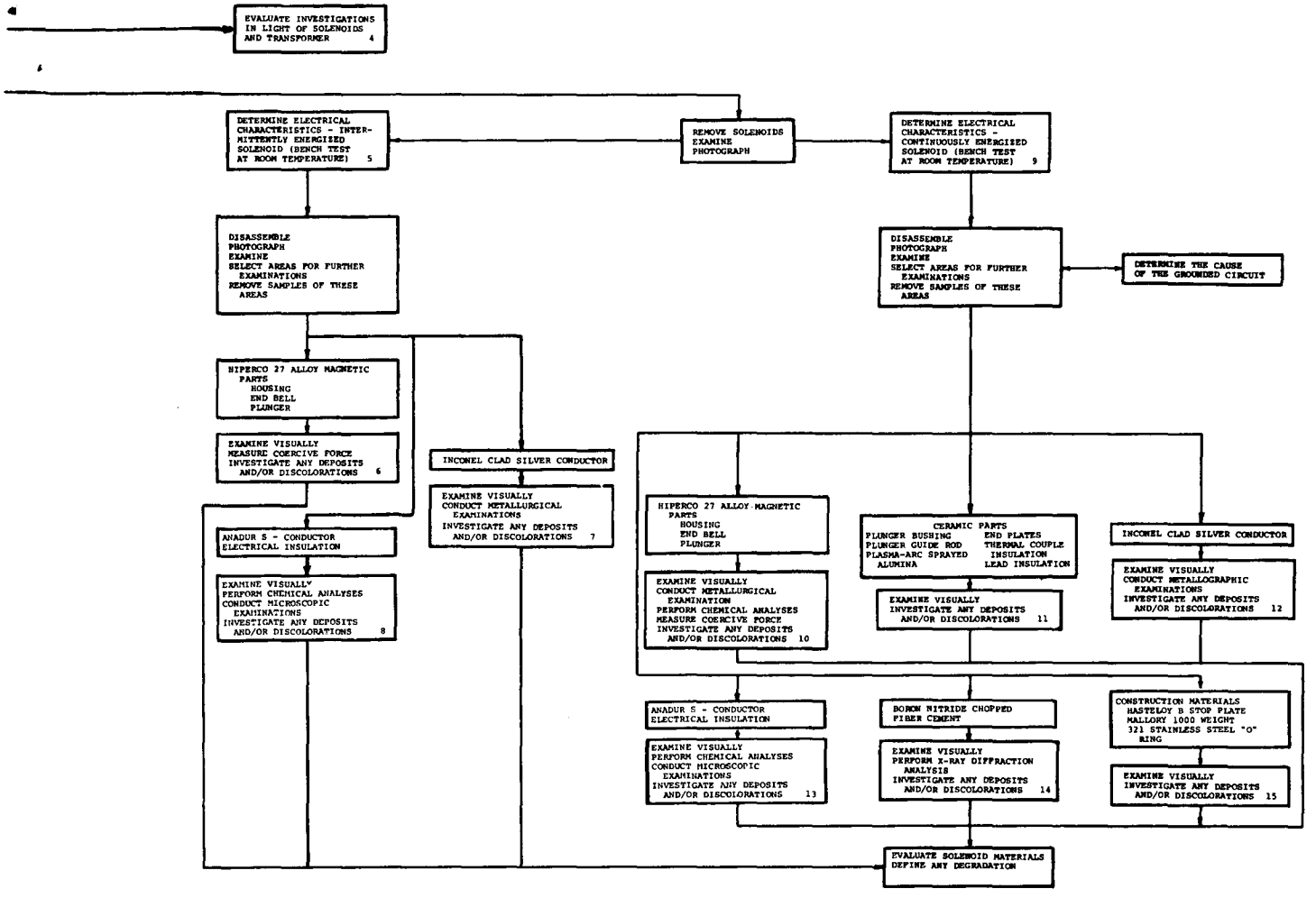
EVALUATE INVESTIGATIONS IN LIGHT OF SOLENOIDS AND TRANSFORMER 4
DETERMINE ELECTRICAL CHARACTERISTICS - INTERMITTENTLY ENERGIZED SOLENOID (BENCH TEST AT ROOM TEMPERATURE) 5
REMOVE SOLENOIDS EXAMINE PHOTOGRAPH
DETERMINE ELECTRICAL CHARACTERISTICS - CONTINUOUSLY ENERGIZED SOLENOID (BENCH TEST AT ROOM TEMPERATURE) 9
DISASSEMBLE PHOTOGRAPH EXAMINE SELECT AREAS FOR FURTHER EXAMINATIONS REMOVE SAMPLES OF THESE AREAS
DISASSEMBLE PHOTOGRAPH EXAMINE SELECT AREAS FOR FURTHER EXAMINATIONS REMOVE SAMPLES OF THESE AREAS
DETERMINE THE CAUSE OF THE GROUNDED CIRCUIT
HIPERCO 27 ALLOY MAGNETIC PARTS HOUSING END BELL PLUNGER
EXAMINE VISUALLY MEASURE COERCIVE FORCE INVESTIGATE ANY DEPOSITS AND/OR DISCOLORATIONS 6
INCONEL CLAD SILVER CONDUCTOR
EXAMINE VISUALLY CONDUCT METALLURGICAL EXAMINATIONS INVESTIGATE ANY DEPOSITS AND/OR DISCOLORATIONS 7
ANADUR S - CONDUCTOR ELECTRICAL INSULATION
EXAMINE VISUALLY PERFORM CHEMICAL ANALYSES CONDUCT MICROSCOPIC EXAMINATIONS INVESTIGATE ANY DEPOSITS AND/OR DISCOLORATIONS 8
HIPERCO 27 ALLOY MAGNETIC PARTS HOUSING END BELL PLUNGER
EXAMINE VISUALLY CONDUCT METALLURGICAL EXAMINATION PERFORM CHEMICAL ANALYSES MEASURE COERCIVE FORCE INVESTIGATE ANY DEPOSITS AND/OR DISCOLORATIONS 10
CERAMIC PARTS
PLUNGER BUSHING
PLUNGER GUIDE ROD
PLASMA-ARC SPRAYED ALUMINA
END PLATES
THERMAL COUPLE INSULATION
LEAD INSULATION
EXAMINE VISUALLY INVESTIGATE ANY DEPOSITS AND/OR DISCOLORATIONS 11
INCONEL CLAD SILVER CONDUCTOR
EXAMINE VISUALLY CONDUCT METALLOGRAPHIC EXAMINATIONS INVESTIGATE ANY DEPOSITS AND/OR DISCOLORATIONS 12
ANADUR S - CONDUCTOR ELECTRICAL INSULATION
EXAMINE VISUALLY PERFORM CHEMICAL ANALYSES CONDUCT MICROSCOPIC EXAMINATIONS INVESTIGATE ANY DEPOSITS AND/OR DISCOLORATIONS 13
BORON NITRIDE CHOPPED FIBER CEMENT
EXAMINE VISUALLY PERFORM X-RAY DIFFRACTION ANALYSIS INVESTIGATE ANY DEPOSITS AND/OR DISCOLORATIONS 14
CONSTRUCTION MATERIALS
HASTELOY B STOP PLATE
MALLORY 1000 WEIGHT
321 STAINLESS STEEL "O" RING
EXAMINE VISUALLY INVESTIGATE ANY DEPOSITS AND/OR DISCOLORATIONS 15
EVALUATE SOLENOID MATERIALS DEFINE ANY DEGRADATION

OUTLINE OF PLANNED POST ENDURANCE EVALUATION PROCEDURES, PROCESSES, ANALYSES, AND EXAMINATIONS

Transformer and Solenoids

1. ELECTRICAL CHARACTERISTICS OF THE TRANSFORMER (IN VACUUM CHAMBER AT ROOM TEMPERATURE)

   A. Electrical Characteristics - The following transformer electrical characteristics will be determined:

      (1) Conductor resistance - secondary (low voltage) winding.

      (2) AC electrical leakage current.

         a. Primary (high voltage) winding to secondary (low voltage) winding.

         b. Primary and secondary to ground.

      (3) DC insulation resistance.

2. ELECTRICAL CHARACTERISTICS OF THE SOLENOIDS (IN VACUUM CHAMBER AT ROOM TEMPERATURE)

   A. Electrical Characteristics - The following electrical characteristics of specified solenoids will be determined:

      (1) Conductor resistance-intermittently energized solenoid.

      (2) DC insulation resistance - both intermittently energized and continuously energized solenoids.

      (3) AC electrical leakage current - intermittently energized solenoid.

      (4) Pickup and minimum hold voltage - intermittently energized solenoid.

3. EXAMINE VACUUM CHAMBER AND FURNACE PARTS, THERMOCOUPLES, LEADS AND INSULATORS - TRANSFORMER AND SOLENOIDS VACUUM TEST CHAMBER

   A. Visual Examinations - Vacuum chamber and furnace parts, thermocouples, leads, and insulators will be examined for deposits and/or discolorations (e.g. silver). Any deposits and/or discolorations will be investigated first by microscopic examinations. Then, if necessary, by appropriate physical and/or chemical examination.

4. EVALUATION OF THE TRANSFORMER AND SOLENOIDS VACUUM TEST CHAMBER AND INSTRUMENTATION PARTS

   Evaluation of any tests or examinations on deposits and/or discolorations will be done in light of findings in the transformer and solenoids areas and to establish the suitability of the test chamber and accessories for the thermal vacuum test.

5. ELECTRICAL CHARACTERISTICS OF THE INTERMITTENTLY ENERGIZED SOLENOID (BENCH TEST AT ROOM TEMPERATURE)

   A. Electrical Characteristics - The following electrical characteristics will be determined:

      (1) Conductor resistance.

      (2) AC electrical leakage current.

      (3) DC insulation resistance.

6. HIPERCO 27 ALLOY MAGNETIC MATERIAL FROM THE INTERMITTENTLY ENERGIZED SOLENOID, HOUSING, END BELL, AND PLUNGER

   A. Visual Examinations - The following Hiperco 27 alloy (iron-27% cobalt) parts will be given visual examinations:

      (1) End bell.

      (2) Housing.

      (3) Plunger.

Typical areas will be selected for further investigation. If critical areas are found, such as ones having deposits and/or discolorations, they will be photographed and investigated; first by microscopic examinations; then, if necessary, by appropriate metallographic, physical, or chemical examination.

B. Coercive Force Measurement - Coercive force will be determined on the following Hiperco 27 alloy (iron-27% cobalt) part:

(1) Plunger. (This plunger was used in a solenoid on NASA contract NAS3-6465 where it was vacuum exposed for 5000 hours in a 1100° F hot-spot test. Typical coercive force measurements on solenoid parts will be determined on the continuously energized solenoid - see 10.D.).

7. INCONEL-CLAD SILVER CONDUCTOR FROM THE INTERMITTENTLY ENERGIZED SOLENOID

A. Visual Examination - Inconel-clad silver will be given visual examinations. Typical areas will be selected for further investigation. If critical areas are found, such as ones having deposits and/or discolorations, they will be photographed and investigated; first by microscopic examinations; then if necessary, by appropriate metallographic, physical, or chemical examination.

B. Metallographic Examinations - Metallographic examinations will be conducted on the following sections of Inconel clad silver conductor:

(1) Longitudinal.

(2) Transverse.

Interpretations will be made and significant observations will be recorded by photomicrographs.

8. ANADUR "S" - CONDUCTOR ELECTRICAL INSULATION FROM THE INTERMITTENTLY ENERGIZED SOLENOID

A. Visual Examination - Anadur "S" insulation will be given visual examinations. Typical areas will be selected for further investigation. If critical areas are found, such as ones having deposits and/or discoloratiens, they will be photographed and investigated; first by microscopic examinations, then, if necessary, by appropriate physical or chemical examination.

B. Chemical Analyses - The following types of chemical analyses will be performed on Anadur "S" specimens:

(1) Qualitative and semi-quantitative chemical analyses (by emission spectrograph) will be performed on samples of the following:

a. Unaged Anadur "S" (control).

b. Anadur "S" from the intermittently energized solenoid.

Interpretations will be made and elements for quantative analyses will be selected.

(2) Quantitative analyses (by emission spectrograph) will be performed for two selected elements (e.g., boron from boron nitride and silicon from Anadur "S" glass (silica) serving) on samples of the following:

a. Unaged Anadur "S" (control).

b. Anadur "S" from the intermittently energized solenoid.

C. Microscopic Examinations - The following Inconel clad silver conductors with Anadur "S" insulation will be mounted and examined as longitudinal cross sections:

(1) Unaged Anadur "S" (control).

(2) Anadur "S" from the intermittently energized solenoid.

Interpretations will be made and significant observations will be recorded by photomicrographs.

9. ELECTRICAL CHARACTERISTICS OF THE CONTINUOUSLY ENERGIZED SOLENOID (BENCH TEST AT ROOM TEMPERATURE)

If the cause of the grounded condition of the continuously energized solenoid can be determined and corrected without disassembly of the solenoid, then this solenoid will be tested to determine the same characteristics as the intermittently energized solenoid, i.e.:

(1) Conductor resistance.

(2) DC insulation resistance.

(3) AC electrical leakage current.

(4) Pickup and minimum hold voltage.

10. HIPERCO 27 ALLOY MAGNETIC MATERIAL FROM THE CONTINUOUSLY ENERGIZED SOLENOID, HOUSING, END BELL, AND PLUNGER

A. Visual Examinations - The following Hiperco 27 alloy (iron-27% cobalt) parts will be given visual examinations:

(1) Housing.

(2) End bell.

(3) Plunger.

Typical areas will be selected for further investigation. If critical areas are found, such as ones having deposits and/or discolorations, they will be photographed and investigated; first by microscopic examinations; then, if necessary, by appropriate metallographic, physical, or chemical examination.

B. Metallographic Examinations - Metallographic examinations will be performed on Hiperco 27 alloy (iron-27% cobalt) specimens from the following:

(1) End bell - next to the boron nitride chopped fiber cement, which was used to secure ceramic parts in place.

(2) End bell - away from the boron nitride chopped fiber cement.

(3) Unaged bar (control) from which plungers and end bells were made.

(4) Plunger stop - plasma-arc sprayed alumina interface.

Interpretations will be made and significant observations will be recorded by photomicrographs.

C. Chemical Analyses - Chemical analyses for the following elements will be performed on a sample of Hiperco 27 alloy (iron-27% cobalt) from the material specified.

(1) Specimens of the following materials will be analyzed for oxygen:

a. End bell

b. Unaged bar (control) from which end bells were made.

2. Specimens of the following materials will be analyzed for nitrogen:

a. End bell - next to the boron nitride chopped fiber cement which was used to secure ceramic parts in place.

b. End bell - away from the boron nitride chopped fiber cement.

c. Unaged bar (control) from which end bells were made.

D. Coercive Force Measurements - Coercive force will be determined on the following Hiperco 27 alloy (iron 27% cobalt) specimens:

(1) End bell.

(2) Unaged bar (control) from which end bells and plungers were made.

(3) Plunger.

11. CERAMIC PARTS FROM THE CONTINUOUSLY ENERGIZED SOLENOID

A. Visual Examinations - The following high alumina ceramic parts will be given visual examinations:

(1) Plunger bushing.

(2) Plunger guide rod.

(3) Plasma-arc sprayed alumina on the plunger stop.

(4) End plates.

(5) Thermocouple insulation.

(6) Lead insulation.

If critical areas are found, such as ones having deposits and/or discolorations, they will be photographed and investigated; first by microscopic examinations; then, if necessary, by appropriate physical or chemical examination.

12. INCONEL-CLAD SILVER CONDUCTOR FROM THE CONTINUOUSLY ENERGIZED SOLENOID

A. Visual Examinations - Inconel-clad silver will be given visual examinations. Typical areas will be selected for further investigation. If critical areas are found, such as ones having deposits and/or discolorations, they will be photographed and investigated; first by microscopic examinations; then, if necessary, by appropriate metallographic, physical, or chemical examination.

B. Metallographic Examinations - Metallographic examinations will be performed on longitudinal and transverse sections of Inconel clad silver conductors from the following locations:

(1) Close to the failure.

(2) Away from the failure.

(3) Unaged material (control).

Interpretations will be made and significant observations will be recorded by photomicrographs.

13. ANADUR "S" - CONDUCTOR ELECTRICAL INSULATION FROM THE CONTINUOUSLY ENERGIZED SOLENOID

A. Visual Examination - Anadur "S" from a minimum of the following locations will be examined:

(1) Near ground circuit.

(2) Outside windings - next to the boron nitride chopped fiber cement which was used to secure ceramic parts in place.

(3) Inside windings - away from the boron nitride chopped fiber cement.

(4) Lead wires.

Typical areas will be selected for further investigation. If critical areas are found, such as ones having deposits and/or discolorations, they will be photographed and investigated; first by microscopic examinations, then, if necessary, by appropriate physical or chemical examination.

B. Chemical Analyses - The following types of chemical analyses will be performed on Anadur "S" specimens.

(1) Qualitative and semi-quantative chemical analyses (by emission spectrograph) will be performed on samples of the following:

a. Anadur "S" from next to the boron nitride chopped fiber cement which was used to secure ceramic parts in place.

b. Anadur "S" away from the boron nitride chopped fiber cement.

Interpretations will be made and elements for quantitative analyses will be selected.

(2) Quantative analyses (by emission spectrograph) will be performed for two selected elements (e.g., boron from boron nitride chopped fiber cement and silicon from Anadur "S" glass (silica serving) on samples of the following:

a. Anadur "S" from next to the boron nitride chopped fiber cement which was used to secure ceramic parts in place.

b. Anadur "S" away from the boron nitride chopped fiber cement.

C. Microscopic Examinations - Anadur "S" insulation from the following locations will be given microscopic examinations in longitudinal sections.

(1) Anadur "S" from both sides of the ground circuit.

(2) Typical Anadur "S" from the solenoid.

14. BORON NITRIDE CHOPPED FIBER CEMENT FROM THE CONTINUOUSLY ENERGIZED SOLENOID

A. Visual Examinations - Boron nitride chopped fiber cement from the following locations will be examined:

(1) Next to Anadur "S".

(2) Away from Anadur "S".

Typical areas will be selected for further investigation. If critical areas are found, such as ones having deposits and/or discolorations, they will be photographed and investigated; first by microscopic examinations, then, if necessary, by appropriate physical or chemical examination.

B. X-Ray Diffraction Analyses - X-ray diffraction analyses on samples of the following materials will be conducted:

(1) Unaged boron nitride chopped fiber cement (control).

(2) Boron nitride chopped fiber cement from the continuously energized solenoid.

15. CONSTRUCTION MATERIALS FROM THE CONTINUOUSLY ENERGIZED SOLENOID

A. Visual Examinations - The following construction materials will be given visual examinations:

(1) Hastelloy B stop plate.

(2) Mallory 1000 weight.

(3) 321 Stainless Steel "O" Ring.

If critical areas are found, such as ones having deposits and/or discolorations, they will be photographed and investigated; first by microscopic examinations; then, if necessary, by appropriate metallographic, physical, or chemical examination.

16. ELECTRICAL CHARACTERISTICS OF THE TRANSFORMER (BENCH TESTS AT ROOM TEMPERATURE)

A. Electrical Tests - The following transformer electrical characteristics will be determined:

(1) Conductor resistance - secondary (low voltage) winding.

(2) AC Electrical leakage current.

a. Primary (high voltage) winding to secondary (low voltage) winding.

b. Primary and secondary windings - each to ground.

(3) DC electrical insulation resistance.

17. HIPERCO 27 ALLOY MAGNETIC MATERIAL FROM THE TRANSFORMER - E AND I LAMINATIONS

A. Visual Examinations - Transformer and unaged Hiperco 27 alloy (iron-27% cobalt) E and I laminations will be given visual examinations.

Typical areas will be selected for further investigation. If critical areas are found, such as ones having deposits and/or discolorations, they will be photographed and investigated; first by microscopic examinations; then, if necessary, by appropriate metallographic, physical, or chemical examination.

B. Metallographic Examinations - Metallographic examinations will be performed on the following Hiperco 27 alloy (iron-27% cobalt) materials:

(1) Transformer lamination.

(2) Unaged lamination (control).

Interpretations will be made and significant observations will be recorded by photomicrographs.

C. Microhardness Surveys - Microhardness surveys will be conducted on the mounted Hiperco 27 alloy (iron-27% cobalt) metallographic examination specimens, i.e.

(1) Transformer lamination.

(2) Unaged lamination (control).

Interpretations will be made and significant observations will be recorded by photomicrographs.

D. Coercive Force Measurements - Coercive force determinations will be performed on the following Hiperco 27 alloy (iron-27% cobalt) materials:

(1) Transformer laminations.

(2) Unaged laminations (control).

E. Chemical Analyses - Specimens of the following Hiperco 27 alloy (iron-27% cobalt) materials will be analyzed for carbon:

(1) Transformer lamination.

(2) Unaged lamination (control).

F. Interlaminar Insulation Examinations - General visual and microscopic examinations will be performed on Hiperco 27 alloy lamination interlaminar insulation (plasma-arc sprayed alumina) surfaces and cross sections.

If critical areas are found, such as ones having deposits and/or discolorations, they will be photographed and investigated; first by microscopic examinations; then, if necessary, by appropriate physical or chemical examination.

G. Interlaminar Insulation Resistance - Interlaminar insulation resistance will be measured on the following:

(1) Transformer laminations.

(2) Unaged laminations (control).

18. CERAMIC COIL FORM FROM THE TRANSFORMER

A. Visual Examination - Ceramic coil form parts will be given visual examinations. If critical areas are found, such as ones having deposits and/or discolorations, they will be photographed and investigated; first by microscopic examinations; then, if necessary, by appropriate physical or chemical examination.

19. INCONEL-CLAD SILVER CONDUCTORS FROM THE TRANSFORMER PRIMARY AND SECONDARY WINDINGS

A. Visual Examinations - Visual examinations will be performed on the following Inconel clad silver conductors:

(1) Primary (high voltage) winding - close to failure.

(2) Primary winding - away from the failure.

(3) Secondary (low voltage) winding.

Typical areas will be selected for further investigation. If critical areas are found, such as ones having deposits and/or discolorations, they will be photographed and in-

vestigated; first by microscopic examinations; then, if necessary, by appropriate metallographic, physical, or chemical examination.

B. Metallographic Examinations - Metallographic examinations will be performed on Inconel-clad silver conductor specimens from the following areas:

(1) Secondary winding.

(2) Primary winding - close to failure.

(3) Primary winding - away from failure.

(4) Unaged primary conductor (control).

(5) Unaged secondary conductor (control).

Interpretations will be made and significant observations will be recorded by photomicrographs.

20. BORON NITRIDE PAPER ELECTRICAL INSULATION FROM THE TRANSFORMER (LAYER-TO-LAYER)

A. Visual Examination - Boron nitride paper insulation from the following areas will be given visual examinations:

(1) Within primary (high voltage) windings.

(2) Between primary and secondary (low voltage) windings.

(3) Unaged material (control).

Typical areas will be selected for further investigation. If critical areas are found, such as ones having deposits and/or discolorations, they will be photographed and investigated; first by microscopic examinations; then, if necessary, by appropriate physical or chemical examination.

B. Electrical Tests - Five ac electrical breakdown tests will be conducted on each of the two samples from the following areas:

(1) Within primary (high voltage).

(2) Between primary and secondary.

(3) Unaged material (control).

C. X-Ray Diffraction Analyses - X-ray diffraction analyses will be performed on samples of boron nitride paper from the following areas:

(1) Transformer - next to Anadur "S".

(2) Unaged material (control).

21. ANADUR "S" - ELECTRICAL INSULATION FROM THE TRANSFORMER PRIMARY AND SECONDARY CONDUCTORS

A. Visual Examinations - Anadur "S" electrical insulation from the following areas will be given general visual examinations:

(1) Primary (high voltage) winding.

(2) Secondary (low voltage) winding.

Typical areas will be selected for further investigation. If critical areas are found, such as ones having deposits and/or discolorations, they will be photographed and investigated; first by microscopic examinations, then, if necessary, by appropriate physical or chemical examination.

B. Microscopic Examinations - Anadur "S" specimens from the following areas will be mounted with Inconel-clad silver conductors, sectioned, and subjected to microscopic examinations:

(1) Transformer primary away from the open circuit.

(2) Transformer primary at the open circuit.

(3) Unaged primary (control).

(4) Transformer secondary.

(5) Unaged Secondary (control).

Interpretations will be made and significant observations will be recorded by photomicrographs.

C. Chemical Analyses - The following types of chemical analyses will be performed on Anadur "S" specimens:

(1) Qualitative and semi-quantitative chemical analyses (by emission spectrograph) will be performed on samples of the following Anadur "S":

a. Transformer primary.

b. Transformer secondary.

c. Unaged material (control).

Interpretations will be made and elements for quantitative analyses will be selected.

(2) Quantitative analyses (by emission spectrograph) will be performed for two specified elements (e.g., boron from boron nitride paper insulation and silicon from Anadur "S" glass (silica) serving) on samples of the following:

a. Transformer primary.

b. Transformer secondary.

c. Unaged material (control).

101. ELECTRICAL CHARACTERISTICS OF THE STATOR (IN VACUUM CHAMBER AT 1300° F HOT-SPOT TEMPERATURE)

A. Electrical Characteristics - The following electrical characteristics will be determined:

(1) Conductor Resistance - each phase.

(2) AC electrical leakage current.

a. Phase-to-phase.

b. Phase-to-ground.

(3) DC insulation resistance.

a. Phase-to-phase.

b. Phase-to-ground.

(4) Electrical breakover voltage.

a. Phase-to-phase.

b. Phase-to-ground.

Chamber pressures will be recorded after the electrical data, as has been done before (approximately one-half hour later).

102. STEADY-STATE-TEMPERATURE ELECTRICAL CHARACTERISTICS OF THE STATOR DURING COOLING TO ROOM TEMPERATURE

A. Electrical Tests and Test Procedures - The following procedures and tests will be used to determine electrical characteristics:

(1) Turn stator power off.

(2) Reset furnace to obtain aging temperature (1300° F).

(3) Perform tests 1, 2, and 3 described in heading 101 (with furnace heat only).

(4) Reduce furnace power to attain a temperature of approximately 1050° F.

(5) At steady-state temperature conditions, perform tests as in (3) above.

(6) Perform items (4) and (5) above a second and third time attaining temperatures of approximately 820° F and 564° F.

103. ROOM TEMPERATURE ELECTRICAL CHARACTERISTICS OF THE STATOR (IN CHAMBER)

A. Electrical Tests - The following electrical characteristics will be determined:

(1) Conductor resistance - each phase.

(2) AC electrical leakage current.

a. Phase-to-phase.

b. Phase-to-ground.

(3) DC Insulation resistance.

a. Phase-to-phase.

b. Phase-to-ground.

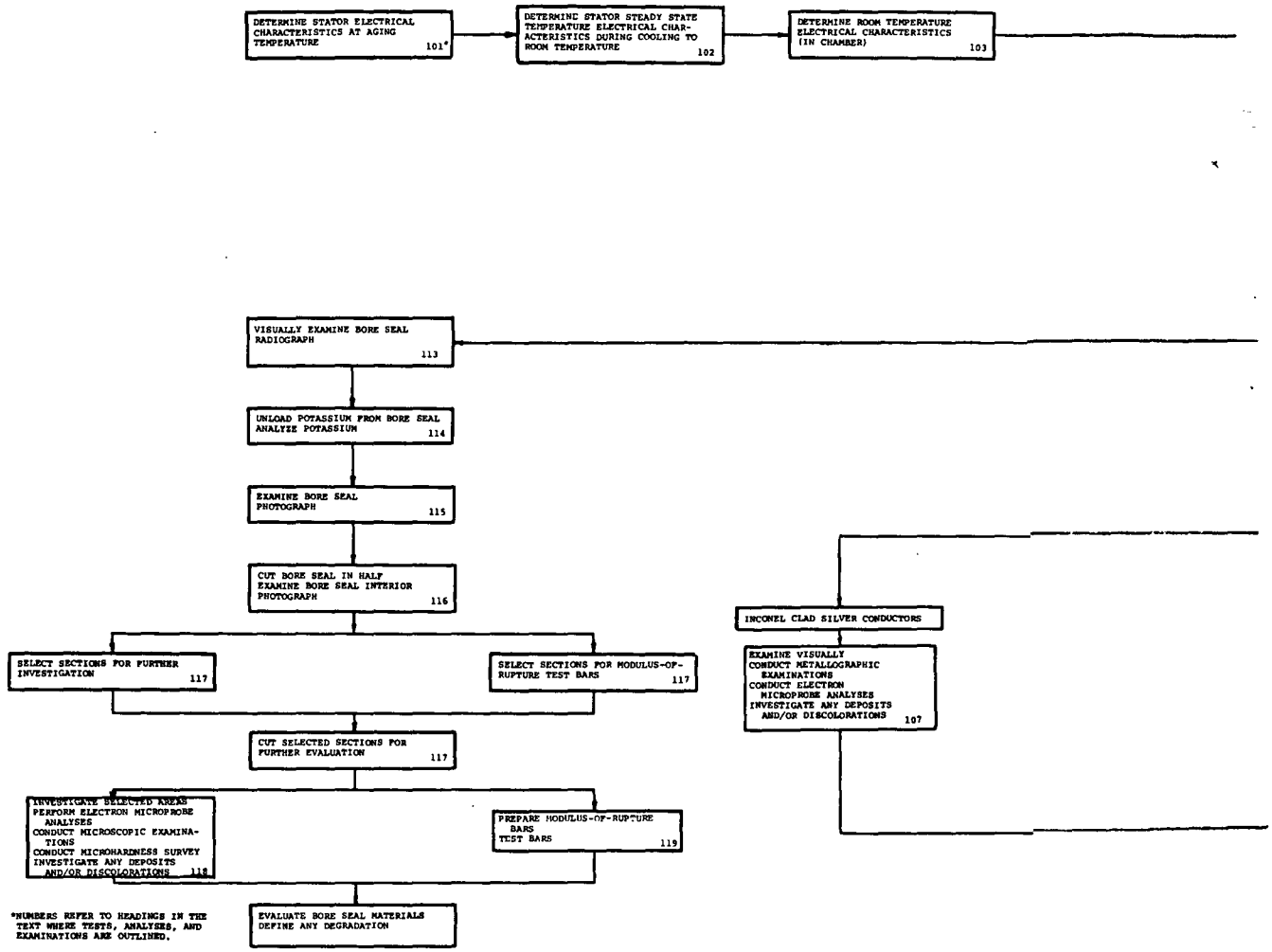

Figure A-2. - Flow Sheet For Post-Test Evaluation Events - Stator and Bore Seal.

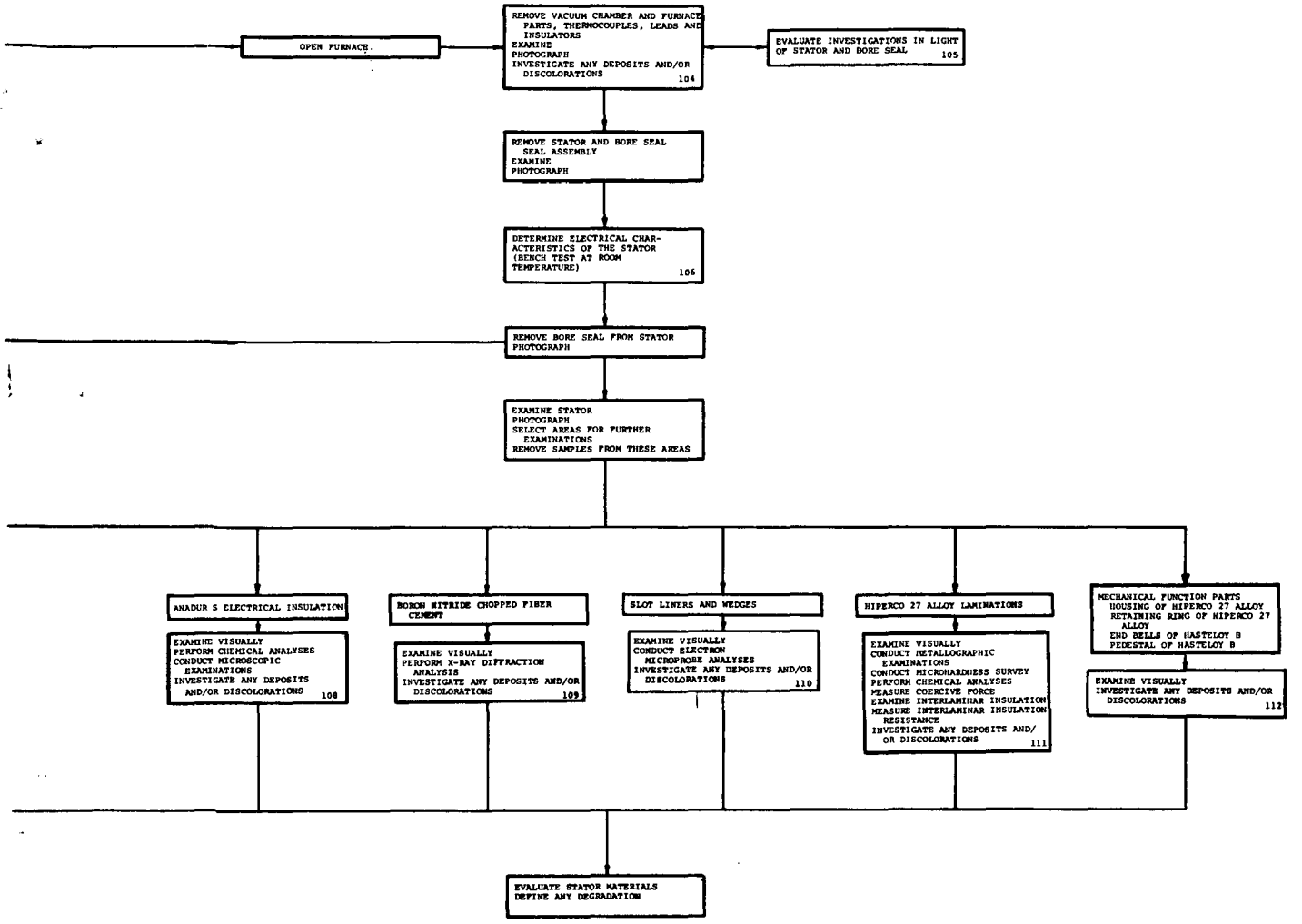
OPEN FURNACE
REMOVE VACUUM CHAMBER AND FURNACE PARTS, THERMOCOUPLES, LEADS AND INSULATORS
EXAMINE
PHOTOGRAPH
INVESTIGATE ANY DEPOSITS AND/OR DISCOLORATIONS
104
EVALUATE INVESTIGATIONS IN LIGHT OF STATOR AND BORE SEAL
105
REMOVE STATOR AND BORE SEAL SEAL ASSEMBLY
EXAMINE
PHOTOGRAPH
DETERMINE ELECTRICAL CHARACTERISTICS OF THE STATOR (BENCH TEST AT ROOM TEMPERATURE)
106
REMOVE BORE SEAL FROM STATOR
PHOTOGRAPH
EXAMINE STATOR
PHOTOGRAPH
SELECT AREAS FOR FURTHER EXAMINATIONS
REMOVE SAMPLES FROM THESE AREAS
ANADUR S ELECTRICAL INSULATION
EXAMINE VISUALLY
PERFORM CHEMICAL ANALYSES
CONDUCT MICROSCOPIC EXAMINATIONS
INVESTIGATE ANY DEPOSITS AND/OR DISCOLORATIONS
108
BORON NITRIDE CHOPPED FIBER CEMENT
EXAMINE VISUALLY
PERFORM X-RAY DIFFRACTION ANALYSIS
INVESTIGATE ANY DEPOSITS AND/OR DISCOLORATIONS
109
SLOT LINERS AND WEDGES
EXAMINE VISUALLY
CONDUCT ELECTRON MICROPROBE ANALYSES
INVESTIGATE ANY DEPOSITS AND/OR DISCOLORATIONS
110
HIPERCO 27 ALLOY LAMINATIONS
EXAMINE VISUALLY
CONDUCT METALLOGRAPHIC EXAMINATIONS
CONDUCT MICROHARDNESS SURVEY
PERFORM CHEMICAL ANALYSES
MEASURE COERCIVE FORCE
EXAMINE INTERLAMINAR INSULATION
MEASURE INTERLAMINAR INSULATION RESISTANCE
INVESTIGATE ANY DEPOSITS AND/OR DISCOLORATIONS
111
MECHANICAL FUNCTION PARTS
HOUSING OF HIPERCO 27 ALLOY
RETAINING RING OF HIPERCO 27 ALLOY
END BELLS OF HASTELOY B
PEDESTAL OF HASTELOY B
EXAMINE VISUALLY
INVESTIGATE ANY DEPOSITS AND/OR DISCOLORATIONS
112
EVALUATE STATOR MATERIALS
DEFINE ANY DEGRADATION

104. EXAMINE VACUUM CHAMBER AND FURNACE PARTS, THERMOCOUPLES, LEADS, AND INSULATORS - STATOR AND BORE SEAL VACUUM TEST CHAMBER

A. Visual Examinations - Vacuum chamber and furnace parts, thermocouples, leads, and insulators will be examined for any deposits and/or discolorations, e.g. silver and potassium.

If critical areas are found, such as ones having deposits and/or discolorations, they will be photographed and investigated; first by microscopic examinations; then, if necessary, by appropriate physical or chemical examination.

105. EVALUATION OF STATOR AND BORE SEAL VACUUM TEST CHAMBER AND INSTRUMENTATION PARTS

Evaluation of any tests or examinations on deposits and/or discolorations will be done in light of findings in the stator and bore seal areas and to establish the suitability of the test chamber and accessories for the thermal vacuum test.

106. ELECTRICAL CHARACTERISTICS OF THE STATOR (BENCH TEST AT ROOM TEMPERATURE)

A. Electrical Characteristics - The following electrical characteristics will be determined:

(1) Conductor resistance - each of three phases.

(2) AC electrical leakage current.

a. Phase-to-phase.

b. Phase-to-ground.

(3) DC insulation resistance.

a. Phase-to-phase.

b. Phase-to-ground.

107. INCONEL-CLAD SILVER CONDUCTOR FROM THE STATOR

A. Visual Examination - Inconel-clad silver will be given visual examinations.

Typical areas will be selected for further investigation. If critical areas are found, such as ones having deposits and/or discolorations, they will be photographed and

investigated; first by microscopic examinations, then, if necessary, by appropriate physical or chemical examination.

B. Metallographic Examination - Metallographic examination will be conducted on the following sections of inconel-clad silver conductor:

(1) Transverse section from a stator slot.

(2) Longitudinal section from a stator end turn.

(3) Longitudinal and transverse sections of unaged material (control).

Interpretations will be made and significant observations will be recorded by photomicrographs.

C. Electron Microprobe Analyses - Electron microprobe analyses for two elements, silver and chromium, will be conducted on a selected aged stator conductor specimen. The silver-Inconel interface will be probed for diffusion of silver into the Inconel and diffusion of chromium from the Inconel into the silver. If diffusion is found to exist, electron microprobe analyses for the same elements will be performed on an unaged stator conductor for comparison. A vacuum exposed surface of the aged stator conductor will be probed for chromium. Interpretations will be made and significant observations will be recorded.

108. ANADUR "S" - CONDUCTOR ELECTRICAL INSULATION FROM THE STATOR

A. Visual Examinations - Anadur "S" insulation from the following locations will be given visual examinations:

(1) End turns.

(2) Slots.

(3) Next to the boron nitride chopped fiber cement which was used to secure ceramic parts in place.

(4) Away from the boron nitride chopped fiber cement.

Typical areas will be selected for further investigation. If critical areas are found, such as ones having deposits and/or discolorations, they will be photographed and investigated; first by microscopic examinations, then, if necessary, by appropriate physical or chemical examination.

B. Chemical Analyses - The following types of chemical analyses will be performed:

(1) Qualitative and semi-quantitative chemical analyses (by emission spectrograph) will be performed on samples from the following areas:

a. Next to boron nitride chopped fiber cement which was used to secure ceramic parts in place.

b. Away from boron nitride chopped fiber cement.

(2) Quantitative analyses (by emission spectrograph) will be performed for two selected elements (e.g. boron from boron nitride chopped fiber cement and silicon from the silica "S" glass serving) on samples from the following areas:

a. Next to the boron nitride chopped fiber cement which was used to secure ceramic parts in place.

b. Away from the boron nitride chopped fiber cement.

C. Microscopic Examination - Inconel-clad silver conductors with Anadur "S" insulation from the following locations will be examined as longitudinal cross sections:

(1) End turn.

(2) Stator slot.

Interpretations will be made and significant observations will be recorded by photomicrographs.

109. BORON NITRIDE CHOPPED FIBER CEMENT FROM THE STATOR

A. Visual Examinations - Boron nitride chopped fiber cement (used to secure ceramic parts in place) from the following locations will be examined:

(1) Next to the Anadur "S" insulation.

(2) Away from the Anadur "S" insulation.

Typical areas will be selected for further investigation. If critical areas are found, such as ones having deposits and/or discolorations, they will be photographed and investigated; first by microscopic examinations, then, if necessary, by appropriate physical or chemical examination.

B. X-ray Diffraction Analyses - X-ray diffraction analyses will be performed on samples of boron nitride chopped fiber cement from the following locations:

(1) Next to the Anadur "S".

(2) Away from the Anadur "S" insulation.

110. SLOT LINERS AND WEDGES FROM THE STATOR

A. Visual Examinations - The following ceramic parts will be given visual examinations.

(1) Slot liners.

(2) Wedges.

If critical areas are found, such as ones having deposits and/or discolorations, they will be photographed and investigated; first by microscopic examinations; then, if necessary, by appropriate physical or chemical examination.

B. Electron Microprobe Analyses - Electron Microprobe analyses to determine the concentration gradient for two contaminating elements shall be made on rigid insulation. Selection of the two elements will depend upon results of chemical analysis.

111. HIPERCO 27 ALLOY LAMINATIONS FROM THE STATOR

A. Visual Examinations - Hiperco 27 alloy laminations from the following locations will be given visual examinations:

(1) Next to boron nitride chopped fiber cement.

(2) Away from boron nitride chopped fiber cement.

Typical areas will be selected for further investigation. If critical areas are found, such as ones having deposits and/or discolorations, they will be photographed and investigated; first by microscopic examinations; then, if necessary, by appropriate metallographic, physical, or chemical examination.

B. Metallographic Examinations - Metallographic examinations will be performed on material from the following locations:

(1) Next to the boron nitride chopped fiber cement which was used to secure ceramic parts in place.

(2) Away from the boron nitride chopped fiber cement.

(3) Unaged stator lamination (control).

Interpretations will be made and significant observations will be recorded by photomicrographs.

C. Microhardness Surveys - Microhardness surveys will be conducted on mounted Hiperco 27 alloy metallographic specimens i.e.:

(1) Next to boron nitride chopped fiber cement.

(2) Away from boron nitride chopped fiber cement.

(3) Unaged stator lamination (control).

Interpretations will be made and significant observations will be recorded by photomicrographs.

D. Coercive Force Measurement - Coercive force determination will be made on the following specimens:

(1) Stator lamination.

(2) Unaged lamination (control).

E. Chemical Analyses - Specimens of Hiperco 27 alloy laminations from specified locations will be analyzed for the following:

(1) Oxygen - Sample from away from boron nitride chopped fiber cement.

(2) Oxygen - Unaged lamination (control).

(3) Carbon - Sample from away from the boron nitride chopped fiber cement.

(4) Carbon - Unaged lamination (control).

(5) Nitrogen - Sample from next to the boron nitride chopped fiber cement which was used to secure ceramic parts in place.

(6) Nitrogen - Sample from away from the boron nitride chopped fiber cement.

(7) Nitrogen - Sample of unaged stator lamination (control).

F. Interlaminar Insulation Examinations - General visual and microscopic examinations will be performed on unaged and aged stator Hiperco 27 alloy lamination interlaminar insulation surfaces and cross sections.

G. Interlaminar Insulation Resistance Measurements - Interlaminar insulation resistance will be measured on the following:

(1) Stator lamination.

(2) Unaged lamination (control).

112. MECHANICAL FUNCTION PARTS FROM THE BORE SEAL AND STATOR

A. Visual Examinations - The following mechanical function parts will be given visual examinations:

(1) Housing of Hiperco 27 alloy.

(2) Retaining ring of Hiperco 27 alloy.

(3) End bells of Hastelloy B.

(4) Pedestal of Hastelloy B.

If critical areas are found, such as ones having deposits and/or discolorations, they will be photographed and investigated; first by microscopic examinations, then, if necessary, by appropriate metallographic, physical, or chemical examination.

113. EXAMINE BORE SEAL EXTERIOR (BORE SEAL LOADED WITH POTASSIUM)

A. Visual Examination - Bore seal exterior will be visually examined.

If critical areas are found, such as ones having deposits and/or discolorations, they will be photographed and investigated; first by microscopic examinations; then, if necessary, by appropriate physical or chemical examination.

B. Radiographic Examination - The bore seal will be radiographed to determine the following:

(1) Location of condensed potassium.

(2) Location of any internal flaws in the metal, ceramic, and brazed joint.

114. UNLOAD POTASSIUM FROM BORE SEAL

The bore seal will have its potassium unloaded and analyzed according to the following procedure:

A. The bore seal (except loading tube) will be heated and the loading tube cooled to vapor transport and flow potassium into the loading tube.

B. The bore seal will be radiographed to verify the location of the majority of the potassium.

C. The loading tube will be cut off to remove the majority of the potassium. This will be done in a glove box under a cover of high purity (99.995 percent) argon.

D. All potassium will be slowly neutralized with spectrographic grade methanol (thus forming potassium methylate) under high purity argon (argon will be flowed directly into the bore seal interior). Potassium exposed surfaces will be rinsed with methanol several times until there is no detecable reaction. This determination will be made by analyzing rinse methanol for potassium with a flame photometer and comparing this with a similar analysis of the starting methanol. Potassium methylate exposed surfaces will be rinsed with distilled water to assure collection of all potassium methylate and to remove any water soluble or insoluble substances. Concentrated high purity hydrochloric acid will be added to the solution and the solution evaporated to potassium chloride (a salt). A standard for reagent impurity analysis will be processed with potassium from the bore seal. This standard will be made using high purity potassium chloride and the same quantity of reagents as above. This will be evaporated to potassium chloride.

E. Bore seal residue from evaporation of clean-up solutions, reagent standard residue, and the standard high purity potassium chloride will be analyzed (by mass spectrograph) for the following metallic impurities:

(1) Columbium.

(2) Beryllium.

(3) Vanadium.

(4) Zirconium.

F. The bore seal parts will be rinsed with methanol to remove residual water.

G. The bore seal parts will be clean fired at 1832° F for 10 minutes at a pressure no greater than $5x10^{-6}$ torr.

H. The bore seal will then be placed in a tight enclosure to keep the device clean during storage and shipment.

115. EXAMINE BORE SEAL EXTERIOR (BORE SEAL EMPTY)

A. Visual Examination - The bore seal will be given visual and microscopic examinations as warranted.

If critical areas are found, such as ones having deposits and/or discolorations, they will be photographed and investigated; first by microscopic examinations; then, if necessary, by appropriate physical or chemical examination.

116. CUT BORE SEAL IN HALF

A. Selecting the plane for cutting - One longitudinal half of the bore seal will be selected, on the basis of visual and radiograph examinations, as the location of specimens for further evaluation.

B. Bore Seal Cutting - The bore seal will be cut in half in a specified longitudinal plane (i.e., a plane containing the axis of the bore seal tube) at a facility that can safely and satisfactorily perform the work.

C. Visual Examinations - The bore seal interior will be given visual and microscopic examinations. If critical areas are found, such as ones having deposits and/or discolorations, they will be photographed and investigated; first by microscopic examinations; then, if necessary, by appropriate physical or chemical examination.

117. SELECT AND OBTAIN SPECIMENS FOR FURTHER INVESTIGATION

A. Select sections for modulus-of-rupture bars - The location of fifteen modulus-of-rupture bars will be specified. Each bar will have an as-cut length of one inch or greater and a width of 0.1 inch or greater. The one inch dimension will be parallel to the axis of the beryllia tube. These bars will be in the selected bore seal half.

B. Select areas for further investigation - Two selections of brazed joints will be selected for examinations and analyses. Any other areas requiring further investigation

will be specified for removal. It is anticipated that all these sections will come from the selected half of the bore seal.

C. Cut specimens - Selected specimens will be cut using a diamond cut off wheel and appropriate safety precautions.

118. INVESTIGATION OF SELECTED AREAS

A. Electron microprobe analyses of brazed joints - Electron microprobe analyses will be conducted on two brazed joint specimens. Each specimen will consist of: back-up ring, beryllia, braze material, columbium-1% zirconium, braze material, and a short length of potassium exposed beryllia tube. Each specimen will be analyzed for zirconium vanadium, columbium, potassium, and oxygen. (Beryllium content will be approximated by a difference calculation.)

B. Microscopic examination of brazed joints - Each of the two electron microprobe specimens will be given microscopic examinations, i.e., the various materials and their respective interfaces. Interpretations will be made and significant observations will be recorded by photomicrographs.

C. Microhardness scans across brazed joints - Microhardness of the various materials and, as possible, interfaces will be determined on the electron microprobe specimens.

Interpretations will be made and significant observations will be recorded by photomicrographs.

D. Investigation of other areas - If other bore seal areas show definite corrosion, they will be investigated first by microscopic examinations; then, if necessary, by appropriate chemical or physical investigations.

119. PREPARATION AND TESTING OF MODULUS-OF-RUPTURE BARS

A. Preparation of modulus-of-rupture bars - As-cut modulus-of-rupture bars will be prepared for testing as follows:

(1) As-cut bars will be diamond ground to a square cross section of slightly less than 0.1 inch dimension. (This will remove the radius of curvature of the tube.) During this operation, the potassium exposed side will remain identified.

(2) Ground-to-size bars will be cleaned and clean-fired at 1832° F for 10 minutes at a pressure no greater than 5×10^{-6} torr (as were the bars on the previous program, NASA Contract NAS3-6465). During this operation the potassium exposed side will remain identified.

B. Testing of modulus-of-rupture bars - Modulus-of-rupture bars will be divided into three five-bar groups. Modulus-of-rupture (flexural strength) will be determined using the same four-point loading fixture as was used on NASA contract NAS3-6465. Groups of bars will be tested as follows:

(1) Longitudinal specimens:

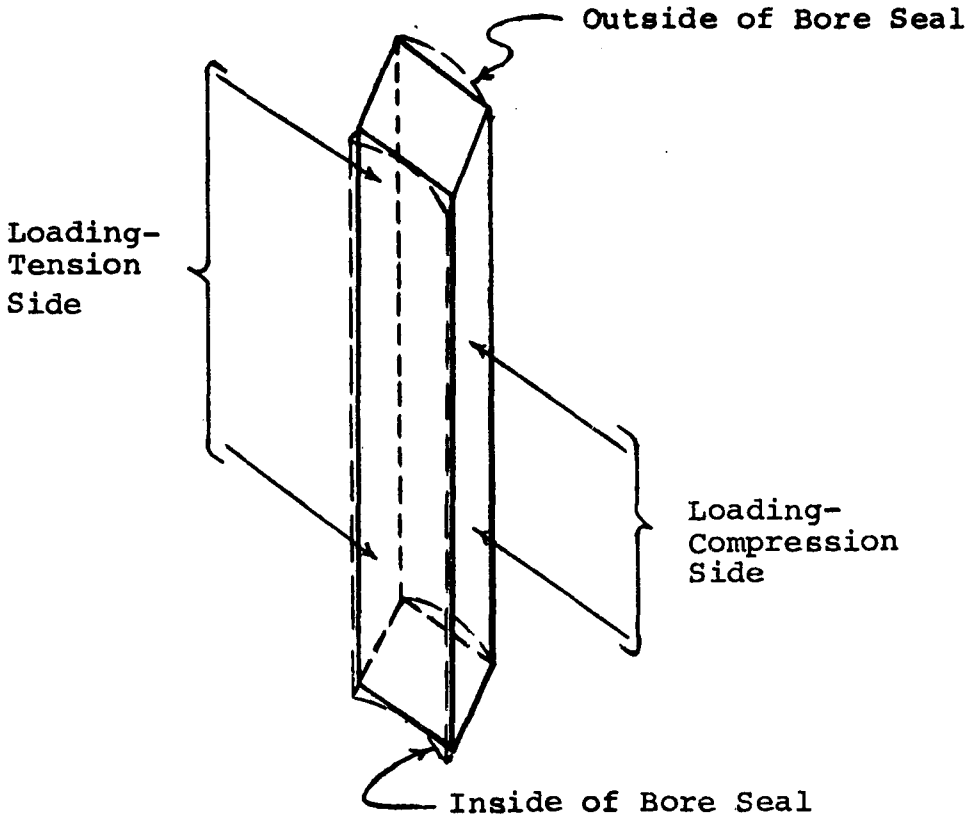

(2) Circumferential specimens (Potassium side in tension).

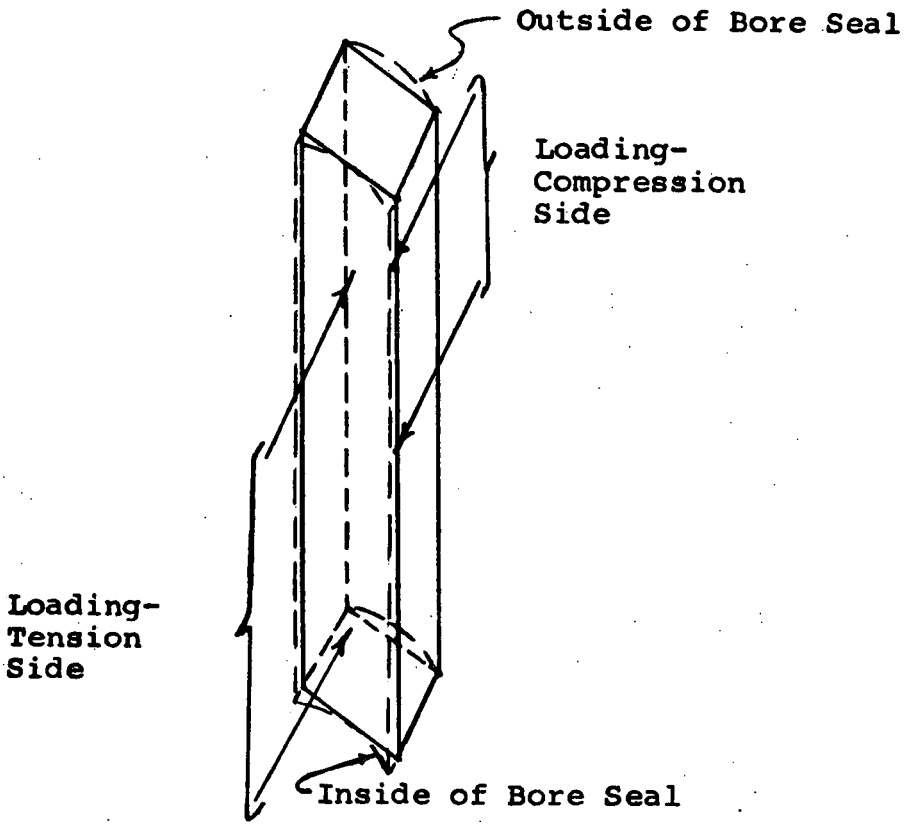

(3) Circumferential specimens (potassium side in compression).

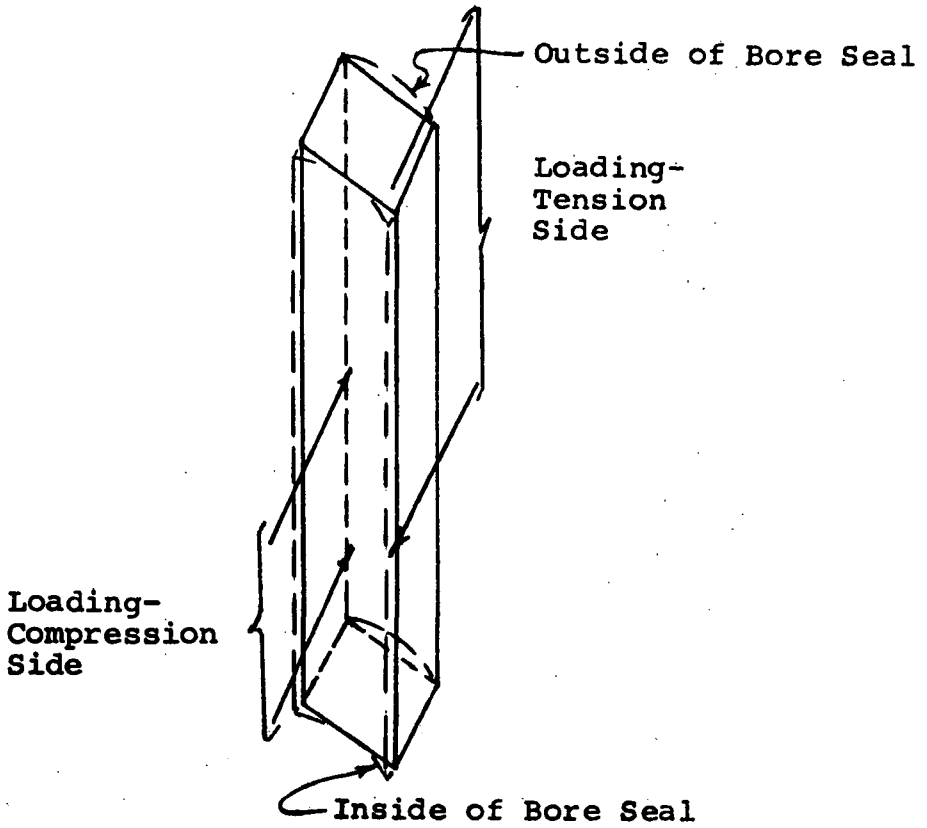

APPENDIX B

NOMINAL COMPOSITIONS OF METALLIC MATERIALS OF CONSTRUCTION USED IN COMPONENTS, FIXTURES, AND THERMAL-VACUUM CHAMBERS

Elements	A Nickel	Inconel 600	Hastelloy B	Hiperco 27	Mallory 1000 (c)	304 SS	321 SS	Fine Silver
Nickel	99.0[b] min.	72.0[b] min.	Balance	0.75 max.	6.0	8.0/12.0	9.00/12.00	
Cobalt			2.50 max.	26.0/28.5				
Iron	0.40 max.	6.0/8.0	4.00/7.00	Balance		Balance	Balance	
Chromium		14.0/17.0	1.00 max.	0.75 max.	< 0.1	18.0/20.0	17.00/19.00	
Manganese	0.35 max.	1.00 max.	1.00 max.	0.80 max.	< 0.1	2.00 max.	2.00 max.	
Silicon	0.35 max.	0.75 max.	1.00 max.	0.45 max.		1.00 max.	1.00 max.	
Carbon	0.15 max.	0.10 max.	0.05 max.		0.000020	0.08 max.	0.08 max.	
Sulfur	0.01 max.		0.03 max.			0.030 max.	0.030 max.	
Phosphorus			0.04 max.			0.045 max.	0.045 max.	
Tungsten					Balance			
Molybdenum			26.0/30.0		< 0.1			
Titanium							5 x C min.	
Vanadium			0.20/0.60					
Columbium & Tantalum		1.75/2.75						
Copper	0.25 max.	0.50 max.			4.0			0.9 max.
Others (each)				0.10 max.				
Others (total)				0.30 max.				
Pb								0.03 max.
Bi								0.01 max.
Li								0.025 max.
O								0.005 max.
Ag								99.875 min.

(a) Tantalum and tantalum-10% tungsten, used as heater elements and support mechanism in the vacuum furnace, contained a total of less than 300 ppm and 600 ppm metallic impurities, respectively.

(b) Plus cobalt.

(c) This is a power metallurgy product.

REFERENCES

1. Kueser, P. E., et al.: "Properties of Magnetic Materials For Use in High-Temperature Space Power Systems," NASA SP-3043, 1967.

2. Kueser, P. E., et al.: "Electrical Conductor and Electrical Insulation Materials Topical Report," NASA CR-54092, October 1964.

3. Kueser, P. E., et al.: "Bore Seal Technology Topical Report," NASA CR-54093, December 1964.

4. Grant, W. L.; Kueser, P. E.; Parkman, M. F.; and Toth, J. W.: "Bore Seal Development and Simulated Space Evaluation of High-Temperature Electrical Materials and Components Topical Report," WAED 67.46E, Contract NAS3-6465, November 1967.

5. Grant, W. L.; and Kueser, P. E.: "Thermal-Vacuum Testing of High-Temperature Electrical Components," NASA CR-1592.

6. Kueser, P. E.; Toth, J. W.; and Grant, W. L.: "Ceramic/Metal Bore Seal Development," NASA CR-1591.

7. Honig, R. E.: "Vapor Pressure Curves for the More Common Elements," RCA Laboratories, 1957.

8. Hansen, Max: "Constitution of Binary Alloys," McGraw Hill, 1958.

9. Pshenchenkova, G. V.; and Skokov, A. D.: "An Investigation of Magnetic Properties and Hardness of Iron-Cobalt Alloys," Physics of Metals and Metallography (U.S.S.R.), Vol. 21, Issue #3, pp. 339-345, (1966), Hereafter Cited as Pshenchenkova and Skokov.

10. Pshenchenkova, G. V.; and Skokov, A. D.: Magnetic Alloys for High-Temperature Service, Elektrichestvo (U.S.S.R.) Vol. 1, Issue #4, pp. 81-83, 1965.